Combating Fibrosis In Mdx Mice With A Novel Antifibrosis Drug – Halofuginone

BY

KYLA DANIELLE HUEBNER

A thesis submitted to the Faculty of Graduate Studies in partial fulfillment of the requirements for the degree of

MASTER OF SCIENCE

Department of Human Anatomy and Cell Science
Faculty of Medicine
University of Manitoba
Winnipeg, Canada

ACKNOWLEGEMENTS

I would like to thank several individuals for their encouragement, support and guidance during this project. This Masters project would not have been completed without your help, and I will always cherish everything you have done for me.

I need to begin by thanking my parents and partner. Mom and Dad – thanks for your help in matters of life and science, and for encouraging my education every step of the way. Matt – thanks for keeping me calm throughout this experience and always opening my eyes and ears to new ideas. I hope to be able to support you in the same manner throughout all of your endeavours.

To the rest of my family and friends – Your support, encouragement, and understanding through this project have made this experience smoother. To my Grandma – I am happy to reach this stage and know how proud you would have been to see this and share this experience with me. I wish you could be here for this, and to continue our discussions on everything from biology to NYC.

To my advisor – Judy Anderson. Thank you very much for all of your help professionally and personally. During these past years of study you have taught me the big picture in the world of science, stimulated me to constantly think about every side of a situation, encouraged me to continue my education, and to set the bar at a higher level. It has been a pleasure working with you and I look forward to continuing working together in the future.

To my advisory committee – Dr. Thliveris and Dr. Scott. This project would not have been possible without you. Thank you very much for all you help and guidance.

I would like to thank Sujata, Sarah and Dr. Halayko for helping with the barometric plethysmography. I would also like to thank Dr. Jassal and Tielan for conducting the echocardiography studies. Thank you for you patience while teaching me all about murine echogardiography. This was truly the icing on the cake for the functional outcome of this study.

Lastly, the lab and department – Jeff, Cinthya, and Alex. Your friendship and support were there on a daily basis. Thank you for your company and friendship. I know we will remain friends for years to come.

This work was supported through funding provided by the Muscular Dystrophy Association (Anderson Lab) and the Manitoba Institute of Child Health (Studentship).

TABLE OF CONTENTS

ABSTRACT

The effects of the antifibrotic drug Halofuginone hydrobromide (Halo) on muscle function, regeneration and cardiorespiratory function were studied using the mdx mouse, a homologue of Duchenne muscular dystrophy (DMD). Halo is an antifibrotic drug that is thought to affect only the "pathological" collagens. Halo prevents fibrosis as well as resolve pre-established fibrosis. It was hypothesized that Halo treatment would resolve pre-established fibrosis and prevent further collagen deposits. This would improve muscle function and regeneration, as well as cardiorespiratory function.

Mice 8-9 months old were treated with saline or Halo for 5 (n = 4/group), 10 (n = 5/group) and 12 weeks (n = 4-5/group). Muscle strength and endurance were evaluated weekly. Plethysmography was done to assess respiration, followed by an injection of Evans Blue Dye and exercise to induce muscle damage. Mice were then euthanized and tissues were collected for protein studies and histological examination. Two additional groups of mice were treated for 10 weeks (young mice 3-4 wks n = 9-10/group; old mice 8-9 mos n = 8-10/group) and echocardiography was performed.

Treatment with Halo significantly increased hepatocyte growth factor (HGF); this is thought to decrease myofibroblast activation and proliferation. Halo significantly reduced expression of collagen and decreased collagen content. As a consequence of reduced fibrosis, muscle repair was more effective and damage was reduced. There were significant functional improvements after treatment for 5 or 10 weeks and the progression of disease was slowed.

This research is especially important because it shows a resolution of pre-existing fibrosis and a reduction of new collagen synthesis. This treatment could potentially improve quality of life and lengthen the lifespan of boys with DMD.

Chapter 1. INTRODUCTION

1. DUCHENNE MUSCULAR DYSTROPHY

Duchenne muscular dystrophy (DMD) is an X-linked disorder that affects approximately 1 in 3500 boys (Brown and Lucy 1993). DMD is a disease which causes muscle wasting, because muscle is easily damaged by exercise. In the initial stages of DMD, damage is followed by muscle regeneration, but muscle is eventually replaced by fat and collagen, so muscle weakness becomes progressively more profound. Initially infants appear normal, but by the age of 3-5 years clinical symptoms are exhibited. Signs are a wide gait, falling often, and employing Gower's maneuver (Iannaccone and Nanjiani 2001). Most DMD-affected boys require the use of a wheelchair by 12 years old, reducing their quality of life. In addition to musculoskeletal deficits, some DMD patients have central nervous system disorders such as cerebral atrophy (Yoshioka *et al* 1980) and abnormal dendrite branching (Jagadha and Becker 1988), causing mild mental retardation and behavioural problems in 20-30% of DMD patients (Blake and Kroger 2000). This also contributes to a diminished quality of life. As the disease progresses, ventilatory assistance is required, and ultimately leads to premature death of DMD patients in their early twenties from cardiac dysfunction and respiratory failure. Notably, recent improvements in medical therapy and support in the Western world are pushing this interval to early thirties and beyond.

DMD is caused by a mutation to the DMD gene coding for dystrophin (Hoffman *et al* 1987a). The gene is located at the Xp21 locus (Roberts *et al* 1992). In DMD, the

mutation of this gene causes dystrophin to be missing, truncated or mutated, depending on the precise location, size, and type of mutation.

a) Dystrophin

Dystrophin is a very large protein (427 kD); the dystrophin gene is also enormous (3.0 MB). This makes it hard to detect mutations and predict phenotypic outcomes and abnormal dystrophin expression. Dystrophin is a rod-like protein located within the sarcolemmal dystrogycan complex (DGC) cytoskeleton of a muscle fiber. It bridges the inner cytoskeleton, the sarcolemma, and the extracellular matrix (ECM), acting like a "shock absorber", and is therefore essential for the integrity of the muscle membrane (Blake *et al* 2002,Durbeej *et al* 1998,Henry and Campbell 1999).

b) Dystroglycan complex (DGC)

The dystroglycan complex (DGC) is located within and just below the sarcolemma and is associated with laminin (in the ECM) (Ervasti and Campbell 1993,Hemler 1999), dystrophin (see *chapter1, section1a* above), and actin filaments (Ibraghimov-Beskrovnaya *et al* 1992);(Ervasti and Campbell 1991). The DGC is composed of many proteins in a wide range of molecular weights; these are either dystrophin-associated proteins (DAP) or dystrophin-associated glycoproteins (DAG). The DGC has been further separated into dystroglycan complex and sarcoglycan complexes. The dystroglycan complex is composed of an α-dystroglycan, binding to laminin (Ibraghimov-Beskrovnaya *et al* 1992), and a β-dystroglycan, binding to the C-terminal of dystrophin (Ohlendieck 1996). There are three sarcoglycan proteins: α-

saroglycan, β-sarcoglycan, and γ-sarcoglycan which form a smaller complex (Lim and Campbell 1998). The dystroglycan and sarcoglycan complexes are both absent in DMD (Love *et al* 1989). During muscle contraction, force from the sarcomeric actin filaments is transmitted to the actin cytoskeleton, through the DCG, across the sarcolemma, and to the ECM. In DMD, the loss of dystrophin causes this transmission of force to be disrupted, disrupting the membrane and causing fibers to degenerate.

2. NORMAL MUSCLE HISTOLOGY

Skeletal muscle is made up of bundles of long multi-nucleated fibers. Nuclei are peripherally located, distinguishing skeletal muscle from other muscle types. Muscle fibers are arranged in organized bundles surrounded by the epimysium (surrounds entire muscle). Septa from the epimysium run within the muscle surrounding each bundle of fibers (uniformly sized); this is called the perimysium. Further in still, each muscle fiber itself is surrounded by connective tissue, called the endomysium, and by the sarcolemma. Connective tissue in the muscle is important for integrating lateral forces from the contracting muscle fibers.

Skeletal muscle is classified as striated muscle; cross-striations delineate the contractile unit of the muscle, the sarcomere (2.2μm to 3.5μm in length). Contractile units are penetrated by T-tubules, which are responsible, along with the sarcoplasmic reticulum, for calcium regulation. For muscle contraction, a neurotransmitter (acetylcholine) is released by the nerve terminal into the synaptic cleft. Acetylcholine causes the muscle membrane to depolarize, which signals T-tubules joined in a triad with

the sarcoplasmic reticulum to signal calcium release from the sarcoplasmic reticulum. Calcium binds to troponin on actin filaments which moves tropomyosin from the myosin-binding site to allow interaction between the actin filament and myosin head (Alberts *et al* 2002). Myosin heads pull along the length of the actin filaments, shortening the sarcomere (sliding filament theory). Coordinated contraction of all fibers ensues and a pull force is exerted on the tendons. Lateral forces are also applied to the sarcolemma and ECM by the dystroglycan complex (see *chapter1, section1b* above). The contraction ends when calcium is rapidly pumped from the sarcoplasm into the sarcoplasmic reticulum by an ATP-dependent calcium pump (Ca^{2+}-ATPase). The muscle is now relaxed.

3. NORMAL MUSCLE REGENERATION

a) Myogenesis

Myogenesis is the process by which repair and development of muscles occurs by the proliferation and differentiation of muscle progenitor cells. These muscle progenitor cells are referred to as satellite cells.

b) Satellite cells

Satellite cells, named for their location, are found between the external lamina and the sarcolemma of muscle fibers (Mauro 1961). There is a visible differentiation between embryonic derived satellite cells and myoblasts (Bischoff and Heintz 1994). Adult skeletal muscle satellite cells are mononucleated cells that sit in a 15nm depression

between the basal lamina and the plasmalemma of the myofibers (Ishikawa 1966). In adult muscle these cells are quiescent (Schultz *et al* 1978) and only enter the cell cycle with a stimulus to form new muscle fibers or to repair damaged muscle fibers (Schultz and McCormick 1994).

c) Injury

Muscle injuries are caused by direct or indirect (stretch/contractile) trauma. Contractile injuries, the source of indirect injury to muscle, result from muscle stretching or contraction. They cause the muscle to tear, leading to an increase in intracellular calcium levels through calcium leakage. Excessive calcium stimulates muscle fiber degradation (Armstrong 1990). The myofibrils subsequently lose their structural architecture (Carpenter and Karpati 1979), and then more calcium enters, which activates proteases and cleaving proteins. Desmin in the sarcolemma is disrupted, causing disruptions in the Z disc and A band; sarcolemmal disruption stimulates an inflammatory process (Best and Hunter 2000).

d) Inflammation

Inflammation due to muscle fiber damage is a T-cell mediated process that is a key feature in muscle pathology. In muscle, inflammatory cells play a critical role in activation of myofibroblasts (the cell that produces connective-tissue collagen in response to injury, see *chapter1, section8c*) and satellite cells (which are muscle precursor cells, see *chapter1, section3b*). After damage the muscle releases chemotatic factors that attract polymophonuclear leukocytes (Orimo *et al* 1991); upon arrival at the site of injury, the

leukocytes produce cytokines and cause the release of reactive oxidase species that up-regulates inflammation (Best and Hunter 2000) and attracts macrophages to the site of damage (Nathan 1987). An initial population of phagocytotic macrophages causes membrane lysis and increase muscle injury (Nguyen and Tidball 2003a,Nguyen and Tidball 2003c,Wehling *et al* 2001), in order to destroy all the damaged muscle fibers (Krippendorf and Riley 1993,St Pierre and Tidball 1994,Tidball *et al* 1999). A second non-phagocytotic population of macrophages invades the muscle (McLennan 1993). These macrophages release interleukin-6 (IL6), thereby stimulating satellite cell proliferation (Allen *et al* 1995) while delaying differentiation (Merly *et al* 1999). Cross-talk between white blood cells and muscle fibers inhibits macrophages once repair is complete, so as not to cause further damage (Allen *et al* 1995,Nguyen and Tidball 2003b). Simultaneously, myofibroblasts (see *chapter1, section8c*) are recruited to the site of injury to regenerate connective tissue. They also appear to release cytokines that activate inflammatory responses (Walther *et al* 1988). To prevent undamaged fibers from becoming damaged, the areas of injury are sealed off by collections of blood-borne inflammatory cells that infiltrate the muscle (Hurme and Kalimo 1992,Robertson *et al* 1992).

e) Activation, proliferation, differentiation and fusion

Muscle regeneration starts when satellite cells are activated, or enter G0 of the cell cycle. Otherwise, satellite cells in normal adult muscle are in a quiescent state. When satellite cells are activated they get larger and migrate from their original fiber (Anderson and Pilipowicz 2002,Schultz *et al* 1985).

After an injury, contact inhibition of satellite cells is stopped and activation and proliferation ensue (Bischoff 1990). Several factors act in stimulating proliferation of satellite cells. Shortly after muscle injury, nitric oxide is released in rapid pulses as a result of nitric oxide synthase-1 (NOS-1) up-regulation. This release activates quiescent satellite cells (Anderson 2000). Hepatocyte growth factor (HGF) is critical in satellite cell stimulation; HGF is involved in most organ regeneration (Nakamura *et al* 1989). HGF binds to c-met, a receptor on quiescent satellite cells, and stimulates satellite cell proliferation (Tatsumi *et al* 1998). Insulin-like growth factor -1 (IGF-1) is upregulated in skeletal muscle after injury and activates and promotes satellite cell proliferation (Adams *et al* 1999,Vierck *et al* 2000). Different isoforms of IGF-1 are involved in regeneration: mechano growth factor (MGF) and IGF-1Ea. MGF expression peaks within one day after mechanical stress, suggesting it is an activator of satellite cell proliferation. While the peak in IGF-1Ea expression is not until several days after injury, it is thought to regulate late rather than earlier stages of proliferation (Hill *et al* 2003b).

Once activated, satellite cells enter the mitotic cycle and proliferate. Markers for satellite cell proliferation include expression of proliferating cell nuclear antigen (PCNA) (Johnson and Allen 1993) and Ki67, which can be detected during DNA synthesis, while markers for S-phase in the cell cycle are BrdU or tritiated-thymidine incorporation into new DNA. These are general markers of early proliferation/activation. An early marker specific for satellite cell activation is a method to detect HGF colocalization with c-met, and c-met expression (Anderson 2000,Tatsumi *et al* 1998). Within 3-6 hours muscle regulatory genes, myoD and myf5 are expressed (Grounds *et al* 1992). Two other markers of satellite cell activation are c-fos and c-jun, which are immediate early genes

and are expressed as soon as thirty minutes in tissue culture (Wozniak and Anderson 2007). Expression of IGF-1Ea in the muscle causes satellite cell proliferation to increase (McKoy *et al* 1999,Yang *et al* 1996).

Satellite cell daughter cells, called myoblasts, also express myf5 and myoD (Grounds *et al* 1992). Myoblasts continue to express myf5 and myoD through proliferation and also express myogenin, sometimes simultaneously with myf5 and myoD, other members of the muscle regulatory-gene family. Cells proliferate until protein expression shifts them to differentiate, or the cell environment limits proliferation signals (Sabourin and Rudnicki 2000).

Myoblasts begin to differentiate. Differentiation is the process by which myoblasts exit the cell cycle and fuse either with existing muscle fibers or form new muscle fibers with centrally located nuclei (Florini and Magri 1989). Myogenin upregulation and the down-regulation of pax7 expression, mark the onset of myogenic differentiation (Weintraub 1993,Yablonka-Reuveni and Rivera 1994) (see figure A in *Appendix A*).

4. PATHOPHYSIOLOGY OF DYSTROPHIN DEFICIENT MUSCLE

Duchenne first described the clinical features of dystrophy (now called Duchenne muscular dystrophy (DMD). Histologists then examined its histopathology, and later Mokri and Engel (Mokri and Engel 1975) further described DMD using electron microscopy. Lesions were observed in the sarcolemma, and they were noted close to

abnormal cytoplasm; this lead to the theory that DMD muscle fibers are fragile and leaky (Mokri and Engel 1975,Rowland 1976). We now know that this permeability is made worse by mechanical stress. This is seen in experiments using Evans Blue Dye (EBD) (Bradley and Fulthorpe 1978) in mdx mice (Matsuda *et al* 1995,McArdle *et al* 1994,Petrof *et al* 1993,Straub *et al* 1997). This marks exercise-induced damage to the sarcolemma, as the dye binds to albumin which leaks into fibers with a permeable sarcolemma. Another marker is plasma creatine kinase (CK) levels. When the sarcolemma is torn, CK leaks out of the muscle cells. With exercise, CK levels are higher in mdx mice compared with control mice (Carter *et al* 1995).

Calcium content is increased in DMD muscle (Bertorini *et al* 1982b,Bertorini *et al* 1984), as seen by high $[Ca^{+2}]_i$ (intracellular calcium concentration) in myofibers and myotubes, and higher levels of Ca^{+2} in the sarcoplasmic reticulum. This observation has led to the calcium-overload hypothesis that describes the ionic basis of many myopathic conditions (Wrogemann and Pena 1976).

Some data suggest that proteases, especially calpains, have a role in the pathophysiology of DMD (Spencer *et al* 1995,Spencer and Tidball 1996). However, details of that activity are not well understood.

5. MYOGENESIS IN DUCHENNE MUSCULAR DYSTROPHY

In DMD muscles there is constant cycling of degeneration and regeneration, but with age the repair phase becomes continually less successful. Muscles become progressively weaker and are replaced with fat and connective tissue. In DMD muscle,

regeneration is insufficient to compensate for this continuous breakdown. Interestingly, the decline in regenerative capacity is not from a morphological difference in satellite cells (Watkins and Cullen 1986) or any reduction in satellite cell numbers (Watkins and Cullen 1988). However, satellite cell lifespan may be shorter in DMD because the telomeres shorten from the repetitive regeneration. This limits the number of cell cycles that one cell can undergo (Decary *et al* 1996). In DMD muscle, nitric oxide synthase-1 (NOS-1) is downregulated, causing an inhibition of nitric oxide (NO) release, so satellite cells are over-activated (Anderson 2000). Early in DMD, satellite cells easily become activated. Activated satellite cells that migrate into the inter-fiber space are called myoblasts. Muscles hypertrophy, apparently as an early consequence of muscle weakness and this is partly enabled by satellite hyperactivity. Ongoing repair produces an increasing value for the central nucleation index, as repaired fiber segments have central nuclei. However, the central nucleation index can decrease as fibers are lost and replaced with fat and connective tissue during the later progression of dystrophy. As regeneration continues and myoblast divisions accumulate, there will be fewer satellite cells able to enter or complete the cell cycle due to telomere shortening; therefore muscles become progressively weaker and fibers are lost.

6. ANIMAL MODELS FOR DUCHENNE MUSCULAR DYSTROPHY

Cat, dog, and mouse models have all been used to study Duchenne muscular dystrophy (DMD). The hypertrophic feline muscular dystrophy (HFMD) cat and the canine X-linked muscular dystrophy (CXMD) dog/ golden retriever muscular dystrophy

(GRMD) dog, for which there are published descriptions of phenotype and histopathology, are available (Carpenter *et al* 1989,Cooper *et al* 1988a,Cooper *et al* 1988b,Winand *et al* 1994). The HFMD cat shows prominent hypertrophy without the other pathologies of dystrophin (Gaschen *et al* 1992); this indicates a feline-specific pathology, and therefore is an unsuitable model for DMD in most studies. Unlike the HFMD cat, the CXMD/GRMD dog is the closest model to DMD in phenotype and histopathology. The CXMD/GRMD dog muscles have a complete absence of dystrophin, and show early muscle degeneration. Dogs lose mobility and die by one year of age from respiratory failure. The CXMD/GRMD dog is the ideal model to study DMD, however, because of the cost and temporal issues associated with using the dog model, most researchers opt to use the mdx mouse model, at least until major pre-clinical trials are undertaken.

a) Mdx mouse

The mdx mouse model was discovered in 1984 in a colony of C57/BL10 mice. They were originally isolated because they had abnormally high levels of pyruvate kinase and abnormal muscle lesions. These mice have an X-linked dystrophy (Bulfield *et al* 1984) that was later found to be due to a mutation at the base pair in position 3185 in the dystrophin gene (Amalfitano and Chamberlain 1996,Sicinski *et al* 1989) affecting the identified gene to that affected in DMD (Hoffman *et al* 1987b).

Unlike DMD patients, the mdx mouse appears to have little “clinical” manifestation of dystrophy, although from regular handling we can establish that mice are weak. The mouse lives a relatively long life, although the lifespan is markedly

shorter than that of normal C57/BL10 mice; the mdx mouse rarely lives past two years of age (Pastoret and Sebille 1995a,Pastoret and Sebille 1995b), while wild-type mice live two and a half to three years (Lynch *et al* 2001).

The muscle phenotype of mdx mice is similar to DMD, except for the severity; the difference in severity is especially notable early in life. Mdx mouse muscles display a higher central nucleation index than DMD muscle (Karpati *et al* 1988), and show less fibrosis and less severe muscle degeneration in limb muscles. However, histopathologically there are many similarities between dystrophin-deficient myopathies in mdx mice and DMD patients. As in DMD, muscles in mdx mice undergo damage repair cycles, have increasing central nucleation with age, and show increasingly wider ranges of fiber size (Carnwath and Shotton 1987,Coulton *et al* 1988b,Torres and Duchen 1987). The damage is more extensive in DMD and has greater functional consequences. Fibrosis and adipose tissue deposits are less extensive in mdx muscle than in DMD muscle. Similar to DMD, mdx mice undergo early degeneration/regeneration, which increases progressively. In DMD, however, there is more muscle to regenerate and the disease is more extensive, so the regeneration capacity is reached earlier than in mdx mice. At this stage the fibrosis and fat infere more with regeneration in DMD tissue. Therefore, both mdx muscle and DMD muscle show disease progression, although at different rates.

Muscle fibers in mdx mice have a greater variation in cross-sectional area compared with the same muscles in C57/BL10 (wild-type) mice due to the appearance of large hypertrophic and small regenerating fibers in the same muscle. There is also an increase in fibrosis with age (Anderson *et al* 1987,Carnwath and Shotton 1987). Mdx

muscles have been shown to generate less twitch and tetanic force per cross-sectional area than muscles in wild-type mice (Anderson *et al* 1988,Coulton *et al* 1988a,Dangain and Vrbova 1984). Later researchers found that the mdx mouse diaphragm muscle was more similar to the severe muscle phenotype in DMD patients than mdx mouse limb muscles (Stedman *et al* 1991). The mdx diaphragm also exhibits a higher level of fibrosis than C57/BL10 mice, and fibrosis is also greater in mdx diaphragm than mdx limb muscles. The muscle of the diaphragm becomes dysfunctional prior to an increase in collagen content (Coirault *et al* 2003).

The mdx model is said to have two limitations for the study of DMD; the first is its delayed progression compared to DMD, and the second is its milder tissue pathology and functional phenotype.

b) Mdx muscle and age

As mdx mice age, the muscles become more similar to those in DMD. Mouse muscles exhibit declining regeneration, decreasing overall weight and muscle weight, and large variations in fiber size, with many atrophic and split fibers (Pastoret and Sebille 1995a,Pastoret and Sebille 1995b). There are also large increases in the amount of fibrosis in skeletal muscle (Pastoret and Sebille 1995a) as the damaged myofibers are replaced with ECM and adipose tissue as part of tissue repair processes. In old mice, the progress of limb muscle weakness is quite advanced, and is accompanied by dystrophic changes in cardiac and respiratory muscles (Lefaucheur *et al* 1995). Kyphosis and spinal deformations progress with age in the mdx mouse (Laws and Hoey 2004). Functionally, the diaphragm, and less so the skeletal muscles are able to generate lower force, and

contractions are slower. As the mice age, they show progressive signs of exhaustion from exercise. After being subjected to involuntary exercise, older mdx mice were fatigued and prostrated for several minutes, and some died shortly after exercise, while controls showed no signs of exhaustion (Vilquin *et al* 1998).

As mdx mice age, their muscles show changes in protein expression. By three months of age proteins involved in energy metabolism, growth and differentiation, serine protease inhibition, calcium homeostasis, and cytoskeleton organization are mostly overexpressed, with the exception of adenylate kinase 1, which is underexpressed as compared to control mice (Ge *et al* 2004).

7. COLLAGEN

a) General information

Collagen is a ubiquitous, structural, filamentous protein that makes up part of the extracellular matrix (ECM) in connective tissue and parenchymal tissue. It is the most abundant protein in the body and more than two dozen types have been described (Brown and Timpl 1995,Kadler 1995,Myllyharju and Kivirikko 2001,Ricard-Blum and Ruggiero 2005). Members of the collagen family all contain proline-rich domains with repetitions of tripeptides Gly-X-Y. In the last few years, collagen functions have been shown to vary widely and are not limited to structural support in tissues.

b) Structure

The word "collagen" generally refers to a large protein made up of three protein chains coiled into a triple helix. The distinguishing feature of collagen is its chemical structure: a right-handed triple helix composed of three α-chains (Kuhn 1995,Piez and Carrillo 1964). The three α-chains, either homotrimers or heterotrimers, are coiled around a central axis to form the triple helix (Fraser *et al* 1983), as originally proposed by Ramachandran and Kartha in 1954. Glycine, the smallest amino acid, is found in every third position of the collagen protein chain domain (Gly-X-Y). Because glycine is small in size, it faces into the helix, while the other larger amino acids point outwards; this enables tight packing of the collagen α-chains and helices. Assembly of the helix takes place in the endoplasmic reticulum, and at this stage the molecule is referred to as a procollagen.

Collagen helices are resistant to most proteases (Bruckner and Prockop 1981) and can only be degraded by collagenase, which is a matrix metalloproteinase (MMP) (Goldberg *et al* 1988). MMP cleavage is thought to be involved in tissue remodelling, inflammation, and bone and cartilage remodelling (Varghese 2006,Yu *et al* 1997).

c) Collagen classification

Based on the structure and molecular organization of the α-chains, collagen can be grouped into one of several classes. These classes are: fibril-forming collagen (I, II, III, V, XI), basement membrane collagen (IV), microfibrillar collagen (VI), anchoring fibrils (VII), hexagonal network-forming collagen (VIII, X), fibril-associated collagen with interrupted triple helices (FACIT collagens) (IX, XII, XIV, XIX, XX, XXI),

transmembrane collagen (XIII, XVII), and multiplexins (XV, XVI, XVIII) (Gelse *et al* 2003).

d) Fibril-forming collagens

Fibril-forming collagens make up about 90% of the collagen in the body. They are divided into different sub-classes by the structure that they form in the body.

Procollagens are secreted into the ECM and converted to collagens by terminal propeptide cleavage actions by procollagen N-proteinase and procollagen C-proteinase (Hulmes *et al* 1995,Kadler *et al* 1996). The cleaved collagens assemble into supramolecular structures called collagen fibrils by spontaneous fibrillogenesis (Kuivaniemi *et al* 1991). During this process, the molecular structures are stabilized by relatively low-energy, polar, hydrophobic, and non-covalent bonds, therefore the collagen fibrils are weak and easily altered by changes in temperature, molecular interactions, and the ionic strength of their environment. At a later stage, strong covalent cross-linkages stabilize the collagen fibrillar structure (Seyedin and Rosen 1990). Lysyl oxidase initiates this cross-linking by oxidative deamination of some lysine residues in the telopeptides which are the cleaved ends of fibrils (Kagan and Trackman 1991). Lysine residues in telopeptides in adjacent collagen molecules react with each other forming Schiff-base cross-links (see figure B in the *Appendix A*).

Once collagen fibrils are formed they aggregate into large bundles called collagen fibers.

e) Collagen I

Collagen I, as classified previously, is a fibril-forming collagen. It is the most abundant collagen, and forms the bulk of the collagen found in most tissues with the exception of only a few tissues (hyaline cartilage, brain, and vitreous humor). Collagen I is a heterotrimer of two α1(I)-chains and one α2(I)-chain. Collagen I is often formed into a composite with collagen III (Von der 1981). Collagen I in musculoskeletal soft tissue allows a considerable amount of tensile and torsional strength.

f) Collagen III

Collagen III, another fibril-forming collagen, is a homodimer of three α1(III)-chains. It is found in most collagen I-containing tissues with the exception of bone (Rossert *et al* 1996). As stated above, collagen III fibrils are often mixed with collagen I fibrils in muscle and other tissues. It is important to note that there is a need for collagen in muscle tissue, as it contributes to the physical properties of the tissue. However, excessive collagen build up in muscle and other tissues affects tissue function and can be sign of pathology.

8. FIBROSIS

Fibrosis is defined as an increased production of collagen in the ECM of a tissue. In DMD, fibrosis is demonstrated by large increases in type I and type III collagens in the muscle (Finsterer *et al* 2006). Fibrosis is correlated with muscle damage (Zhao *et al* 2003) and thought to play a crucial role in the mechanisms that lead to death.

a) Fibrosis in DMD

The loss of muscle function in DMD is closely associated with fibrosis. Fibrosis builds up as the muscle tissue is damaged, and accumulates via inflammatory and regenerative processes. Fibrosis and loss of muscle function together lead to respiratory and heart failure (due to DMD effects on respiratory and cardiac muscles) as well as to the decline in limb muscle function and contractile strength. Fibrosis is characterized by an increase in connective tissue in the ECM, specifically collagen (see *chapter1, section7*). Increases in both collagens I and III in skeletal muscle have been observed in DMD (Duance *et al* 1980,Hantai *et al* 1985). Cardiomyopathy in DMD is especially marked by large amounts of fibrosis of the myocardium, especially in the left ventricle. This is most likely due to increased myofibroblast activity. Fibroblast cultures from DMD patients secrete large levels of collagen, much higher than those from healthy individuals (Ionasescu *et al* 1977).

b) Fibrosis in mdx mouse muscle

Mdx mice (described above) also have fibrotic muscles and eventually die from fibrosis and loss of contractile function in the heart and respiratory muscles, similar to DMD. There is an increase in collagen I and III observed in mdx mouse muscles and also in non-muscle tissue, especially as the disease progresses, and more so than in aging normal (C57/BL10) mice (Goldspink *et al* 1994). This is most evident in the heart and diaphragm (Quinlan *et al* 2004), although still significant in limb muscles.

c) Myofibroblasts

Myofibroblasts were first identified by electron microscopy in granulation tissue of wound healing (Gabbiani *et al* 1971). Gabbiani and colleagues observed that myofibroblasts were modified fibroblasts that exhibited features of smooth muscle cells, such as microfilaments and gap junctions. Later, contractile structures (stress fibers) were identified, in addition to expression of contractile proteins including α-smooth muscle actin (α-SMA) (Darby *et al* 1990).

The contractile units of myofibroblasts contain bundles of actin with non-muscle myosin (Dugina *et al* 2001,Serini and Gabbiani 1999,Singer *et al* 1984). Intracellular actin fibers link to extracellular fibronectin via transmembrane integrins (Dugina *et al* 2001,Singer *et al* 1984), and thereby provide a mechano-transduction system that transmits forces generated by the stress fibers to the ECM (Burridge and Chrzanowska-Wodnicka 1996). In addition, extracellular mechanical signals can become intracellular signals by reversal of the direction of force transmission (Burridge and Chrzanowska-Wodnicka 1996).

Unlike connective tissue fibroblasts, myofibroblasts have gap junctions between adjoining cells. It has been suggested that gap junctions allow myofibroblasts to form muticellular contractile units (Gabbiani *et al* 1978).

Upon injury, signals from inflammatory cells cause fibroblasts to migrate to the granular tissue (see *chapter1, section3c*). Fibroblasts then undergo morphological changes and stress fibers appear. However, these cells do not express α-SMA; they are poorly differentiated myofibroblasts called proto-myofibroblasts. Proto-myofibroblasts differentiate into myofibroblasts by the cellular fibronectin splice variant ED-A (Serini *et*

al 1998), and express α-SMA. Myofibroblasts are responsible for matrix reorganization as a result of changes in contractile forces (Grinnell 1994,Harris 1988), thereby remodelling tissue and matrix and promoting wound closure. Once the wound is healed, myofibroblasts become apoptotic and are removed by phagocytosis. However, if myofibroblasts do not undergo apoptosis and continue to remodel the ECM, the connective tissue becomes increasingly strong. In muscle, this is demonstrated as contractures which shorten the whole muscle and tighten it between attachments.

d) Transforming growth factor β (TGFβ)

Transforming growth factor β (TGFβ) is a member of a family of polypeptide growth factors. Members include: activins and inhibins, bone morphogenetic proteins, growth and differentiation factors, Mullerian inhibitory substance, glial cell line-derived neurotropic factor, and TGFβ (Kingsley 1994). All these proteins fall within the TGFβ superfamily. TGFβ family members are dimeric molecules comprised of two monomers, a β-strand and an α-helix.

TGFβ is known to play a role in fibrosis in DMD. It is highly expressed in DMD muscle (Bernasconi *et al* 1995,Ishitobi *et al* 2000,Murakami *et al* 1999). TGFβ is also a major player in connective tissue cell proliferation (Bernasconi *et al* 1999). It contributes to both the influx of inflammatory cells as well as the activation of fibroblasts to become myofibroblasts.

Recent studies have examined the role of cytokines in fibrosis. Cytokines play an important role in TGFβ signalling. One cytokine that has been shown to play an important role is interleukin-6 (IL-6). Recently, cross-talk between IL-6 and TGFβ was

identified in epithelial cells (Walia *et al* 2003). Zhang *et al.* (Zhang *et al* 2005) examined TGFβ and IL-6 cross-talk in the kidney. They found that IL-6 enhanced TGFβ-receptor internalization and thereby enhanced TGFβ signalling. IL-13 has also been examined as an inducer of TGFβ. Fichtner-Feigl *et al.* (Fichtner-Feigl *et al* 2006) identified that interleukin-13 (IL-13) induces TGFβ expression in macrophages. This is a two-stage process involving induction of IL-13Rα_2 (formerly thought to function as a decoy receptor) by IL-13 and tumor necrosis factor α (TNFα), and IL-13 signaling through IL-13Rα_2 activation of a TGFβ promoter.

TGFβ is secreted as a latent precursor molecule that must be activated to bind to receptors and activate signal transduction. The receptor is composed of two homodimers, one each of type I and type II serine/threonine kinase receptors (Massague 1998). Receptors sit in lipid-raft and non-raft domains in a membrane (Di Guglielmo *et al* 2003). Alterations to membrane compartmentalization thereby regulate TGFβ signalling (Di Guglielmo *et al* 2003,Ito *et al* 2004). TGFβ binds to the type II receptor, which signals and recruits a type I receptor. A cascade involving Smads ensues.

e) Smad signalling

Smads are signal transducers, named for signal intermediates identified in the *drosophila* (Mad) and the c*aenorhabditis elegans* (Sma). Smads are grouped into three families, receptor-activated Smads (R-Smads), common mediator Smads (Co-Smads), and inhibitory Smads (I-Smads).

The activation of the type I TGFβ receptor propagates a signal in the cell which phosphorylates the R-Smads, Smad2 and Smad3 (Eppert *et al* 1996,Nakao *et al*

1997c,Nakao *et al* 1997b,Yingling *et al* 1996). Smad2 and Smad3 are localized to the membrane by Smad anchor receptor activation (SARA) (Tsukazaki *et al* 1998) and Hgs (Miura *et al* 2000) prior to type I receptor activation. Once phosphorylated, an R-Smad binds with a Co-Smad, Smad4 (Hahn *et al* 1996). Smad4, like the R-Smads, is also shuttled to the membrane; this is done by binding with TGFβI-associated protein-1 (TRAP1). TRAP1 is bound to TGFβ receptors at rest, but upon TGFβ receptor activation, TRAP1 is released and is free to bind to Smad4. Once Smad4 interactes with the R-Smads, the complex can enter the nucleus (Hoodless *et al* 1996,Liu *et al* 1996a), where Smads bind to target DNA sequences via their MH1 domains and regulate transcriptional events. Smads recruit Smurf (Zhang *et al* 2001,Zhu *et al* 1999a,Zhu *et al* 1999b) and APC to degrade SnoN (Stroschein *et al* 2001,Wan *et al* 2001), and therefore degrade Smads in the nucleus. There is some debate on whether this degradation is Smurf-mediated or not (Bonni *et al* 2001,Kavsak *et al* 2000).

The I-Smad, Smad7, inhibits TGFβ signalling. Smad7 is translocated from the nucleus to the cytoplasm, the opposite direction to the R-Smad pathway, in response to relevant signalling (Itoh *et al* 1998,Nakao *et al* 1997a). Smad7 binds to the TGFβI receptor to inhibit further TGFβ signal transduction. These receptor-bound I-Smads act as adaptors for Smurf ubiquitin ligases, and can catalyze the degradation of the R-Smad complex.

The R-Smad, Smad3, has been identified as the regulator of collagen production (Zhang *et al* 2000). Therefore, Smad3 is the critical R-Smad involved in the signal cascade above for the production of collagen in fibrosis.

f) Matrix metalloproteinase (MMP) and Tissue inhibitor of metalloproteinase (TIMP)

TGFβ and Smad3 not only enhance collagen synthesis in the ECM, they also inhibit collagen degradation. This is through the down-regulation of tissue inhibitor of metalloproteinases (TIMPs) (Verrecchia *et al* 2001) and the upregulation of matrix metalloproteinases (MMPs) (Yuan and Varga 2001). MMPs are part of a group of zinc metalloproteinases involved in enzyme degradation of ECM. MMPs share similar mode of activation and mode of action to TIMPs (Edwards *et al* 1996). The balance between TIMPs and MMPs determines the extent of collagen degradation. In skeletal muscle injuries, MMPs can act by proteolytically releasing growth factors from the ECM during regeneration. These growth factors stimulate myogenic cells (Allen *et al* 1995,Bischoff 1997,Clegg *et al* 1987,Tatsumi *et al* 1998). Many researchers are exploring MMP inhibition for cancer treatment; MMPs and TIMPs are also potential targets in developing new treatments for fibrotic diseases and DMD.

9. MYOSTATIN

Myostatin, also known as growth/differentiation factor 8 (GDF-8), is a member of the transforming growth factor β (TGFβ) family, and was originally discovered by McPherron *et al.* (McPherron *et al* 1997). They developed a GDF-8 null mouse and found it had increased mass; when carcass weights were examined, GDF-8 null mice had an increased muscle mass, contributing to an overall larger size, with no change to adipose tissue. Upon histological examination, there was muscle hypertrophy noted. On the basis of this phenotype, GDF-8 was renamed myostatin. Natural myostatin gene

mutations in cattle (Belgium-Blue and Piedmontese) demonstrate a similar "double-muscled" phenotype (Grobet *et al* 1997,Kambadur *et al* 1997). Nishi *et al.* (Nishi *et al* 2002) created a myostatin missense mutant mouse to further investigate histology of the McPherron mouse (McPherron *et al* 1997). These missense mutant mice show muscles with an increase in fiber number (fiber hyperplasia), but without hypertrophy, and authors reported that this phenotype resulted from expression of a dominant-negative form of myostatin compared to the myostatin null mutant.

Myostatin mRNA is expressed initially in somites that give rise to skeletal muscle (McPherron *et al* 1997); later in development it is expressed in muscle; in adults it is expressed in skeletal muscle, heart (Sharma *et al* 1999), and adipose tissue (Lin *et al* 2002,McPherron and Lee 2002).

A mature myostatin dimer and two pro-peptides, cleaved off the immature myostatin C-terminals, produce a non-covalently linked complex; in this form, myostatin cannot bind with its receptor (Hill *et al* 2002,Hill *et al* 2003a). When the complex disassociates, myostatin binds to an ActRIIB receptor (Thies *et al* 2001), which triggers a signal cascade. Myostatin follows a similar signal transduction pathway to the other TGFβ members (see *chapter1, section8d*), and initiates Smad-protein activation. Zhu *et al.* (Zhu *et al* 2004) have shown that Smad2, Smad3 and Smad4 are responsible for myostatin signaling, while Smad7 reduces the signalling via the myostatin signal transduction pathway. Smad7 expression itself is stimulated by myostatin though the interaction of Smad2, Smad3, Smad4 and the Smad binding element. This feature suggests that Smad7 regulates myostatin signal transduction by negative feedback.

Myostatin inhibits myoblast differentiation by repressing myoD, myf5 and myogenin levels via the Smad3 pathway (Langley *et al* 2002). Myostatin has also been shown to inhibit cell proliferation and myoblast apoptosis (Joulia *et al* 2003).

10. TREATMENT FOR DUCHENNE MUSCULAR DYSTROPHY

Many treatments for Duchenne muscular dystrophy (DMD) are under investigation, with major headway in the last few years indicating a treatment is not too distant. There have been three major approaches to the treatment of DMD; pharmacological, cell therapy, and gene therapy. Animal and human studies will be discussed together except where more detail is required.

a) Pharmacological

Pharmacological studies use drugs/molecules to try to improve muscle function and alleviate the severity of the disease phenotype. In the case of DMD, pharmacological treatments have aimed to decrease inflammation and fibrosis, improve calcium homeostasis, upregulate utrophin, increase muscle progenitor cell proliferation, and promote muscle regeneration. Most pharmacological therapies are designed to tackle only the secondary problems associated with DMD, which is a disadvantage since the disease continues to progress and treatment must be repetitive. However, there are many advantages to pharmacological treatments, as they are easy to administer, are more likely

to be affordable than cell or gene therapies for patients, and they avoid the immunological and some systemic toxicity issues involved with gene and cell therapies.

a1. Corticosteroids and anti-inflammatory agents

Corticosteroids are one of the oldest therapies used to alleviate the symptoms and progression of DMD (Barthelmai 1965,Drachman *et al* 1974). The most studied and commonly used corticosteroids for DMD are prednisone and its derivative prednisolone. Prednisolone has been shown to improve muscle force and function as well as delay the progress of DMD (Backman and Henriksson 1995). Its long-term benefits are currently being studied by Keeling and colleagues. Prednisone and prednisolone have been shown to cause loss of bone mass (Khan 1993), latent growth and delayed maturation, and suppression of the immune system. Similar results were found with prednisone and prednisolone in mdx mice (Fisher *et al* 2005,Keeling *et al* 2007). With the concern about the adverse effects of prednisone and prednisolone, scientists have explored the use of deflazacort, an oxazoline derivative of prenisolone. In pre-clinical trials on mdx mice, deflazacort decreased fibrosis and inflammation, increased fiber size (Anderson *et al* 1996), increased expression of laminin, a stabilizer of the sarcolemma (Anderson *et al* 2000), and improved myogenic repair in limb muscles and diaphragm (Anderson and Vargas 2003,McIntosh *et al* 1998). Further study of deflazacort in mdx mice showed it prevented a significant degree of the progression of cardiomyopathy (Skrabek and Anderson 2001) and improved muscular strength and endurance (Archer *et al* 2006). As well, deflazacort was partly protective against exercise-induced fiber damage (Archer *et al* 2006). While there are concerns about the effects of long-term steroid treatment (dose-

dependent side effects), steroids are the gold standard treatment today for DMD (Biggar *et al* 2001).

Inflammation, although only a part of DMD, has been investigated extensively for pharmacological therapies. As seen above, corticosteroids have been shown to reduce inflammation and restrict it to one fiber to three fibers with a membrane injury. The inflammatory process that removes the damaged regions makes the damaged area worse, *i.e.* it extends the region of damage to ten to twelve fibers. Therefore anti-inflammatory drugs can have a large positive effect without changing the occurrence of the primary injury. Corticosteroids also decrease fibrosis that results from primary tissue damage and that which occurs from secondary inflammation. The use of an anti-inflammatory treatment, including antibody-mediated depletion of circulating $CD4^+$ and $CD8^+$ T cells resulted in decreased fibrosis in mdx muscles (Spencer *et al* 2001). Treatment with some mast-cell stabilizers, normally used in asthma, has also been accompanied by increased muscle strength in mdx mice (Granchelli *et al* 1996).

a2. Calcium homeostasis

DMD patients accumulate large amounts of intracellular calcium in skeletal muscle (Bodensteiner and Engel 1978). Extraocular muscles, which are unaffected by DMD, are able to maintain calcium homeostasis (Khurana *et al* 1995); since this differs from the other muscles in DMD, the observation was explored further by researchers. It is not yet determined whether a loss of calcium homeostasis initiates fiber dystrophy or if calcium dysregulation is a result of fiber membrane tearing. According to the calcium-overload theory, calcium rises after an insult to the muscle fiber (membrane permeability)

(Wrogemann and Pena 1976). However, dystrophin is described by some (Franco, Jr. and Lansman 1990) as being involved in the calcium-leakage, which causes membrane damage. In either event, pharmacologists began to examine the use of calcium-channel blockers, such as nifedipine and diltiazem to prevent disease progression by fiber injury. Neither was proven to be effective in this regard. In pilot studies by Bertorini *et al.* (Bertorini *et al* 1982a,Bertorini *et al* 1988), treatment with calcium-release inhibitiors, diltiazem and dantrolene, resulted in a reduction in calcium levels and CK levels as well as alleviating the deterioration in manually tested muscle strength, but no further studies have explored this avenue of treatment. Researchers have also explored effects of calcium dysregulation using calpastatin-overexpressing mdx mutant mice (Spencer and Mellgren 2002) and by treating mdx mice with leupeptin, a calpain inhibitor (Badalamente and Stracher 2000). Both these studies reported some success in regulating calcium homeostasis and partly normalized the dystrophic phenotype. The problem that remains with all the above calcium-homeostatic treatments is that their action is not specific to muscle or to the dysfunctional state, and could therefore disrupt corporal cell metabolism.

a3. Muscle strength

Deflazacort and prednisone have been shown to improve strength in mdx mice and DMD patients, while anabolic steroids have not, despite their popular use for strength enhancement among athletes. This may be due to lack of ability to do exercise training in DMD patients. However, non-steroidal treatment with β_2-adrenoceptor agonists

increases protein production, stimulates satellite cell proliferation, and improves muscle strength in both animal models and humans with muscular dystrophy (Zeman *et al* 1994).

Creatine is another potential treatment that aims to improve the strength of muscles in DMD patients. It is also commonly used among athletes to improve performance and has been shown in some reports to improve muscle strength in many neuromuscular diseases (Walther *et al* 2000).

In mdx mouse studies, myostatin was targeted for inhibition with the aim of improving strength. When blocking-antibodies for myostatin were injected, muscle mass and strength increased and muscle degeneration decreased (Bogdanovich *et al* 2002,Wagner *et al* 2002). Amthor *et al.* (Amthor *et al* 2004) were able to block myostatin with follistatin, showing similar improvements. Myostatin antagonists therefore, have huge pharmacological potential for treating DMD, although the effect of large contractile forces on the susceptibility to exercise-related injury in dystrophin-deficient muscle fibers is not well reported, and is a deficiency in the literature.

b) Gene and cell therapy

Successful gene therapies have been very challenging to achieve because of the large size of the dystrophin gene (3.0 MB). Only a small part of the dystrophin gene will fit in a viral vector or plasmid. Researchers, however, have not given up and are working on achieving high-efficiency viral gene transfer (Cerletti *et al* 2003,Rossert *et al* 1996) and successful treatment with non-viral gene transfer treatment success (Gollins *et al* 2003,Thioudellet *et al* 2002). There is similar success in some reports with the use of micro- and mini-dystrophin gene constructs for insertion in vectors (Scott *et al* 2002).

Other studies have examined the use of antisense strategies to produce functional proteins (Bartlett *et al* 2000,Lu *et al* 2003), destroying dysfunctional genes, so new constructs can be inserted.

Myoblast transfer for cell transplantation has also been explored for a number of years, and not without controversy (Belles-Isles *et al* 1993,Law *et al* 1997a,Law *et al* 1997b,Morgan 1990). However, this treatment cannot be obtained at this time as a long-term treatment. Sampaolesi *et al.* (2006) have recently made a large break-through in cell therapy for DMD. Using the dog model, they were able to transplant donor mesoangioblasts isolated from muscle vessels. Mesangioblasts act as muscle precursors (Sampaolesi *et al* 2006). After a long term treatment in older dogs and accompanying immunosupression, there was extensive reconstitution of fibers that expressed dystrophin. There was also significantly improved function *in vivo*, shown by smooth walking, mobility, and greater contractile force produced by the muscles. This treatment modality is extremely promising for future cell therapies in DMD, since the muscle architecture was vastly improved and the fibrosis present at the start of treatment was resolved. Exactly how such resolution occurs is open to further investigation.

11. TREATMENT FOR FIBROSIS

Fibrosis is a wide-spread condition that affects people suffering from many different disorders. Treatment for fibrosis, therefore, has been extensively explored, mostly in relation to pulmonary and liver fibrosis.

a) Pharmacological treatment

Corticosteroids are the most common antifibrotic modality used today and several other non-steroidal anti-inflammatory agents have also been studied (see corticosteroids and anti-inflammatories).

Stein (Stein 1993) observed that an anti-parasitic drug, suramin, could bind to the TGFβ-receptor and inhibit TGFβ actions by competitive binding. Suramin can decrease fibroblast proliferation and fibrotic-protein expression in fibroblast cultures. It has also been shown to inhibit fibrosis in mice after a muscle injury (Chan *et al* 2003). The drug, suramin must be administered intravenously and in combination with low doses of prednisone, making this an unappealing treatment. Suramin has also had variable effects on fibrosis outside muscle tissue, with little to no benefit reported for use in lung fibrosis (Lossos *et al* 2000).

Treatment with pirfenidone, an antifibrotic agent, has induced improvement in some patients suffering from fibrotic conditions in the lung. Pirfenidone also ameliorates bleomycin-induced pulmonary fibrosis (Tian *et al* 2006), and decreases fibroblast proliferation and collagen synthesis *in vitro* (Di Sario *et al* 2004).

Relaxin, a protein secreted from the testes and corpus luteum in pregnancy, inhibits TGFβ-induced collagen and fibronectin production by human lung fibroblasts. It also increases the expression of MMPs and decreases the production of TIMPs (Unemori *et al* 1996). However, application of this knowledge as a treatment would need to avoid systemic effects of treatment by targeting relaxin to a particular process or tissue.

Eicosanoids, such as the prostaglandin PGE2, which is a potent inhibitor of fibroblast proliferation and matrix production, may also ameliorate fibrosis. An oral

analogue of PGE2 is a potential candidate for therapeutic intervention, but has not been studied yet in any models of fibrosis.

Interferon β (IFNβ) is widely used for the treatment of chronic hepatitis C and multiple sclerosis and has anti-inflammatory properties. In mice, IFNβ inhibits irradiation-induced pulmonary fibrosis (Ziesche and Block 2000). Interferon α (INFα) has been shown to decrease fibroblast proliferation in human tenon capsule (Gillies *et al* 1993), and might have a similar effect in other fibrotic models.

B-aminoproprionitrile, a blocker for collagen cross-linking, has been shown to be beneficial in many mouse studies of schistoma treatment (Giboda *et al* 1994). B-aminoproprionitrile works by inhibiting lysyl oxidase and D-penicillamine. However, because of a tendency to cause extreme joint laxity over long-term use, this is an undesirable treatment for fibrosis in DMD or progressive neuromuscular disease.

a1. Cellular and genetic treatments for fibrosis

An alternative genetic treatment using antisense technology was used to inhibit collagen I synthesis in dystrophic mice. However, the results were extremely variable, and did not show significant promise in dystrophy (Khillan *et al* 1994,Laptev *et al* 1994). Targeting post-transcriptional enzymes is another method by which collagen production and accumulation could be reduced (Prockop and Kivirikko 1995).

The major disadvantage with all of the above treatments is their lack of specificity in muscle or on abnormal fibrosis. Therefore, they could inhibit synthesis and organization of the normal, non-pathological collagens, and have significant adverse and toxic effects.

12. HALOFUGINONE HYDROBROMIDE

a) Origin and structure

Halofuginone hydrobromide (Halo) is a recently discovered antifibrosis drug. The drug, an analogue of an alkaloid isolated from the plant *dichroa febrifuga*, was originally used as a coccidiostat in poultry, as it arrested the development of coccidial infections. As a side effect to treatment, it was observed that the poultry were developing thin skin; this stimulated scientists to think about the properties of Halo as an inhibitor of collagen synthesis. The structure of Halo is 7-bromo-6chloro-3-[3-(3-hydroxy-2-piperidinyl)-2-oxopropyl]-4(3H)-quinazolinone.

The lethal dose (LD50) of Halo in a mouse is 4.4mg/kg - 4.9mg/kg. Interestingly studies in mice using treatment doses below the LD50 show no adverse effects.

b) Specificity

Experiments that have examined the effects of Halo treatment on intimal hyperplasia in rabbit smooth muscle (Choi *et al* 1995) and Halo treatment of avian skin fibroblasts (Granot *et al* 1991) indicated that only collagen I expression is inhibited, while collagens II and III were unaffected by Halo treatment. In these models, only collagen I accumulation was pathological. This suggested that the mode of action of Halo is very specific and tailored to affect the "pathological" collagens. In further studies, halo was shown to prevent increased collagen synthesis in several animal models in which excessive collagen is a key part of the disease process. These animal models

include: tight-skin (Tsk) mice, murine chronic graft versus host disease (cGvHD), murine scleroderma (Levi-Schaffer *et al* 1996,Pines *et al* 2001,Pines *et al* 2003), pulmonary fibrosis in the rat (Nagler *et al* 1996), liver fibrosis in the rat (Bruck *et al* 2001,Gnainsky *et al* 2004), urethral stricture (Nagler *et al* 2000), and adhesion in rat abdomen and uterine horn (Nagler *et al* 1998,Nagler *et al* 1999).

c) Prevention and resolution

Halo inhibits formation of fibrosis in some tissues, but more interestingly, Halo has also been demonstrated to resolve already-established (pre-existing) fibrosis in other tissues. The ability to resolve fibrosis makes Halo unique among other preventative antifibrosis drugs. In most models, Halo was used as a preventative agent, in which it was administered either with or before a stimulus that induced fibrosis. However, a few studies have examined its potential to treat established fibrosis. In a liver fibrosis model in rats, Halo induced almost full resolution of fibrosis as seen by a decrease to baseline levels of collagen content and collagen I gene expression in the liver. Halo also inhibited proliferation of the fibroblasts in the fibrotic liver (Bruck *et al* 2001). Similarly in the Tsk mouse, with a topical application of Halo, skin fibroblast proliferation decreased and there was a significant reduction in collagen I gene expression (Pines *et al* 2001). Therefore, fibrosis was resolved in animal models of liver fibrosis and tight skin. There are no reports of Halo treatment for muscle fibrosis conditions.

d) Mode of action

Halo was originally thought to inhibit collagen I gene expression by DNA methylation (Rhodes *et al* 1994,Thompson *et al* 1991). After examining [^{3}H]-proline incorporation into collagen and non-collagen proteins, DNA methylation was not determined to be part of the mode of action of Halo (Halevy *et al* 1996). Another thought was that Halo affects the collagen I gene directly, for example when new protein synthesis is needed. While Halo does not act by affecting the collagen promoter (Pines and Nagler 1998), Halevy *et al.* (1996) demonstrated that the stimulation of new protein synthesis is required for Halo to inhibit collagen I production.

TGFβ has been shown to play a major role in fibrosis, causing an increased production of extracellular matrix (ECM) proteins and inhibiting matrix-degrading proteins. Therefore, hypotheses about the mode of action of Halo shifted toward the idea that Halo might affect TGFβ. McGaha *et al.* (2002a,2002b) evaluated the effect of Halo on TGFβ-induced upregulation of collagen synthesis. They found that when Halo was administered to fibroblasts *in vitro* and this was followed by TGFβ stimulation, that the induction of collagen was three-fold less than without Halo. Further effects of Halo on the expression and activation of TGFβ-receptors were examined, and showed that Halo had no effect on these two components of TGFβ signalling pathway. McGaha *et al.* (2002b) then contemplated intracellular events of TGFβ signaling (*i.e.*, Smads). They found Halo inhibited Smad3 phosphorylation and affected Smad3 activation, without affecting Smad2. This suggests that Halo inhibits TGFβ-induced Smad3 activation.

Since Smad3 is also involved in the TGFβ-like pathway of myostatin, it is thought that Halo may play an additional role in muscle growth as well as in the reduction of

fibrosis. Further work on this part of our research studies on Halo is being conducted by Drs. Pines and Halevy (Israel).

e) Clinical applications

Halo has passed phase I and phase II clinical trials for use in chronic graft versus host disease (cGvHD), an inflammatory condition that arises after allogeneic bone marrow transplantation. cGvHD results in skin fibrosis (as well as graft rejection), and a loss in range of motion (ROM) secondary to joint restriction from skin. Prior to clinical testing, patients suffering from cGvHD provided biopsies. Cell cultures of biopsied skin fibroblasts were treated with Halo, and collagen I content and expression were evaluated (Halevy *et al* 1996). Collagen I synthesis was inhibited with Halo treatment in fibroblasts *in vitro*. Nagler and Pines (1999) continued this work with clinical trials using Halo as a topical cream applied to the neck skin of patients with cGvHD. After three months of treatment, there was a marked reduction in collagen expression and collagen content in patient skin biopsies. These results were accompanied with an increased ROM of the neck. When Halo treatment was stopped, collagen levels and expression, and skin tightness returned to pre-treatment levels within three months. A trial of orally administered Halo (either a single dose of 0.07-2.5mg; or a daily dose of 1.5mg) was also conducted in cGvHD patients and demonstrated that an effective dose (ED) was achieved and that therapeutically effective plasma levels could be reached with no adverse effects (Pines *et al* 2003).

13. FUNCTIONAL STUDIES

Therapeutic success of treating DMD can be evaluated with measures of muscle strength and endurance testing (Brooke *et al* 1983). The Brooke's upper and lower extremity grading scale is used to assess muscle strength after treatment in DMD patients (Brooke *et al* 1983,Lord *et al* 1987). Mendell *et al.* (1989) have also created a test of lower extremity function, which was successfully employed as an assay or outcome measure in prednisone trials in DMD patients.

Both *in vivo* and *in vitro* models can be used to evaluate muscle strength and endurance. Bressler *et al.* (1983) looked at whole-muscle strength and speed of contraction by stimulating a motor nerve or stimulating the muscle directly. Anderson *et al.* (1988) and Ikeda and Mitsumoto (1993) have also examined mdx mouse muscle strength using contractility measures in an *in vitro* muscle bath. Semi-*in vitro* tests can also be used to mimic physiologic conditions, in which muscle origin is fixed to the stabilized limb and the insertion is attached to a force transducer (Dangain and Vrbova 1984). In this model, the blood and nerve supplies remain intact. However, this test does not truly maintain physiologic conditions; *in vivo* studies are ideal for testing muscle strength and endurance.

Several tests have been developed to examine muscular endurance. Swimming tests are commonly used in mice to determine swim times (*e.g.*, the duration of time that mice can remain afloat in warm water) (Leeuwenburgh and Ji 1995). Since the mice are not fond of water, they undergo extreme stress, which might affect the muscle physiology. The University of Manitoba Animal Care does not approve this method for dystrophic mice, because they are already compromised from disease. Treadmill tests are a good

alternative to swimming for measuring endurance. This is a voluntary exercise, and captive animals tend to enjoy running when given the opportunity. Mdx mice run from two to nine kilometres over 24 hrs (Archer *et al* 2006,Carter *et al* 1995,Hara *et al* 2002) which is significantly less than C57 mice (Dupont-Versteegden *et al* 1994,Hayes and Williams 1996). Mdx mice also have a stop and go pattern, as opposed to the continuous running by C57 mice (Hara *et al* 2002). This may be because mdx mice lack motivation due to pain, or because of lower muscle function. Archer *et al.* (2006) saw that deflazacort treatment prevented a progressive loss of function with a 24 hr treadmill runs.

To complement muscle-endurance treadmill testing, strength testing is a good accompaniment. Meyer *et al.* (1979) reported a method to test muscle strength over time. They used a Chatillon gauge (a force tranducer) to test forelimb grip strength. This method is inexpensive and fast. Grip strength was later used to show improved muscle function in mdx mice following deflazacort treatment (Anderson *et al* 2000).

Many recent tests have assessed cardiorespiratory function in DMD patients and mdx mice (Hahn *et al* 1997) as a reflection of disease progression and/or treatment outcome. Although not explored previously in mdx mice, barometric plethysmography is an excellent way to measure respiratory function in rodents (*e.g.*, (Levitt and Mitzner 1988,Mishima *et al* 1996). This technique is commonly used in asthmatic or allergic mice to test airway responsiveness after a methacholine challenge (Hamelmann *et al* 1997), and could easily be applied to mdx mice to test function of respiratory muscles.

Murine echocardiogram is a growing research tool. It is being used in a wide variety of application, such as examining phenotypes of transgenic mice and as a functional measure for many treatments (Doevendans *et al* 1998). Echocardiography is

especially desirable because once the apparatus is purchased the costs are low, sampling is rapid, and it is non-invasive to the mice. A full assessment of the heart structure and cardiovascular function can be done with echocardiogram, including left ventricular function and size (hypertrophy), heart rate, ejection fraction, valvular function, and chamber sizes. This is an extremely valuable tool for assessing murine cardiac function.

Chapter 2. HYPOTHESIS AND AIMS

1. HYPOTHESIS

Halo has aided in the inhibition, reduction and suppression of fibrosis in many organs. In a pilot study (Pines and Anderson, unpublished) mdx mice were treated with either 3μg/mouse Halo or saline (intraperitoneally) for 4 weeks beginning at 5 weeks of age. C57Bl mice were used as controls. Examination of several muscles showed lower collagen I expression and decreased fibrosis. This suggested that Halo is an inhibitor of fibrosis in the mdx mice.

We hypothesize that from the previous research and the preliminary data on Halo, treatment will reduce tissue fibrosis, and thereby improve muscle function and myogenesis by inhibition of the Smad3 pathway. This will be seen as decreased collagen content quantified by Sirius red staining, Masson's trichrome staining, and Western blotting, and reduced levels of collagen I and collagen III expression. We expect that these results will be significant in the diaphragm, heart and limb muscles. With the reduction of fibrosis, cardiomyopathy and respiratory dysfunction should be diminished. Without an extensive collagen network, satellite cells may be able to migrate more freely and proliferate, and tissue will be less susceptible to exercise-induced damage. We expect that overall function will improve post-treatment.

2. AIMS

Pines and colleagues (Halevy *et al* 1996,Nagler and Pines 1999)have shown that Halo administered by injection, topical administration and oral administration inhibited,

suppressed or reduced fibrosis in several organs and models. To date there are no studies examining the use of Halo in fibrosis of muscle caused in Duchenne muscular dystrophy (DMD); this project aims to fill that gap.

Aim #1: To study histological and molecular effects of Halo on the mdx mouse model of DMD using a resolution protocol.

Aim #2: To study the effect of Halo on target genes and proteins that regulate fibrosis.

Aim #3: To study functional effects of Halo on the mdx mouse model of DMD using a resolution protocol.

Chapter 3. MATERIALS AND METHODS

1. EXPERIMENTAL ANIMALS

Mdx mice were used in this study to test the effects of Halofuginone on fibrosis, muscle repair, and muscle function. Animals were housed in the Central Animal Care facility at the University of Manitoba. Animals were given water and food *ad libitum*. All treatments were approved by the University of Manitoba Animal Care Committee (Protocol # 05-056).

2. TREATMENT

Experimental mice eight to nine months old were treated with Halofuginone (ip injections: 3μg/gram of body weight) and control mice were treated with 0.9% saline (ip injections: 2μL/g body weight) every second day for five (n = 4/group), ten (n = 5/group) or twelve weeks (n = 4-5/group). Mice were randomly assigned to treated or control groups. A Hamilton syringe was used (Hamilton Company, Reno, Nevada) for accuracy. Prior work in Isreal indicated that injection doses from 1μg to 5μg/gram body weight was effective in fibrotic treatment in mice, therefore the mean was selected for the dose in the current study.

3. TISSUE COLLECTION

Mice were anesthetized using ^{Pr}AErrane isoflurane (Baxter Corp, Mississauga, Ontario) and sacrificed by cervical dislocation. After euthanasia, an incision was made in the dorsal skin and the skin and fur from the lower half of the mouse were removed. The fascia surrounding the muscles of the lower limb was removed with fine forceps and scissors. Using the forceps, the distal tendon of the tibialis anterior (TA) was separated from the bone and the muscle was gently lifted away from the leg and cut at the proximal insertion, with care not to damage or remove the extensor digitorum longus (EDL). The quadriceps and gastrocnemius were similarly removed with care not to take the deeper muscles.

Using an abdominal approach, the diaphragm was collected. The anterior inferior border of the rib cage at the xiphisternum was located, the skin and muscle around the subcostal margin were cut, and the vertebral column was severed. The abdominal viscera were retracted to reveal the descending aorta and esophagus, which were then cut; any blood was blotted away with a Kimwipe® (Kimberly-Clark, Mississauga, Ontario). The perimeter of the diaphragm was gently cut from the costal margins using scissors. Once the diaphragm was removed, the heart was located in the thoracic cavity. Forceps and scissors were used to sever the vessels entering and exiting the heart. Excess blood was blotted away, and blot clots and fat tissue were cleaned off the heart.

4. TISSUE PREPARATION AND FROZEN SECTIONS

Muscles that would be used for frozen sections were either arranged longitudinally in a cryo-mold containg OCT compound (Shandon Cryomatrix™ Thermo, Pittsburgh, Pennsylvania), or transected at the midbelly and arranged in the cryomold (Tissue-Tek®, Sakura Finetek, Torrance, California) so that cross sections could be taken. The diaphragm was cut into right and left halves or left whole, rolled up and placed in the cryomold for either longitudinal or cross sections. The heart was separated into right and left halves. The left half was arranged longitudinally in the cryomold. The molds containing OCT compound were immersed in cold isopentane (≤ -50° C) with care not to disrupt the tissue orientation.

For studies of gene expression at the RNA and protein levels, the TA, quadriceps, and gastrocnemius were bisected at the muscle belly and each half was placed in an eppendorf® tube (Eppendorf, Westbury, New York). The remaining half of each muscle was divided into halves again and each part was placed separately into an eppendorf® tube. The muscles were snap frozen by immersing the tubes in liquid nitrogen. The tubes were colour-coded so sets of muscle samples could be easily identified for studies using a particular assay technique (e.g., for Western or Northern blots, etc.)

5. TISSUE SECTIONING

Prior to tissue sectioning, slides were silanated. Slides were placed in metal racks and washed in warm soapy water, rinsed well with distilled water (dH_2O), and air dried.

After drying, slides were wrapped in aluminum foil and baked at 180-200°C overnight. Slides were cooled and immersed in freshly prepared 2% aminopropyltriethoxy silane (Sigma, St. Louis, Missouri) in acetone for 10 seconds. Slides were rinsed with diethyl pyrocarbonate (DEPC) (Sigma, St. Louis, Missouri) double distilled water (ddH_2O) to remove any RNAse and air-dried overnight.

Tissues were sectioned at a thickness of 5 μm. Tissue blocks frozen in OCT compound were mounted onto a chuck with fresh OCT compound. Once the tissue was frozen on the chuck (approximately three minutes) the superficial layers of the block were shaved off until the muscle tissue was exposed. The block was then faced by taking 10 to 20 5 μm sections (total 50-100μm). Forty serial sections of each tissue were then collected. Two sections of diaphragm, heart or gastrocnemius, quadriceps and TA were on each slide. Several slides of thymus, skin and intestine were taken for use as control slides in proliferation studies.

6. ASSAYS OF FIBROSIS

a) Sirius Red

Collagen content was quantified using a Sirius Red stain on sectioned tissues. Slides containing sections of diaphragm, heart, quadriceps and TA were hydrated by passage through two changes of 100% ethanol, one change of 95% ethanol, one change of 70% ethanol, and one change of water. Slides were then stained for 30 minutes in 0.1% sirius red F3B (ESBE Laboratory Supplies, Toronto, Ontario) in saturated picric acid, and dehydrated rapidly in 100% ethanol. Slides were cleared with Slide Brite™

(Sasco of Georgia Inc., Albany, Geaorgia) and mounted with Permount (Fisher, Hampton, New Hampshire).

Slides were examined with a Zeiss Photo II microscope (Carl Zeiss Inc., Thornwood, New York) and images were captured with a Sony 3 chip colour CCD Camera (Sony, USA). The stained tissues were analyzed using Northern Eclipse Imaging Software (Empix Imaging, Mississauga, Ontario). Using polarizing filters, twenty image-samples were taken of the diaphragm and quadriceps from each animal at each of 180°, 135°, 90° and 45°. Images were converted to the Red plane, and the average, maximum and minimum gray intensities (representing red) were calculated. Data were compiled in Excel spreadsheets (Microsoft, USA) for further study.

b) Masson's Trichrome

Masson's trichrome stain was used to examine muscle histology and fibrosis. Slides were hydrated through two changes of 100% ethanol, one change of 95% ethanol and one change of 70% ethanol. Sections were fixed for one hour in Bouin's fixative (Fisher, Hampton, New Hampshire) at 56°C, and rinsed in running water until sections were clear. Slides were counterstained using Weigerts Iron Hematoxylin (Fisher, Hampton, New Hampshire) for ten minutes, rinsed in running water for ten minutes, stained in filtered Biebrick Scarlet Acid Fuschin (Matheson, Coleman and Bell, Norwood, Ohio), and rinsed in running water for ten minutes. Slides were differentiated in 5% phosphotungstic acid for twenty minutes and counter-stained in filtered Light Green SF Yellowish (Matheson Coleman and Bell, Norwood, Ohio) for ten minutes. Sections were

dehydrated rapidly in two changes of 95% ethanol and two changes of 100% ethanol, cleared in Slide Brite™ and mounted with Permount.

Slides were analyzed with an Olympus BH2 fluorescence microscope (Center Valley, Pennsylvania). Collagen content was measured over 5 areas along the long axis of the section, using a 10x10 ocular grid (500squares). If squares were a quarter or more full of green (collagen) they were considered positive.

c) Western Blots

c1. Protein isolation

Muscles were weighed, transferred to a cooled Petri dish and chopped finely using a cooled razor blade. Chopped muscles were transferred individually to 15mL polystyrene conical tubes (Falcon, Lincoln Park, New Jersey) and protein isolation buffer was added at 300-500 μL/tube. Samples were vortexed for thirty seconds, left on ice for one hour and re-vortexed for thirty seconds. Samples were transferred to eppendorf® tubes and centrifuged at 3000 rpm for five minutes at 4°C to remove particulate matter. The supernatant was then transferred to clean eppendorf® tubes and frozen at -80°C. A protein assay was used to determine the concentration of the protein samples using a bovine serum albumin (BSA) stock standard to create a standard curve.

c2. Dot Blots

To quantify the amount of collagen protein, the protein samples were diluted with loading buffer, boiled and immediately quenched on ice. Diluted samples were loaded

onto a Polyvinylidene Fluoride (PVDF) membrane (Osmonics, Minnetonka, Minnesota) that had been pre-soaked in methanol and rinsed in dH_2O. Membranes were incubated in a blocking solution of 5% skim milk powder (Nestle Carnation, USA) for thirty minutes, rinsed for one hour in 1xPBS, and immunostained for two hours at room temperature with a polyclonal antibody to either collagen I (1:1000, Orbigen, San Diego, California) or collagen III (1:8000, Abcam, Cambridge, Massachusetts). Membranes were washed for an hour in 1xPBS to rinse off any excess, unbound antibody. Membranes were then incubated with an goat anti-rabbit-AP secondary antibody (1:1250; Santa Cruz, Santa Cruz, Califonia) for two hours at room temperature and washed for an hour in 1xPBS. Membranes were incubated with chemiluminescent substrate (CSPD) (Roche Diagnostics, Indianapolis, Indiana) and exposed to visualize the collagen protein. Vitrogen (a commercial solution of 98% collagen I and 2% collagen III) (Cohesion, Palo Alto, California) was diluted and blotted at different concentrations to establish a standard curve against which the optical density of the CSPD-detected collagen proteins could be quantified.

c3. Gels

After the protein was isolated were prepared (see *chapter3, section6c1*), protein concentration was determined by measuring the wavelength of the samples (Bio-Rad Assay Dye Reagent and protein sample). Samples were then incubated with collagenase (at a concentration of 0.2%) at 37° C for one and a half hours. Samples were then mixed with a sample buffer, boiled for 8 minutes, quenched on ice until cool, and centrifuged for 30 seconds. The prepared samples were loaded in to an 8% acrylamide gel with a

marker and a positive control (Vitrogen), and run for one and a half hours at 120mV in a running buffer. After the samples had run they were transferred to a PVDF membrane at 100mV for 2 hours in a transfer buffer solution. Membranes were then stained with Ponceau Red (Sigma, St. Louis, Missouri), and rinsed with dH_2O to ensure transfer had occurred. The membranes were photocopied, so that the marker ladder could be used as comparison at a later stage. Membranes were blocked with a 0.5% milk blocking buffer for 30 minutes to prevent non-specific binding. Membranes were rinsed in 1 x PBS, and incubated with a monoclonal collagen I antibody (1: 4000; Sigma, St. Louis, Missouri) at room temperature for 2 hours and at 4° C overnight. The next day membranes were rinsed in 1 x PBS (3 x 15 minutes), blocked with a blocking buffer, and incubated with a rabbit anti-mouse-Alkaline Phosphatase (AP)-conjugated secondary antibody (1:1000; Abcam, Cambridge, Massachusetts) for 2 hours at room temperature. The membranes were rinsed with 1 x PBS (3 x 15 minutes) and rinsed with Buffer 3 (3 x 5 minutes). Membranes were then washed in a chemiluminescent substrate (CSPD) (Roche Diagnostics, Indianapolis, Indiana) solution for five minutes, incubated for 15 minutes at 37° C, and left to expose for 40 minutes in a dark place. The film was developed and scanned with a densitometer to measure optical densities.

The membranes were stripped with a stripping solution in a 70° C water bath for 30 minutes. Membranes were rinsed in 1 x PBST (3 x 10 minutes), blocked with a bovine serum albumin (BSA) blocking buffer, and incubated for 2 hours at room temperature with an anti-GAPDH antibody (1:1000; Abcam, Cambridge, Massachusetts) to allow for the internal control of loading conditions. Membranes were then left to rinse in 1 x PBST (3 x 15 minutes) and then were blocked again with a BSA blocking buffer.

The membranes were then incubated with a goat anti-rabbit-AP secondary antibody (1:1000; Santa Cruz, Santa Cruz, Califonia), rinsed in 1 x PBST (3 x 15 minutes), and rinsed in Buffer 3 (3 x 5 minutes). To develop the membranes, they were washed with CSDP for 5 minutes, incubated for 15 minutes, and exposed for 40 minutes. The film was developed and analyzed with a densitometer (accumulated densities).

The optical densities of Collagen I incubated membranes were divided by the optical densities of the GAPDH incubated membranes, to account for any loading errors.

7. HGF

Muscle fractions of the quadriceps after 10 weeks of treatment were run on a gel (see *chapter3, section6c3*) to assess the effect of Halo on HGF protein levels. Membranes were probed with an anti-HGF antibody (1:500; Sigma, St. Louis, Missouri). A rabbit anti-mouse-AP secondary antibody was used (1:500; Abcam, Cambridge, Massachusetts). Membranes were incubated with CSPD and exposed to visualize the HGF protein. Optical densities were calculated, and background was subtracted.

8. ALPHA-SMOOTH MUSCLE ACTIN

Muscle fractions of the quadriceps after 10 weeks of treatment were run on a gel (see *chapter3, section6c3*) to assess the effect of Halo on myofibroblast activity. Membranes were probed with an anti-α-smooth muscle actin antibody (1:2500; Santa Cruz, Santa Cruz, California). A goat anti-rabbit-AP secondary antibody was used

(1:20000; Santa Cruz, Santa Cruz, California). Membranes were incubated with CSPD and exposed to visualize the α-smooth muscle actin protein. Optical densities were calculated, and background was subtracted.

The membranes were stripped with a stripping solution in a 70° C water bath for 30 minutes. Membranes were rinsed in 1 x PBST (3 x 10 minutes), blocked with a bovine serum albumin (BSA) blocking buffer, and incubated for 2 hours at room temperature with an anti-GAPDH antibody (1:1000; Abcam, Cambridge, Massachusetts) to ensure equal loading. Membranes were then left to rinse in 1 x PBST (3 x 15 minutes) and then were blocked again with a BSA blocking buffer. The membranes were then incubated with a goat anti-rabbit-AP secondary antibody (1:1000; Santa Cruz, Santa Cruz, California), rinsed in 1 x PBST (3 x 15 minutes), and rinsed in Buffer 3 (3 x 5 minutes). To develop the membranes, they were washed with CSDP for 5 minutes, incubated for 15 minutes, and exposed for 40 minutes. The film was developed and analyzed with a densitometer (accumulated densities).

9. IN SITU HYBRIDIZATION

The expression of collagens I and III was determined using in situ hybridization. Collagen I or III digoxygenin-labeled riboprobes were prepared by the laboratory technician for probing the tissue with collagen I and III clones.

A riboprobe of collagen I alpha-1 was synthesized from an ATTC cDNA clone (catalogue number 5876788, designation 3823337, GenBank Accession # BF662620) using standard protocols. The riboprobe was approximately 400 base pairs in length and

detected the gene sequence from bases 143 to 408 down to 0.005 ng RNA. The original accession was from Dr. Robert Strausberg, www.ncbi.nlm.nih.gov/ncigap, in 1997).

A riboprobe of collagen III alpha-1 was synthesized from an ATTC cDNA clone (catalogue number 1058119, designation 789709, GenBank Accession # AA387470) using standard protocols. The riboprobe was 1337 to 1754 base pairs in length and detected the gene sequence between bases 2053 and 3473 of the rat collagen III sequence, down to less than 0.0187 ng RNA. The original accession was from M. Marra, Hillier, Allen, Bowles et al including the senior author Waterston R (1996).

For the in situ hybridization protocol, slides were dried, rinsed with 1xPBS and fixed in 4% paraformadehyde. An RNAse working solution was added to a control slide; the slide was then coverslipped and incubated for twenty minutes at room temperature. Slides were rinsed in 1xPBS for thirty minutes keeping the RNAse control separate. All slides were incubated under a coverslip in a humid chamber for one hour at 42°C with a hybridization buffer. The labeled probe was placed in a block heater for thirty minutes at 65°C to, quenched on ice and added to the hybridization buffer at a concentration of 500ng/mL. 160 µL of hybridization cocktail were pipetted onto each slide and a coverslip was gently laid on top of the slide while avoiding bubble formation. Slides were left to hybridize overnight at 42°C in a humid chamber. The next morning, coverslips were removed and sections were washed (2 x 15 minutes) with 2xSSC in 0.1%SDS using a gentle rotary shaker to remove any unbound probe. Slides were then transferred to a solution of 0.1xSSC in 0.1% SDS and rinsed again (2 x 15 min.) to remove any unbound or non-specifically bound riboprobe. Slides were rinsed with Buffer 1 (again using a shaker) and blocked for one hour (under a coverslip) with Buffer

2. An anti-digoxigenin-AP antibody (anti DIG-AP) (Roche Diagnostics, Penzberg, Germany) was diluted to 1:500 with Buffer 2 and 160µL was pipetted onto each slide. Slides were coverslipped for overnight incubation in a humid chamber at 4°C. Slides were then rinsed (3 x ten minutes) in Buffer 1 and then three times for five minutes each in Buffer 3. A colour solution was added to the slides and left in the dark to develop; development was monitored using a microscope (2-4 hours). Slides were rinsed with Buffer 3, then Buffer 4 and finally dH_2O. Slides were lightly counter-stained with Harris Hematoxylin (Fisher, Hampton, New Hampshire), rinsed with dilute Lithium carbonate (Fisher, Hampton, New Hampshire) and rinsed in dH_2O until blue before they were mounted under coverslips using an aqueous mounting media, Immunomount. Slides processed in an identical manner, except for the omission of either the anti-digoxygenin antibody or the digoxigenin-labelled riboprobe were used as negative controls for the procedure.

Slides were analyzed with an Olympus BH2 fluorescence microscope. Nuclei were ranked 1 to 3 based on the number of nuclei visible in the positively stained area. A grade of 1, represented one stained nuclei; a grade of 2 represented two to five stained nuclei; a grade of 3 represented five or more stained nuclei. Positive areas were counted along the long axis of the section over 5 grid lengths (in the ocular lens) at 400x magnification. Central nuclei expressing collagen were also counted in the same manner as previously described (Anderson *et al* 1996).

The central nucleation index (CNI) was also assessed on these slides. Central nuclei were counted in 3 images taken of the tibialis anterior and quadriceps at 100x

magnification. The CNI was calculated as the proportion of fibers with entral nuclei divided by the total number of fibers. A minimum of 250 fibers was counted per muscle.

11. PROLIFERATION AND REPAIR

a) Ki67

Immunocytochemistry (ICC) using a monoclonal antibody, Ki67 (Abcam, Cambridge, Massachusetts), which recognizes an antigen expressed by cells in G1, S, G2, and M phases of the cell cycle but which is not expressed in the G0 phase, was used examine cell proliferation in skeletal muscle.

Slides with sections of diaphragm, heart, quadriceps and TA muscles were dried for an hour at room temperature and rinsed briefly in PBS. Slides were blocked with the primary-antibody diluent for one hour, rinsed three times for five minutes each in PBS, incubated under a coverslip with a monoclonal antibody against Ki67 (1:4000; Abcam, Cambridge, Massachusetts) for five hours at room temperature in a humid chamber and rinsed overnight in PBS. Sections were blocked with the secondary-antibody diluent for one hour, rinsed in PBS (3 x five minutes), incubated for two hours under a coverslip with a donkey anti-rabbit-HRP secondary antibody (1:200; Amersham, Buckinghamshire, England) and again rinsed in PBS. The HRP-conjugated antibody was then thoroughly rinsed off with 1 x PBS. A DAB solution was applied and the slides were left to develop colour. Once the colour was developed the slides were rinsed in 1 x PBS. Tissue

sections were counterstained with Fast Green, fixed in 95% ethanol and then mounted with Immunomount (GelTol, Thermo, Pittsburgh, Pennsylvania).

Slides were analyzed with an Olympus BH2 fluorescence microscope. Ki67-positive nuclei were counted along the long axis of the section over 5 grid length. Ki67 positive cells were categorized based on their location (at the periphery or within muscle tissue or in the ECM).

12. FUNCTIONAL STUDIES

a) Grip strength

Forelimb grip strength was measured with a calibrated (Meyer *et al* 1979) Chatillon gauge (Chatillon, DFM-2.0kg, Greensboro, North Carolina) to determine whether halofuginone treatment affects muscle function. The gauge was mounted at 45° to the horizontal on a thick plexiglass stand as reported (Anderson *et al* 2000). A 3 mm diameter aluminum rod of a 3.2 cm equilateral triangle was attached to the strain gauge for the mice to grip.

Grip strength was assessed by holding mice by their tail, approximately one inch from the base and lowering the mice towards the bar until their forelimbs grasped the bar. Once the mice had securely gripped the bar with both paws, they were gently pulled away from the rod by their tail until their grasp was broken. The peak tension resulting from this maneuver (pull force) was displayed on the Chatillon gauge and recorded in grams. Each test consisted of five one-minute trials.

Mice were tested for strength at the beginning of the treatment period (the baseline measure) and each week throughout the treatment period.

b) Running

Limb strength, muscle endurance and cardiovascular endurance were assessed with a running wheel device. Metal rodent wheels (12.7cm diameter) were outfitted with a doubled-over strip of fiberglass netting cut to the circumference of the wheel. The netting was woven in and out of the crossbars of the wheel to make running easier for the mice. Using strong, double-sided tape, two 1-cm magnets were attached at opposite sides of the wheel for balance. The wheel was then taped down in a plastic rat cage, to ensure it was stable in the cage. A magnetic switch (Guard^{TM}) was attached to a battery-powered counter (Omron^{TM} H7EC-N, Japan) with copper wire. The switch was suspended from the lid of the cage approximately 1 cm above the wheel magnets. The wheel was rotated to ensure the counter recorded every rotation. As the wheel passed the magnets, the switch would be pulled shut and the counter would register it. Every half rotation of the wheel was counted (i.e., the transit of each magnet); therefore, using simple mathematics, the circumference could be calculated. Each mouse was housed separately for 24 hours, giving a full day-and-night period in a rat cage that had a wheel setup. The cages were placed beside each other, so there was visual contact between mice.

Mice in a group of 3-4 were placed in a cage for approximately 30 minutes to become familiar with the setup and learn from one another. Mice were then separated, one per cage, each with a clean wheel; the counters were zeroed and the mice were left to

run for 24 hours. This procedure was carried out weekly, to examine progressive changes in this global measure of function, including muscle endurance, behaviour and cardiovascular function.

c) Evans Blue Dye

In this experiment, nine mice (5 controls and 4 halofuginone-treated) were treated for a period of twelve weeks and were used to assess the level of physiologic muscle damage induced by a 24-hour period of voluntary exercise, as described (Archer et al., 2006). Mice were injected intraperitoneally with Evans Blue Dye (EBD) (1 mg EBD in 0.1mL of a 0.9% solution of saline per 10 g of body weight). One mouse was injected with a lower dose of EBD initially (1 mg/0.01mL 0.9%saline/10g body weight) which was found to be insufficient for quantification; therefore, data from this animal were eliminated from the EBD portion of the study.

Once mice were injected they were subjected to 24 hours of voluntary exercise in the rat cages described above. After euthanasia, muscles were dissected from the mice, tissues were frozen in OCT compound and sectioned as described earlier, and sections were analyzed as follows.

Using a fluorescence microscope (Nikon Eclipse TE2000-E, Japan) with an X-Cite^{TM}120 Fluorescence Illumination system (EXFO, Quebec, Canada), digital pictures at 10x were taken over an entire section of quadriceps in monochrome and red fluorescence. Images were captured (as *.jpeg files) with Simple PCI6 (Compix Inc., Cranberry Township, Pennsylvania), and monochrome and red fluorescent images were merged. Image J software (NIH, USA) was then used to create a collage, arranging the

photographs to form a single, continuous image of each section. Using the Cell Counter option of the program, the number of muscle fibers that were positive for EBD (fluorescing red) and or negative for EBD (no fluorescence) were counted so a ratio of the proportion of EBD-positive over the total number of fibers in each section could be calculated.

d) Barometric Plethysmography

Airway responsiveness was measured by barometric plethysmography (Buxco, Troy, New York). Prior to beginning the experiments, all the animal chambers (4 chambers) and the main chamber were calibrated for pressure. Responsiveness was expressed as Penh (an enhanced pause), which was derived from changes in the chamber pressure caused by bronchioconstriction during peak expiratory pressure (PEP) and peak inspiratory pressure (PIP). Penh was calculated as Pause x PEP/PIP. Methacholine was administered in increasing doses using a Buxco aerosol delivery system (Buxco, Troy, New York), beginning with a baseline 'dose' of saline, and then increasing from 3 mg/mL to 50mg/mL. Between each dose, mice were given time for their tidal volume and responsiveness to return to baseline levels.

Airway-responsiveness tests were conducted within 1-2 days before animals were euthanized.

13. CARDIOMYOPATHY

a) Vimentin

Muscle protein fractions of the quadriceps, heart, tibialis anterior, and diaphragm were prepared from tissues collected from mice after 5 and 10 weeks of treatment and were run on a gel (see *chapter3, section6c3*) to assess the effect of Halo on cardiac fibrosis. Nitrocellulose membranes were probed with an anti-vimentin antibody (1:500; Santa Cruz, Santa Cruz, California). A goat anti-rabbit-AP secondary antibody was used (1:1000; Santa Cruz, Santa Cruz, California). Membranes were incubated with chemiluminescent substrate (CSPD) (Roche Diagnostics, Indianapolis, Indiana) and exposed to visualize the vimentin protein. Optical densities were calculated, and background was subtracted.

b) Echocardiography

Echocardiography was conducted to assess cardiac function after Halo treatment in young and old mice. Mice were prepared for echocardiography without anesthesia after removal of hair using two applications of Nair™. They were positioned by manual restraint in a horizontal position on their left side, and a non-invasive 13 MHz probe (Vivid 7, General Electric Medical Systems, Milwaukee, Wisconsin) covered in gel was applied to the chest wall over the heart. Mice were assessed by positioning a non-invasive probe on the chest. Hearts were imaged in the 2D parasternal short axis view and three different M-mode echocardiograms were recorded. LV end-diastolic diameter

($LVID_{ED}$), LV end-systolic diameter ($LVID_{ES}$), posterior end-diastolic wall thickness (PWT), and LV fractional shortening (FS) were measured. The LV end-systolic (LVESV) and diastolic volumes (LVEDV) are measured from a parasternal long axis view using the prolate ellipsoid geometric model and the LV ejection fraction (EF) is calculated. Cardiac output is calculated as the product of stroke volume (LVEDV–LVESV) and simultaneous heart rate. Tissue Doppler imaging (TDI) was acquired on a parasternal short axis view at the level of the papillary muscles, at a rate of 483 frames per second. For peak systolic endocardial velocity (V_{ENDO}), a region of interest (0.2mm x 0.2mm) in the posterior wall was analyzed. Radial strain rate (SR) was measured over a distance of 0.6mm (Echopac PC, General Electric Medical Systems, Milwaukee, Wisconsin). The temporal smoothing filters were turned off for all measurements. The values obtained in five consecutive cardiac cycles were averaged.

14. STATISTICS

Statistical comparisons appropriate to each parameter were made using SPSS (Chicago, Illinois), Excel (Microsoft, Redmond, Washington) and NCSS and PASS (Kaysville, Utah). Statistical tests employed in these analyses included: ANOVA, t-test, Chi-square and regression studies. Data were recorded to represent: weight, overall function measured as exercise capacity (running distance), muscle function (grip strength), respiratory function (barometric plethysmography), cell proliferation (Ki67), cardiac function (echocardiogram), fibrosis (Collagen I and III content by Western blot,

Sirius Red, Masson's trichrome, *in situ* hybridization), and membrane permeability (EBD). Significance was determined at the $p<0.05$ level.

15. SUMMARY TABLE

The following table summarizes the assays that were utilized in this study, including the gene or protein of interest, the method employed, and the feature under characterization.

Gene or Protein of interest	**Method**	**Characterization**
Collagen (I and III)	Sirius red stain	Fibrosis
	Masson's trichrome stain	
	Western blot	
	In situ hybridizatiom	
HGF	Western blot	Fibrosis and myogenesis
Alpha-smooth muscle actin	Western blot	Fibrosis
Ki67	Immunocytochemistry stain	Myogenesis
Grip Strength	Force measure	Function
Muscle fatigue	Distance	Function
Membrane permeability	EDB stain	Function
Respiration	Barometric plethysmography	Respiratory function
Cardiology	Echocardiogram	Cardiomyopathy
Vimentin	Western blot	Cardiomyopathy

Chapter 4. RESULTS

1. BODY WEIGHT

Mouse body weight was monitored throughout treatment and recorded. There was no significant difference in weight between the Halo+ group compared to the Untreated group during the treatment period (repeated measure ANOVA; $p = 0.924$).

2. GENERAL OBSERVATIONS

Mice in both the treated and untreated group remained active and healthy. Neither group showed any unexpected overt signs of disease progression or severe deterioration although muscle weakness (compared to normal mice) and marked kyphosis were notable in the aged dystrophic animals.

3. FIBROSIS

a) Sirius Red

To determine whether Halo reduced the amount of collagen in muscle tissue, a picrosirius red stain was used. Quadriceps and diaphragm from treated and untreated mice, at 5 (diaphragm only) and 10 weeks were collected and sectioned. Slides were stained and red colour intensity using polarized filters was used as a measure of collagen

content. Sampling was at 20 pre-set intervals from each section. One representative photomicrograph was selected to show staining.

Halo did not result in any reduction of collagen content in dystrophic muscle (figure 1A and B). Results show that there were no significant differences in diaphragm at 5 and 10 weeks of treatment (ANOVA; $p = 0.985$) (figure 2A and B) and the quadriceps at 10 weeks of treatment (Student's T test; $p = 0.48$) between tissues in treated and untreated mice (figure 2C).

As an aside, we saw that Sirius red stains the central nuclei in dystrophic muscle. However, the nuclear staining did not demonstrate the birifingence that is the marker of Sirius red staining for collagen.

Junquiera *et al.* (Junquiera *et al* 1979) proposed that different types of collagens could be identified with Sirius red, by analyzing the colours with polarizing filters. As they reported red-stained collagen is collagen I, blue-stained collagen is collagen II, and green-stained collagen is collagen III. Using a similar approach to the red intensity measurement, red and green planes were separated (collagen II was not of interest) and a red/green ratio was calculated. Results varied significantly based on the slide position and filter position, therefore this analysis was abandoned after a few trial slides.

b) Masson's trichrome

In addition to Sirius red, slides were stained with Masson's trichrome stain for collagen-content analysis (figure 3). Green-positive areas (green = collagen) of the heart (5 and 10 weeks) and diaphragm (5, 10 and 12 weeks) were assessed as follows. Data were analyzed by taking a sample area and measuring a ratio of green to background area

(200x magnification). However, there was no statistically significant difference in collagen content among groups (two way ANOVA; diaphragm $p = 0.46$, heart $p = 0.94$).

Qualitative observations of the muscle histology were also done as these techniques displayed nuclei, muscle fibers and collagen. Fibrosis and fat content appeared unchanged; there was no difference in heterogeneity of fiber size, and no visible difference in fiber lesion size and amount. The number of fibers containing central nuclei also appeared no different between the respective muscles from treated and untreated mice (quantitative analysis below). There was no observable difference between untreated and Halo+ groups at 5, 10, or 12 weeks.

c) Collagen protein content

Collagen I and collagen III proteins were analyzed in homogenized fractions of muscle. A number of methods were used to approach this assay. First, diaphragm samples were analyzed using Western dot-blot protocols and standardized against the sample weights (figure 4). A standard curve was plotted using vitrogen (98% collagen I and 2% collagen III) as a reference for optical density. There was no significant difference between Halo+ and Untreated groups at 5 or 10 weeks of treatment.

The dot-blot approach was taken initially, because after several trials and speaking to other researchers (personal communications with Dr. J.E. Scott and Dr. I. Dixon), we learned collagen is a sticky, large protein that does not run in a gel. However, since the question was still important, we tried a collagenase digestion approach for running collagen on a gel. The rationale for this approach was that partial digestion of the large, sticky collagen protein complex might yield fragments that were small enough

to run in a gel and large enough to be recognized by an antibody. After several trials (with different trials of collagenase incubation duration, and different collagenase concentrations) bands appeared (assayed using vitrogen as a positive control) (figure 5A). There was a significant difference after 5 weeks of treatment (two way repeated measure ANOVA Tukey's; $p = 0.006$) in the quadriceps, tibialis anterior, and heart, but not in the diaphragm or after 10 weeks of treatment (two way repeated measure ANOVA; $p = 0.07$) in collagen content between untreated and Halo+ groups by this method in the dystrophic tissues (figure 5B). There was a significant difference in collagen content between the 4 muscle tissues (*i.e.*: the tibialis anterior had significantly more collagen than the diaphragm) that was consistent in treated and untreated groups (two way repeated measure ANOVA; 5 weeks treatment $p < 0.001$, 10 weeks treatment $p = 0.004$). This was consistent with observations of the tissue sections, stained with Sirius red and Masson's trichrome; the levels of collagen expression also varied between tissues.

4. HGF PROTEIN CONTENT

The level of HGF protein, a protein active in satellite cell activation and proliferation and in the development of renal and pulmonary fibrosis, was assessed in protein extracts prepared from homogenized quadriceps muscle. Samples were analyzed using Western blotting protocols and values of the scanned optical density for each band were standardized against the protein concentration of the samples (figure 6).

After 10 weeks of Halo treatment, there was an increase in the amount of HGF detected in the quadriceps. Untreated mice had a significantly lower level of HGF protein than Halo+ mice (Student's T test; $p = 0.03$).

5. ALPHA-SMOOTH MUSCLE ACTIN

The concentration of Alpha-smooth muscle actin, which is a protein produced by myofibroblasts at a site of injury, was analyzed in quadriceps muscle. Samples were analyzed using Western blotting protocols and values of the scanned optical density for each band were standardized against the protein concentration of the samples (figure 7).

After 10 weeks of Halo treatment, the amount of a-SMA detected in the quadriceps was reduced. Untreated mice had a significantly higher level of α-smooth muscle actin protein than Halo+ mice (Student's Ttest; $p = 0.01$).

6. COLLAGEN I AND COLLAGEN III EXPRESSION

The amount of collagen production, or abnormal production in dystrophic muscles with and without Halo treatment was determined by measuring collagen I and collagen III gene expression in muscles using *in situ* hybridization protocols. The relative number of cells expressing one of these genes was ranked (1 to 4) based on the number of nuclei in the positively stained cytoplasm and if the nuclei were centrally located (figure 8A, B and C). After 5 and 10wks of treatment there were fewer cells

expressing collagen I and III in Halo+ mice in all tissues (Chi square; χ^2 <0.001; χ^2 <0.025).

Interestingly, central nuclei contained in muscle fibers throughout the quadriceps and tibialis anterior muscles were observed to express both collagen I and collagen III. In both the dystrophic quadriceps and tibialis anterior, Halo+ mice had fewer central nuclei that were positive for collagen I or collagen III after 5 weeks of treatment than Untreated mice (Chi squared; χ^2 <0.025). However, there was no significant difference after 10 weeks of treatment.

The same slides were analyzed for central nucleation index. There was no significant difference in the proportion of fibers that displayed central nuclei in the tibilalis anterior and the quadriceps among any of the treatment groups.

7. PROLIFERATION AND REPAIR

a) Ki67 staining

Ki67 expression, as measured by immuno-staining, was used as a marker of cell proliferation. Positive cells were counted and counted separately based on their location (in an area of fibrosis/ECM or in the muscle) (figure 9).

After 5 weeks of Halo treatment, the diaphragm, quadriceps and tibialis anterior had fewer Ki67-positive cells in areas of fibrosis/ECM than untreated mice (Student's Ttest; $p = 0.031$, $p = 0.012$, $p = 0.041$ respectively). This was accompanied by an increase in

muscle cell proliferation in the quadriceps and tibialis anterior with Halo treatment (Student's Ttest; $p = 0.01$, $p = 0.03$ respectively).

After 10 weeks of Halo treatment cell proliferation in fibrotic areas was greater in the quadriceps than in untreated mice (Student's T test; $p = 0.035$), while cell proliferation in areas scored as muscle was decreased in the tibialis anterior of Halo+ mice compared with untreated control mice (Student's T test) (figure 10A, B, C and D).

8. FUNCTIONAL STUDIES

a) Grip strength

After peak grip strength data were collected with a Chatillon gauge (figure 11A), they were analyzed by numerous strategies, including calculating the mean peak-pull strength and measuring fatigue over the five trials for each mouse. Data were normalized to body weight. However, there was no significant change in forelimb grip strength at any time point with Halo treatment compared to strength in untreated mice regardless of the approach (figure 11B). The mean grip strength in the group of untreated mice varied largly from week to week, while Halo+ mice pulled consistently from week to week.

b) Running

Total distance run was calculated weekly using the circular relationship (circumference = πd) using an automated count of the half-rotations of a mouse wheel over 24 hours (figure 12A). Animals ran between 0.2km and 21km over a 24 hour period.

The distance run at a given time point over the experimental period was standardized to body weight in each animal. There were no differences run between Halo+ mice and Untreated mice after 10 weeks of treatment (ANOVA; $p = 0.774$) (figure 12B).

Running exercise was also used to induce damage under non-stressful, physiologic conditions (Archer *et al* 2006), in addition to its use as a general monitor of animal or muscle endurance. The final running test was conducted 4 days after the previous running session for each mouse. In this session Halo+ mice ran significantly further than Untreated mice (Student's T test; $p = 0.009$) (figure 12B and C).

c) Fiber permeability (Evans Blue Dye)

Using a dye which penetrated fibers with membranes damaged by dystrophy and exercise, the effects of treatment and exercise on muscle-membrane stability were determined (figure 13A). The quadriceps of mdx mice after 12 weeks Halo treatment showed a significantly smaller proportion of EBD-positive fibers than saline treated mice (Student's T test; $p = 0.015$) (figure 13B).

In muscle from untreated mice, the amount of fiber damage increased as distance increased; however, Halo+ mice had the same proportion of EBD positive fibers regardless of the distance they ran (figure 13C).

Please note that EBD counts could not be made on tissues of one mouse due to an error in the EBD concentration.

d) Barometric Plethysmography

Barometric plethysmography was used to as an indirect measure of respiratory muscle dysfunction by quantifying the response to a bronchoconstrictor, methacholine (figure 14A). Normally methacholine induces an immediate bronchoconstriction, which mice need to work hard to overcome using increased respiratory excursions and muscle work, whereas mice with respiratory dysfunction (or allergic-sensitization) are less able to overcome the challenge. We would predict that improved respiratory function would reduce or delay the stepwise response to methacholine and allow mice to recover better from the challenge at each concentration of methacholine.

After 10 weeks of treatment, Halo+ mice showed an attenuated response to the methacholine challenge, as well as a decreased response over increasing doses of methacholine (repeated measures ANOVA; $p = 0.008$) (figure 14B and C). This was similarly seen after 12 weeks of Halo+ treatment (figure 14C).

9. CARDIOMYOPATHY

a) Heart histology

Qualitative observations of the heart muscle histology were also made on Sirius red and Masson's trichrome slides. Fibrosis and fat content appeared unchanged with treatment, and there was no difference in heterogeneity of fiber size. No observable difference could be seen between untreated and Halo+ groups at 5, 10, or 12 weeks.

b) Vimentin content

The level of vimentin protein, a protein active in promoting cardiac fibrosis was analyzed in the heart muscle (figure 15A). After 5 and 10 weeks of treatment there was no significant difference between Halo+ mice and Untreated mice (Two way ANOVA; $p = 0.399$) (figure 15B).

c) Echocardiography

While not originally included in this thesis research project, the opportunity to conduct echocardiography studies on groups of Halo+ and untreated mice was provided by a new collaboration between Dr. Davinder Jassal (St. Boniface Research Center, Center of Cardiovascular Science) and Dr. Anderson. Significant organizational efforts supported the collection of data on treated and untreated groups of old mdx mice (treated for 5 weeks; n=8-10/group), and an additional group of young mdx mice (3-4 weeks of age treated for 10 weeks; n=9-10/group). Observations during the echocardiography studies indicated this is a very reliable and sensitive technique when applied by experts (Butler *et al* 2007,Doevendans *et al* 1998,Jassal *et al* 2006,Neilan *et al* 2006).

There were major dykinesias of the left ventricle (LVD) noted by Dr. Jassal, as well as left ventricular hypertrophy (LVH) and ventricular septal functional deficits, as the animals were examined one at a time. Dr. Jassal was blinded to the treatment status of each animal, and this allows us to say that observations by Dr. Jassal at the time of the echocardiography studies strongly show that the LVD were in all the untreated mice (young and old).

LVD was significantly lower than baseline after Halo treatment in the old mdx mice (Chi squared; $\chi^2 = 8.82$; $p<0.025$). There was significantly less LVD after 5 weeks of treatment with Halo compared to untreated mice (Chi squared; $\chi^2 = 8.25$, $p<0.025$). In a separate study on a group of young mice treated with Halo for 10 weeks, a qualitative assessment showed that only one of the young Halo+ mice showed evidence of LVD; there was significantly less LVD after 10 weeks of treatment with Halo (Chi squared; $\chi^2 = 5.84$, $p<0.05$). All mice (young and old, Halo+ and untreated) showed LVH. See attached echocardiography CD for video of Halo+ - normal function, and untreated – LVD echocardiograms (normal speed and one-sixth speed). Note that the right side of the abnormal LV moves dys-kinetically, while the normal LV contracts synchronously

Quantitatively there was no significant difference (Student's T test; $p>0.05$) between untreated and Halo+ mice in either the young or old groups measuring intraventricular septum thickness, posterior wall thickness, left ventricular end diastolic diameter, fractional shortening, and ejection fraction (by tissue Doppler).

Again, these observations are only available to us through a very generous collaboration with Dr. Jassal, his expertise in interpreting cardiac imaging studies in real-time, and the professional assistance of the animal care staff reporting to Dr. Randy Aitkens at St. Boniface Reasech Centre.

Chapter 5. FIGURES

Figure 1: Sirius red photos and measurements

A: longitudinal sections of diaphragm showing picrosirius red-stained slides with birefringence (on the right) and red-plane conversion (images captured in RGB, were transferred into red plane, *i.e.,* the green and blue planes were removed from the image of slides to remove anything that is not collagen) (on the left) (160x magnification) after 10 weeks of treatment. Top row shows representative muscle sections from untreated animals (Untreated). The bottom row shows representative muscle sections from treated animals (Halo+). These definitions (group identification) will be used in many figures to follow. Slides were photographed at 160x magnification.

B: longitudinal sections of quadriceps showing picrosirius red-stained slides with birefringence (on the right) and red plane conversion of slides (on the left) (160x magnification) after 10 weeks of treatment. Top row shows representative muscle sections from untreated mice. The bottom row shows representative muscle sections from Halo+ mice.

A

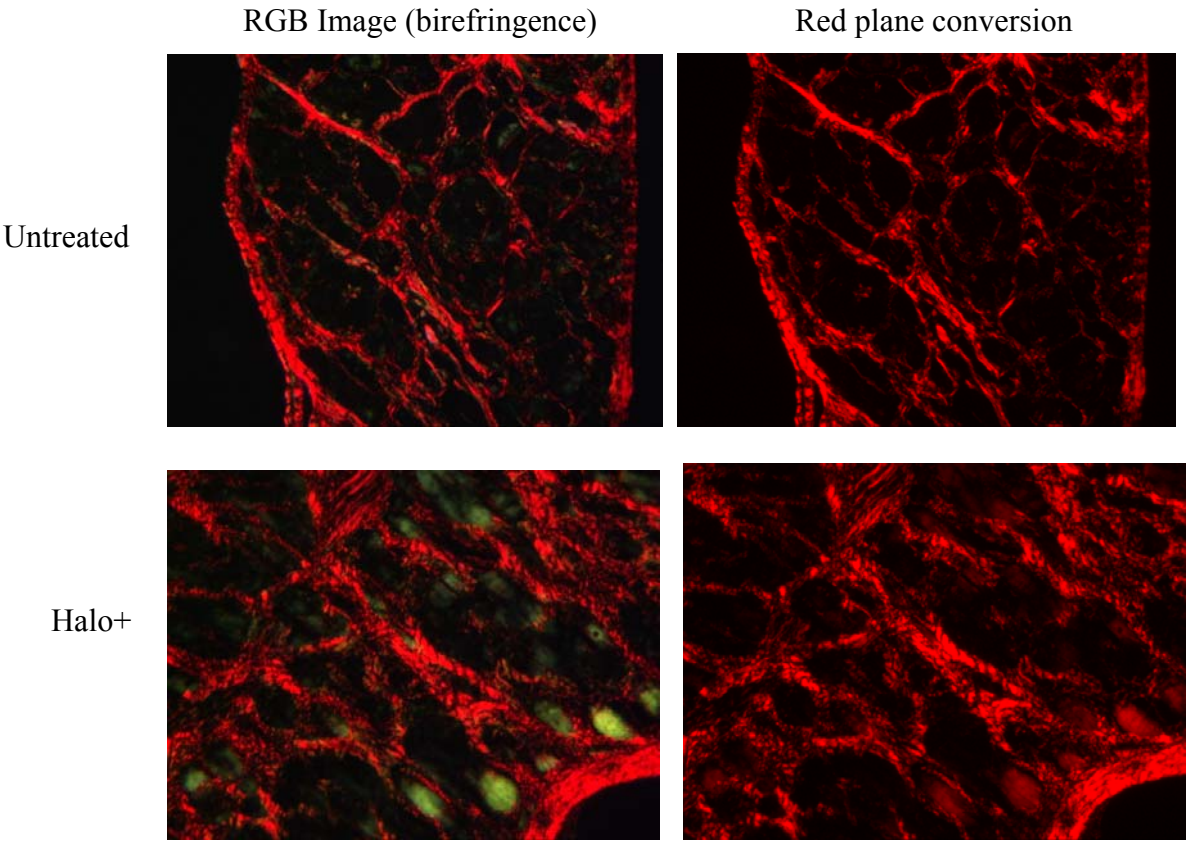
RGB Image (birefringence)
Red plane conversion
Untreated
Halo+

B

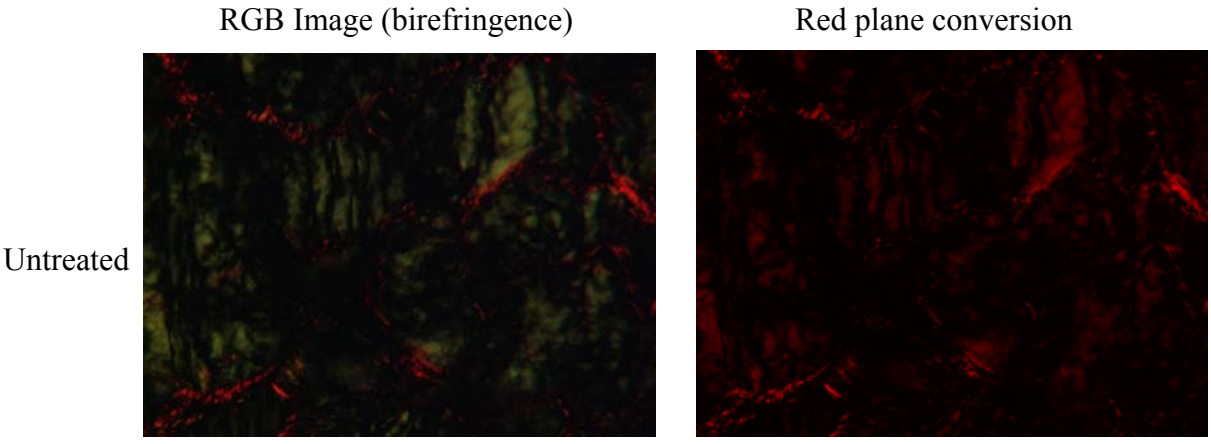
RGB Image (birefringence)
Red plane conversion
Untreated

	RGB Image (birefringence)	Red plane conversion
Halo+	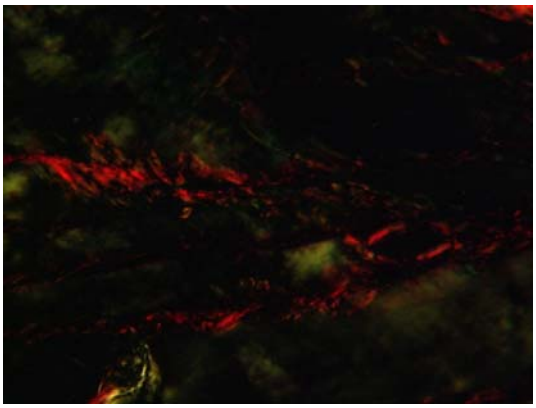	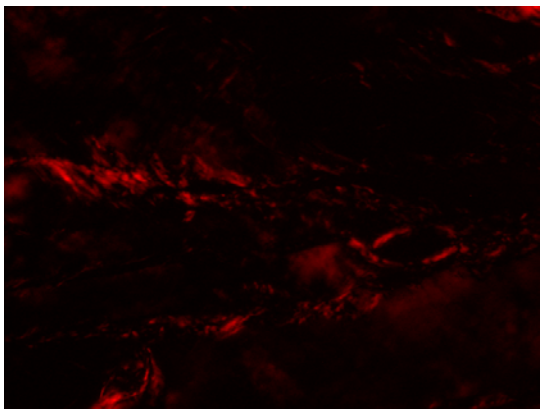

Figure 2: Sirius red measurements

A: Graphs representing the average red intensity in the diaphragm after 5 and 10 weeks of treatment, measured by Northern Eclipse. There was no significant difference between Untreated and Halo+ after either treatment period.

B: Graphs representing the average red intensity in the dystrophic quadriceps measured by Northern Eclipse. There was no significant difference between Untreated and Halo+ after 10 weeks of treatment.

A

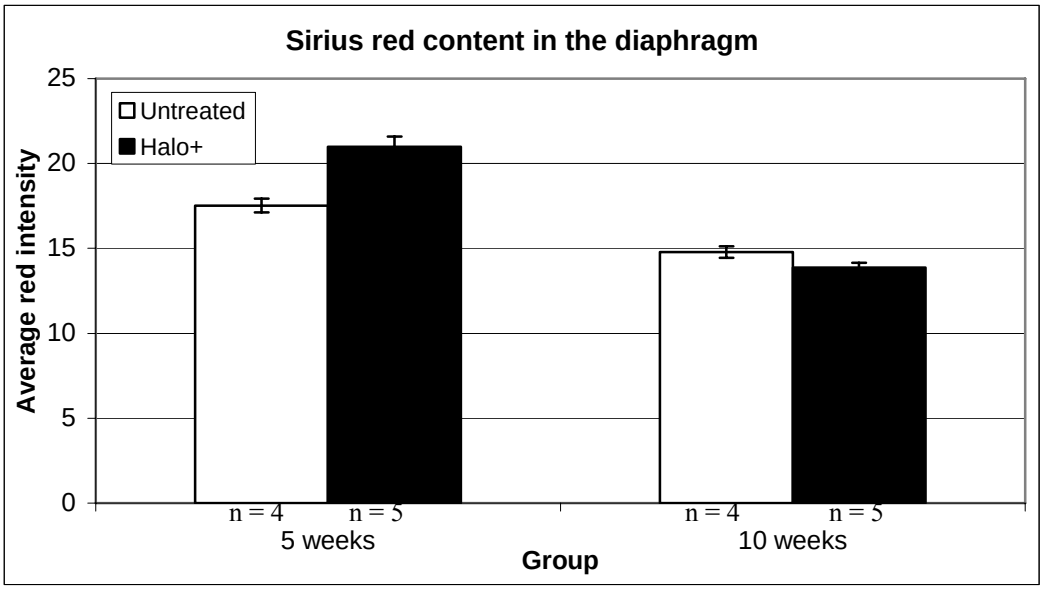
Sirius red content in the diaphragm
Untreated
Halo+
Average red intensity
25
20
15
10
5
0
n = 4
n = 5
n = 4
n = 5
5 weeks
10 weeks
Group

B

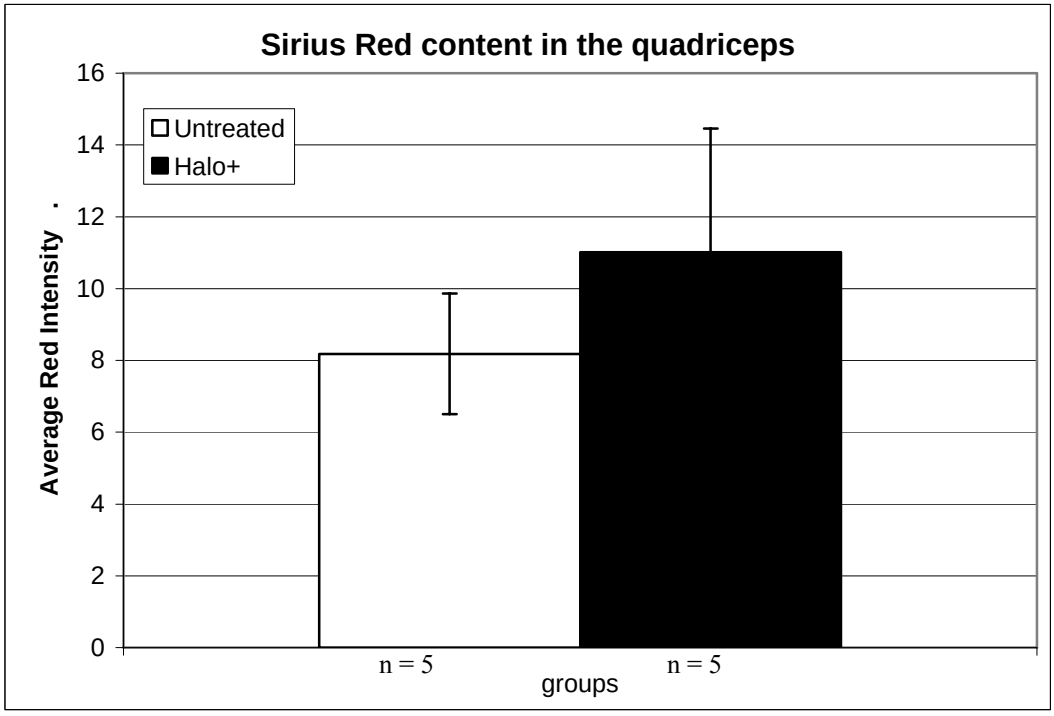
Sirius Red content in the quadriceps
Untreated
Halo+
Average Red Intensity .
16
14
12
10
8
6
4
2
0
n = 5
n = 5
groups

Figure 3: Masson's trichrome photos and measurements

This panel shows photomicrographs of the following tissues.

I: Untreated mouse diaphragm at the 5 weeks treatment time point (200x magnification).

II: Untreated mouse diaphragm at the 10 weeks treatment time point (200x magnification)

III: Halo + mouse diaphragm after 5 weeks of treatment (200x magnification)

IV: Halo + mouse diaphragm after 10 weeks of treatment (200x magnification)

V: Halo + mouse diaphragm after 12 weeks of treatment (200x magnification)

The areas of muscle (red) and fibrosis (green) are distributed focally throughout the muscles, with no apparent differences between the respective muscles from Halo+ and untreated mice. The diaphragm had more fibrosis (green) that the other tissues observed.

I

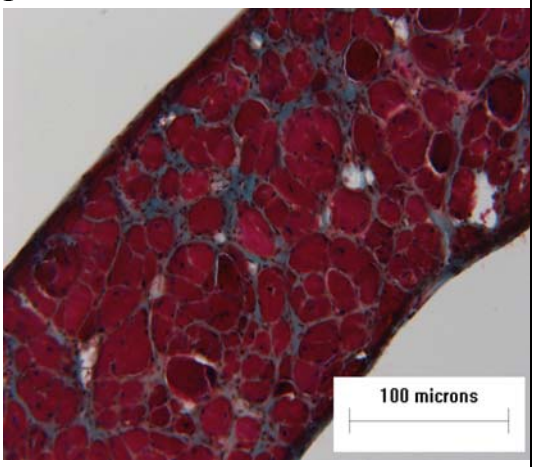
100 microns

III

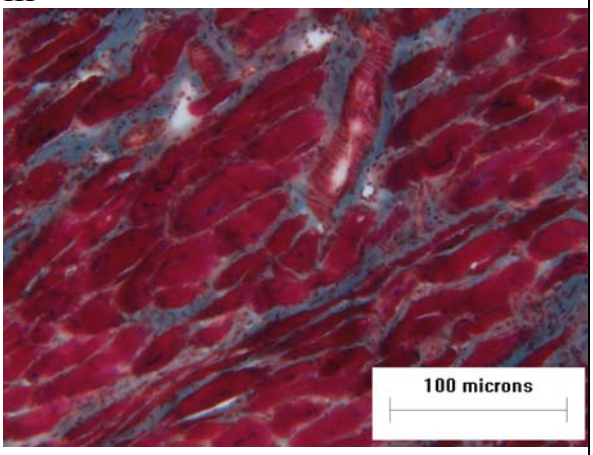
100 microns

II

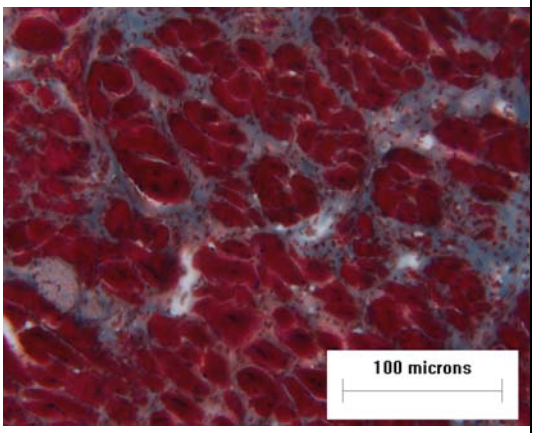
100 microns

IV

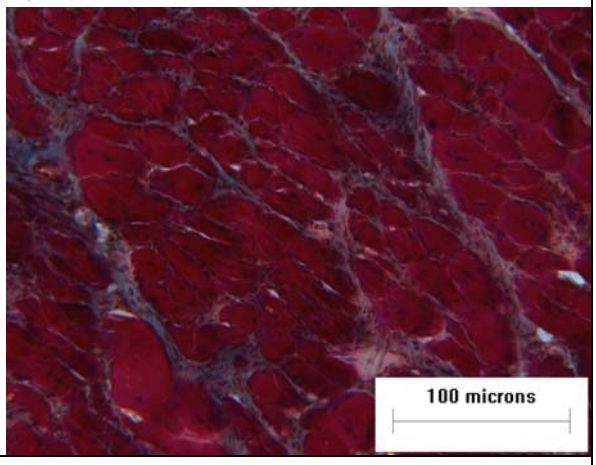
100 microns

V

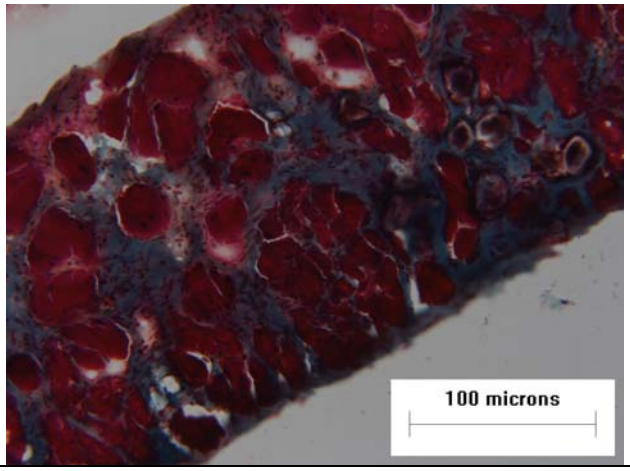
100 microns

Figure 4: Collagen I and collagen III protein content

Graphs of optical density per mg muscle scanned from Western dot blots probed

A: for collagen I (n = 4-5)

B: for collgen III. (n = 4-5)

There was no significant change in collagen content in the diaphragm of any group.

A

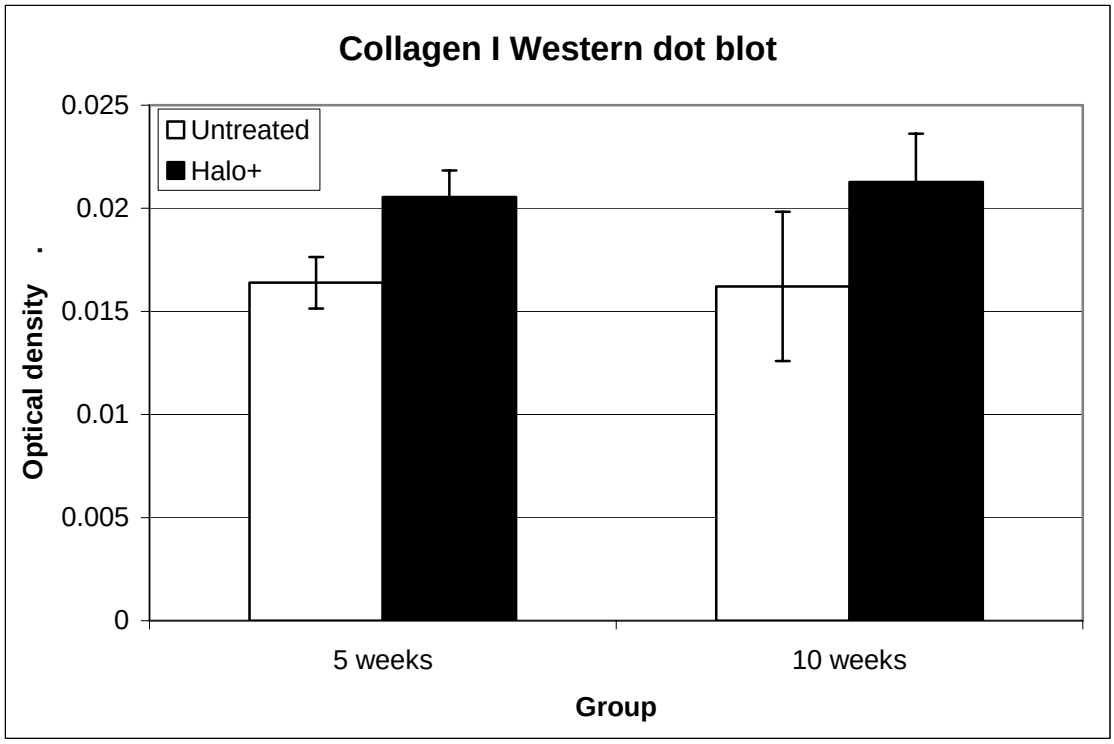
Collagen I Western dot blot
Untreated
Halo+
0.025
0.02
0.015
0.01
0.005
0
Optical density
5 weeks
10 weeks
Group

B

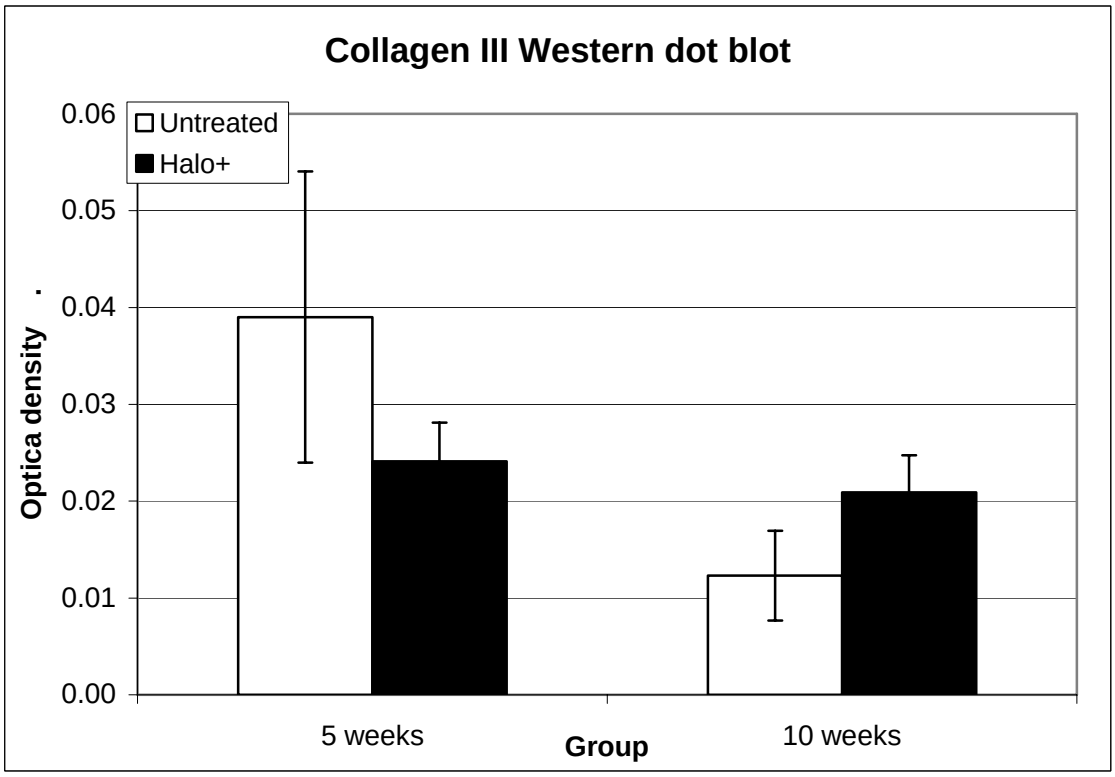
Collagen III Western dot blot
Untreated
Halo+
0.06
0.05
0.04
0.03
0.02
0.01
0.00
Optica density
5 weeks
Group
10 weeks

Figure 5: Collagen I protein content

A: Western blots of gels that were processed for immunodetection of collagen I; below each blot, the same blot probed for GAPDH. The blots show no obvious difference at 5 weeks (n = 4/group) or 10 weeks (n = 5/group) between Untreated (UT) and Halo+ (H) groups in any of the dystrophic tissues. Note that while there were multiple bands (at least 5) on each lane of the collagenase-digest western blots, only the bands at the 190kD (MW of collagen) weight are presented.

B: Graphs of optical density per mg concentration of protein scanned from Western blots probed for collagen I in

I: Quadriceps

II: Heart

III: Tibialis anterior

IV: Diaphragm

There was a significant difference in the quadriceps, tibialis anterior and heart after 5 weeks of treatment, but no significant difference between groups after 10 weeks of treatment in any of the tissues. However, there appeared to be a trend for that Halo to decrease collagen content in the tibialis anterior, quadriceps and heart after 10 weeks of treatment. The diaphragm was unchanged with treatment. There is a significant difference in the amount of collagen per mg muscle, in between the different muscles in both treated and untreated groups (*i.e.* there was significantly more collagen/mg muscle in the tibialis anterior than in the quadriceps).

A

Quadriceps:

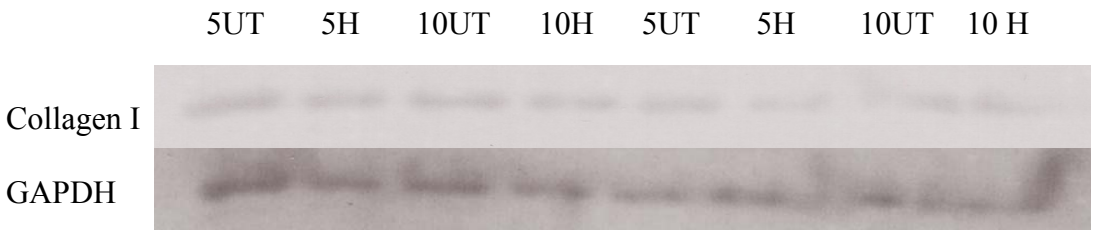

Heart:

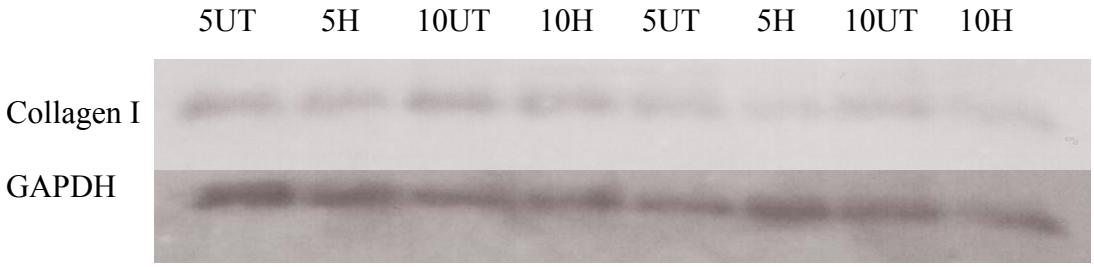

Tibialis anterior:

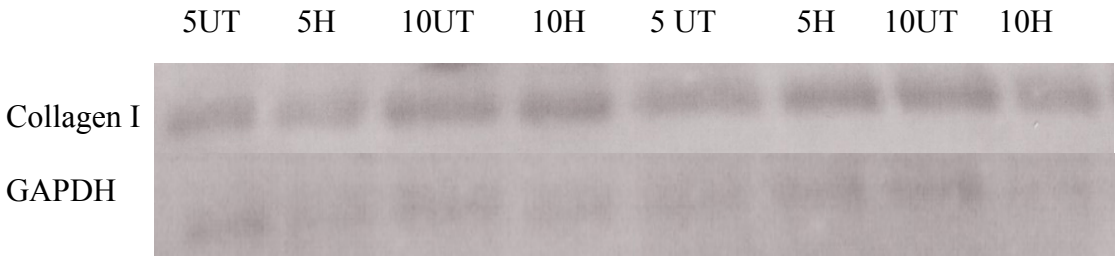

Diaphragm:

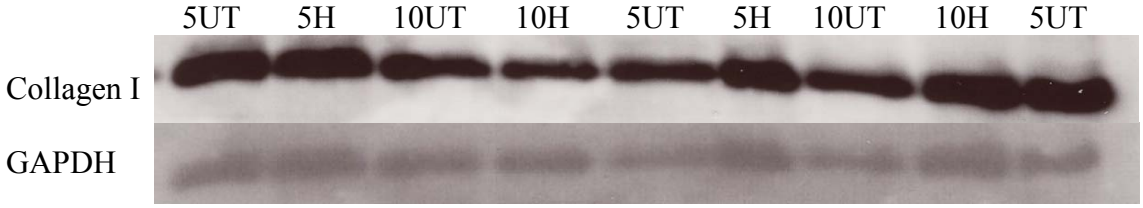

B

I

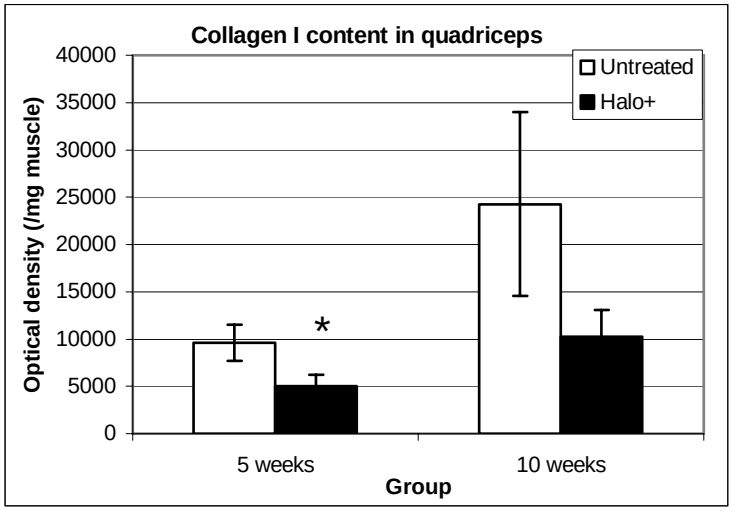
Collagen I content in quadriceps
Optical density (/mg muscle)
40000
35000
30000
25000
20000
15000
10000
5000
0
Untreated
Halo+
*
5 weeks
10 weeks
Group

II

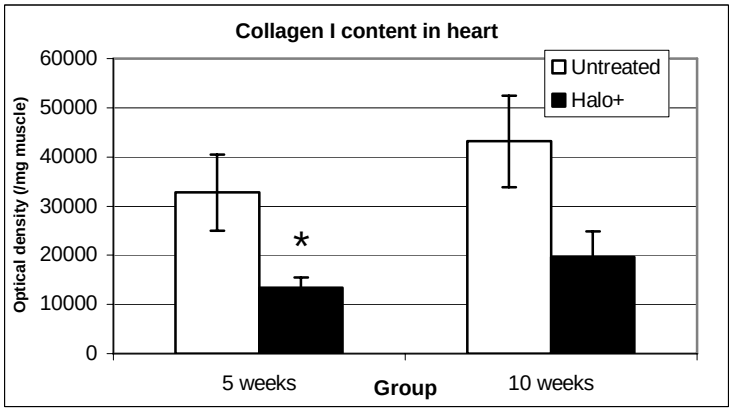
Collagen I content in heart
Optical density (/mg muscle)
60000
50000
40000
30000
20000
10000
0
Untreated
Halo+
*
5 weeks
Group
10 weeks

III

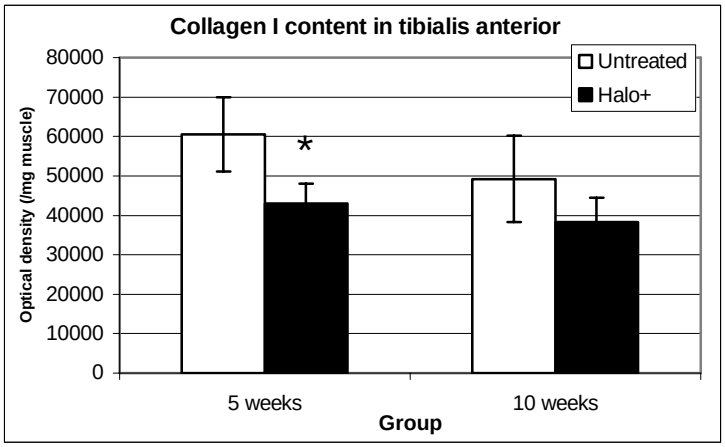
Collagen I content in tibialis anterior
Optical density (/mg muscle)
80000
70000
60000
50000
40000
30000
20000
10000
0
Untreated
Halo+
*
5 weeks
10 weeks
Group

IV

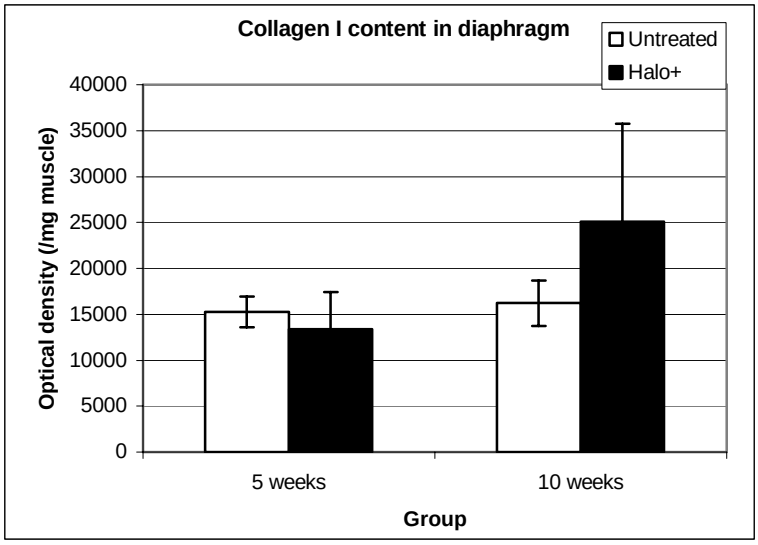
Collagen I content in diaphragm
Untreated
Halo+
Optical density (/mg muscle)
40000
35000
30000
25000
20000
15000
10000
5000
0
5 weeks
10 weeks
Group

Figure 6: HGF protein content

Graph of optical density per mg protein concentration scanned from a Western blot probed for HGF. There was a significant increase in HGF concentration in the Halo+ group after 10 weeks of treatment compared to saline controls (Untreated). (n = 5/group)

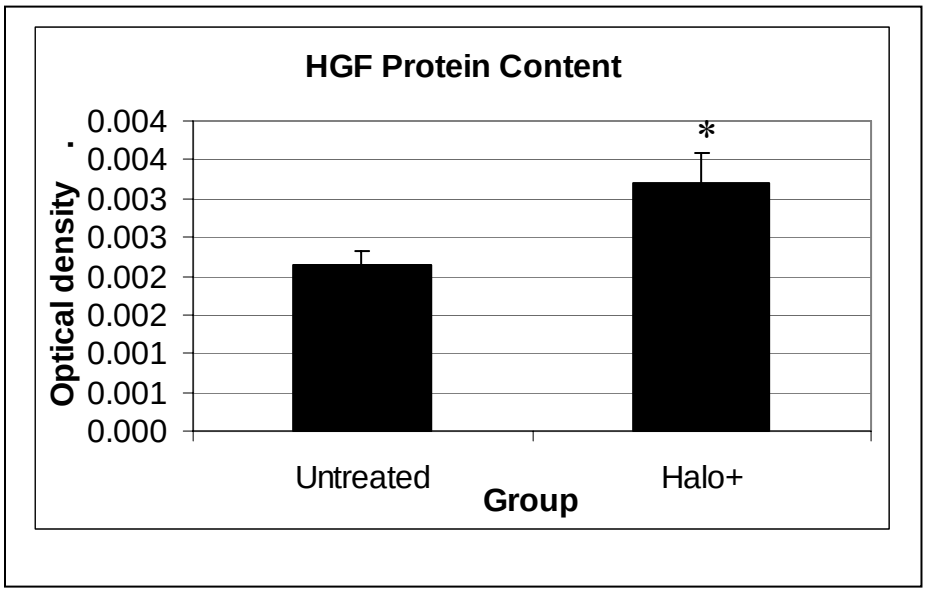
HGF Protein Content
Optical density
0.004
0.004
0.003
0.003
0.002
0.002
0.001
0.001
0.000
*
Untreated
Halo+
Group

Figure 7: Alpha-smooth muscle actin protein content

Graph of optical density per mg protein concentration scanned from a Western blot using immunodetection for α-smooth muscle actin. There was a significant decrease in α-smooth muscle actin concentration in the Halo+ group after 10 weeks of treatment compared to the untreated group (n = 5/group). For comparison, we tested the level of sma in normal muscle; the level is shown in the graph, and C57 control mice had significantly lower α-smooth muscle actin than mdx mice (Untreated). Halo treatment therefore reduced a-smooth muscle actin levels in treated dystrophic muscle to normal (C57) levels.

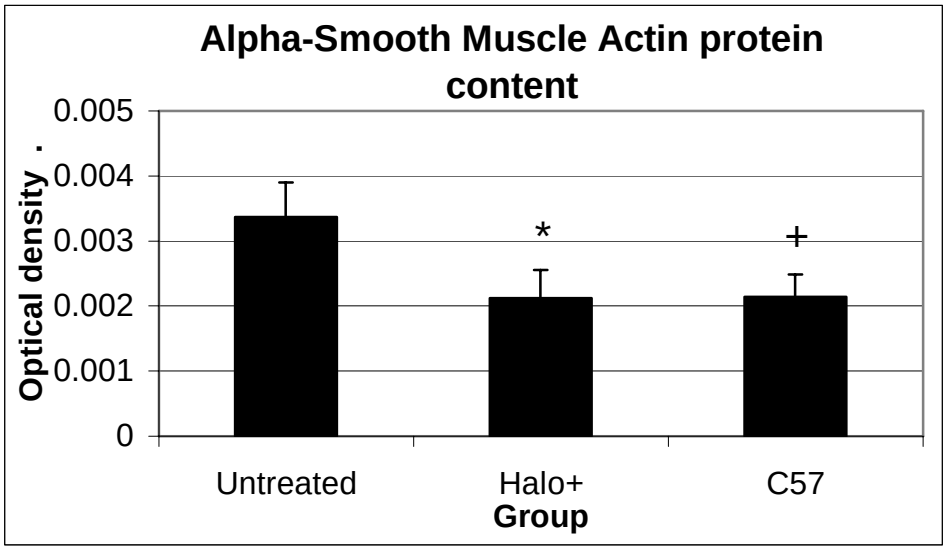
Alpha-Smooth Muscle Actin protein content
Optical density .
0.005
0.004
0.003
0.002
0.001
0
*
+
Untreated
Halo+
C57
Group

Figure 8: Collagen I and collagen III expression

A: A micrograph of skeletal muscle prepared for in situ hybridization, in which the riboprobe detection of collagen transcripts in the cytoplasm is stained brown, while nuclei are counterstained blue with hematxylin. This micrograph shows a collagen-positive cell (rank 1- 1 nucleus in the positive staining cytoplasm) (400x magnification). The blue arrow indicates a nucleus (blue) in the collagen-positive mRNA of the cytoplasm (brown).

B: A micrograph of skeletal muscle prepared for in situ hybridization, in which the riboprobe detection of collagen transcripts in the cytoplasm is stained brown, while nuclei are counterstained blue with hematxylin. This micrograph shows collagen-positive centrally located nuclei (green arrow).

C: A micrograph of skeletal muscle prepared for in situ hybridization, in which the riboprobe detection of collagen transcripts in the cytoplasm is stained brown, while nuclei are counterstained blue with hematxylin. This micrograph showscollagen-positive cells (400x magnification). The blue arrow indicates nuclei in the collagen-positive mRNA (rank 2- 2-5 nuclei in the positive staining cytoplasm). The yellow arrow indicates an area positively stained for collagen mRNA containing multiple nuclei (rank 3).

Positively-stained cells were ranked and counted along the long axis of each section to determine the number of cells expressing collagen. There was a significant decrease in the number of cells expressing collagen for all rankings after treatment with Halo.

A

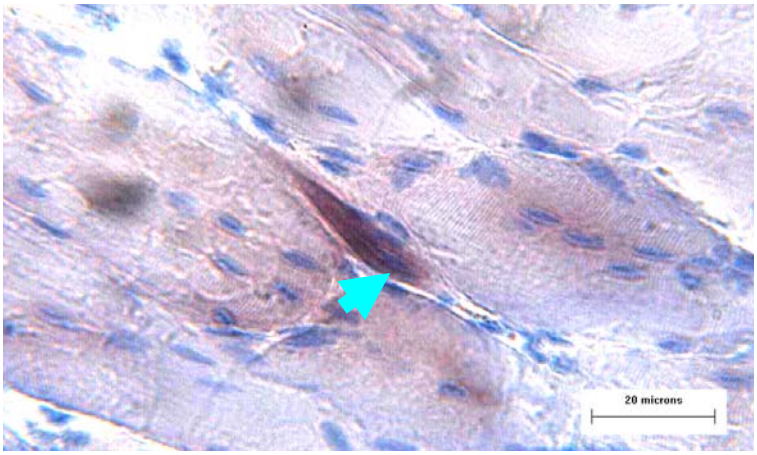

B

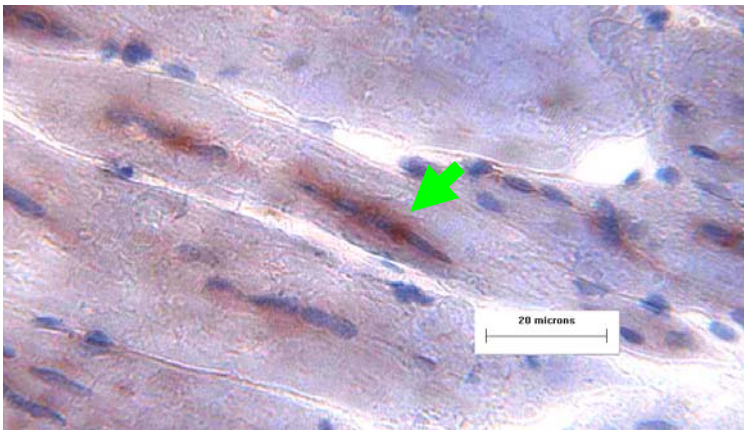

C

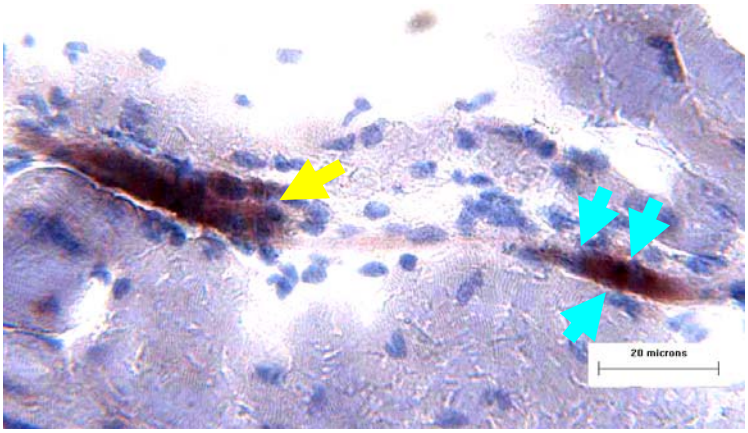

Figure 9: Ki67 staining

Table of the number of Ki67-positive (proliferating) cells 5 fields in sections of muscle tissue collected from mdx mice, either treated or untreated with Halo for 5 or 10 weeks. The asterisks indicate changes as follows: * indicates a decrease at $p<0.05$; ** indicates a decrease at $p<0.025$; $^{+}$ indicates an increase at $p<0.05$; $^{++}$ indicates an increase at $p<0.025$). There was generally a decrease in proliferation within fibrotic regions and an increase in proliferation in muscle regions in quadriceps, tibialis anterior and diaphragm muscles after 5 weeks treatment, while after 10 weeks, there were no significant differences between proliferation in any of the muscle tissues from treated and untreated mice.

Tissue	Location	5 weeks		10 weeks	
		Untreated	Halo+	Untreated	Halo+
Diaphragm	**ECM**	51.8 ± 10.7	31.3 ± 3.5 *	39.0 ± 17.8	27.8 ± 7.2
	Muscle	15.0 ± 3.5	11.0 ± 2.9	20.8 ± 7.0	11.0 ± 2.9
Heart	**ECM**	19.3 ± 4.6	8.3 ± 3.0	17.0 ± 7.5	17.4 ± 8.9
	Muscle	6.0 ± 1.7	4.8 ± 1.6	4.6 ± 2.1	4.2 ± 1.5
Quadriceps	**ECM**	12.3 ± 2.9	5.5 ± 0.6 **	2.2 ± 0.7	6.3 ± 1.7
	Muscle	4.3 ± 2.2	16.0 ± 3.5 $^{++}$	5.8 ± 3.1	8.3 ± 3.5
Tibialis Anterior	**ECM**	21.3 ± 3.5	12.0 ± 4.4 *	9.0 ± 2.9	20.0 ± 11.6
	Muscle	5.0 ± 2.8	12.5 ± 5.5 $^{+}$	8.6 ± 3.8	3.3 ± 1.2

Figure 10: Ki67 proliferation index

A: Graph of the number of Ki67-positive cells in areas of muscle and extracellular matrix (ECM) (as assessed by the method explained in Figure 9) in the diaphragm after 5 and 10 weeks of treatment. There was a significant decrease in ECM cell proliferation after 5 of weeks of treatment with Halo ($p < 0.05$). However, there was no significant difference in any other group.

B: Graph of the number of Ki67-positive cells in areas of muscle and extracellular matrix (ECM) (as assessed by the method explained in Figure 9) in the heart after 5 and 10 weeks of treatment. There was no significant difference with treatment.

C: Graph of the number of Ki67-positive cells in areas of muscle and extracellular matrix (ECM) (as assessed by the method explained in Figure 9) in the quadriceps after 5 and 10 weeks of treatment. There was a significant decrease in ECM cell proliferation after 5 of weeks of treatment with Halo ($p < 0.05$) and a significant increase in muscle cell proliferation after 5 weeks of treatment with Halo ($p < 0.05$). However there was no significant difference after 10 weeks of treatment in the ECM of muscle.

D: Graph of the number of Ki67-positive cells in areas of muscle and extracellular matrix (ECM) (as assessed by the method explained in Figure 9) in the tibialis anterior after 5 and 10 weeks of treatment. There was a significant decrease in ECM cell proliferation

after 5 of weeks of treatment with Halo ($p < 0.05$). However, there was no significant difference in any other group.

A

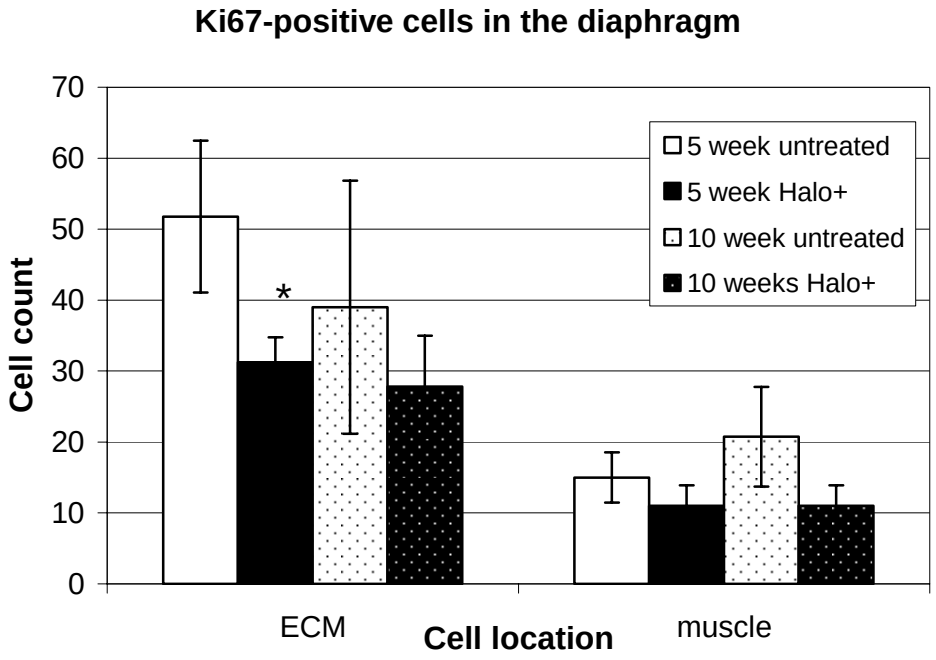
Ki67-positive cells in the diaphragm
70
60
50
40
30
20
10
0
Cell count
*
5 week untreated
5 week Halo+
10 week untreated
10 weeks Halo+
ECM
Cell location
muscle

B

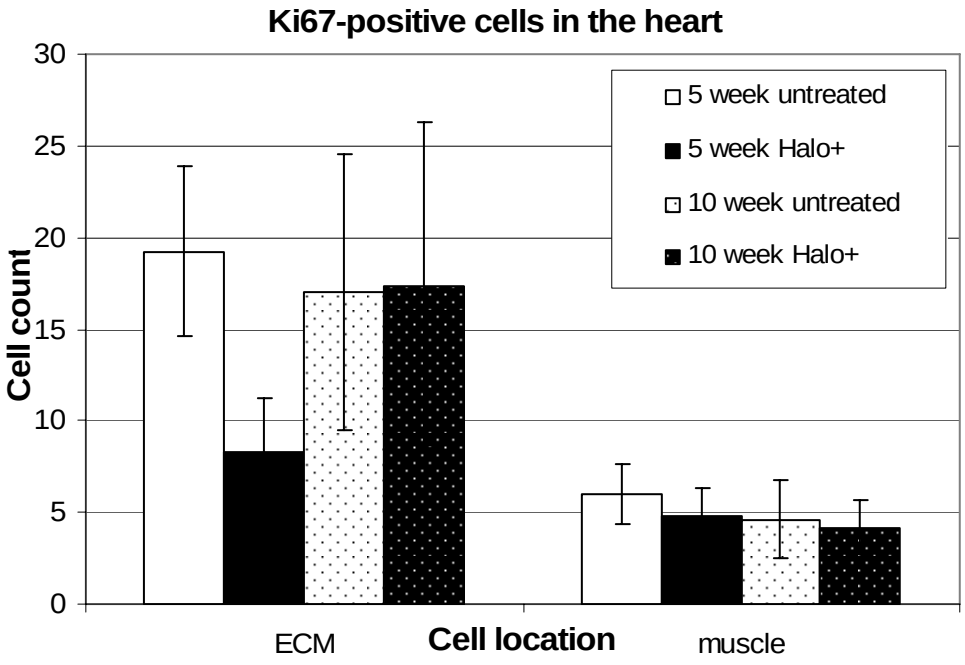
Ki67-positive cells in the heart
30
25
20
15
10
5
0
Cell count
5 week untreated
5 week Halo+
10 week untreated
10 week Halo+
ECM
Cell location
muscle

C

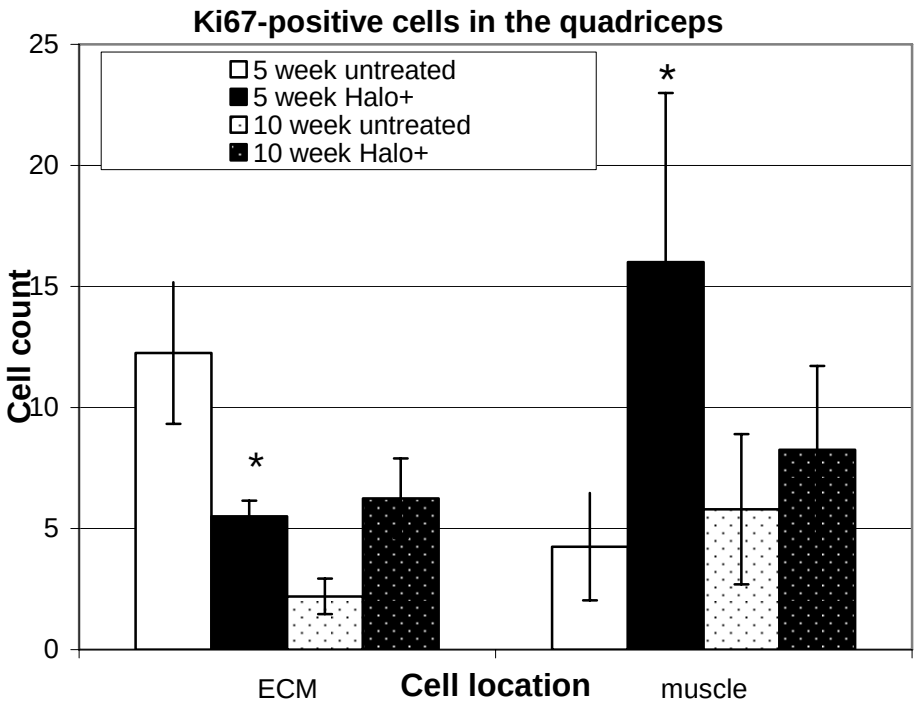
Ki67-positive cells in the quadriceps
5 week untreated
5 week Halo+
10 week untreated
10 week Halo+
Cell count
25
20
15
10
5
0
*
*
ECM
Cell location
muscle

D

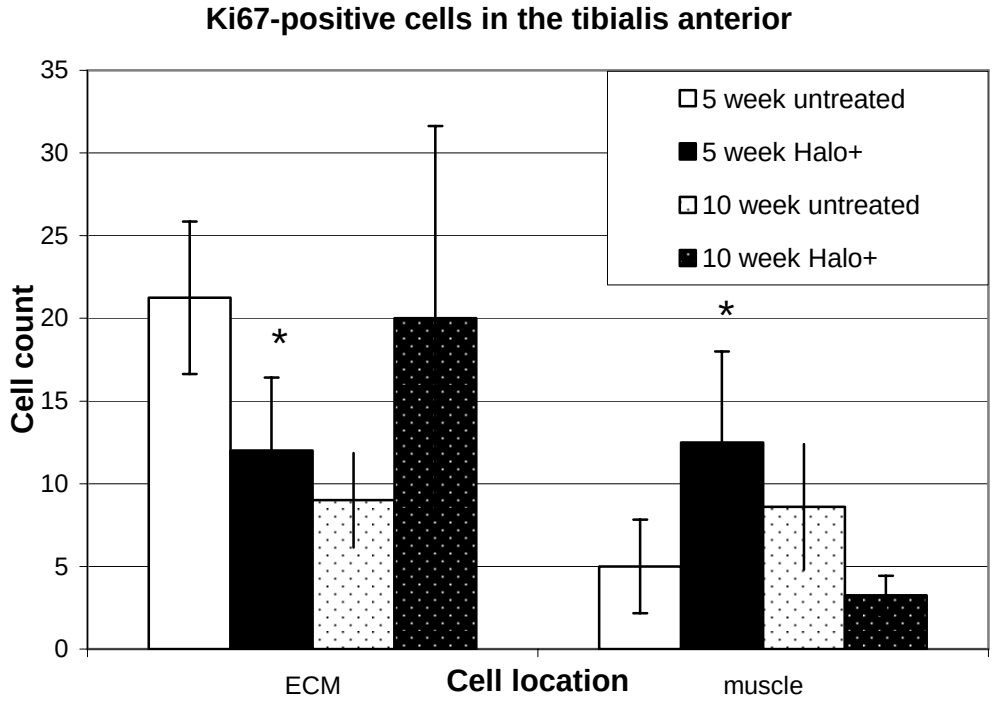
Ki67-positive cells in the tibialis anterior
5 week untreated
5 week Halo+
10 week untreated
10 week Halo+
Cell count
35
30
25
20
15
10
5
0
*
*
ECM
Cell location
muscle

Figure 11: Grip strength

A: Apparatus for strength testing using a Chatillon gauge with a bar attached for the mouse to pull on.

B: Graph representing forelimb grip strength measured as peak pull at weeks 1 through 10 in Untreated or Halo+ groups, as indicated. No significant difference was observed between groups at any time point (ANOVA; $p>0.05$). This is one example of how the data were analyzed. Note that the force exerted (peak pull) by the Untreated mice is irregular and varies a great deal from week to week and more so as time increases, while the Halo+ mice pulled a relatively consistent force level from week to week.

A

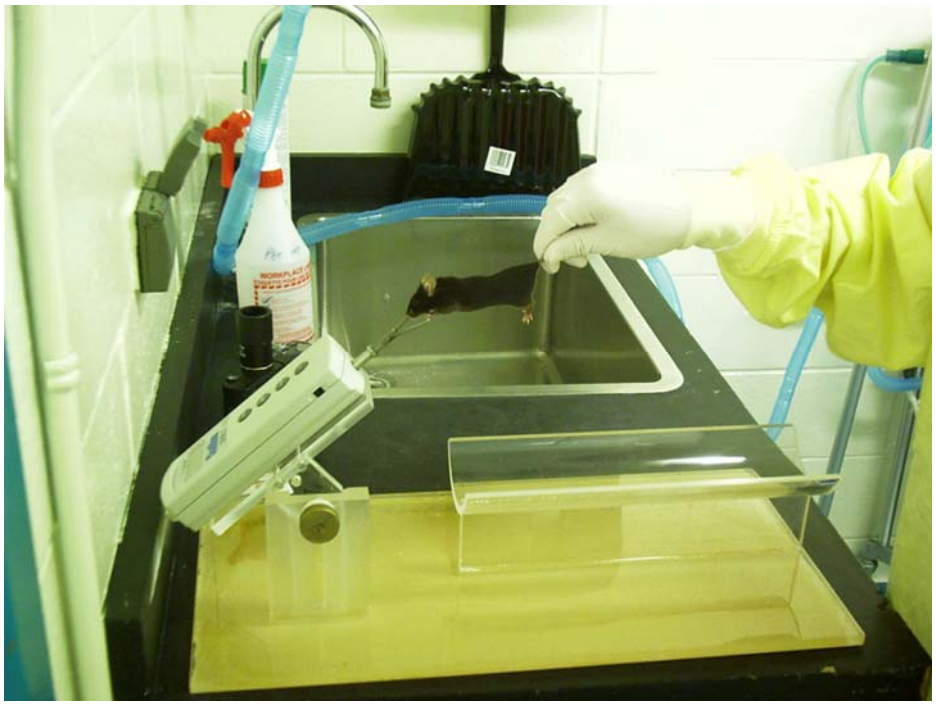

B

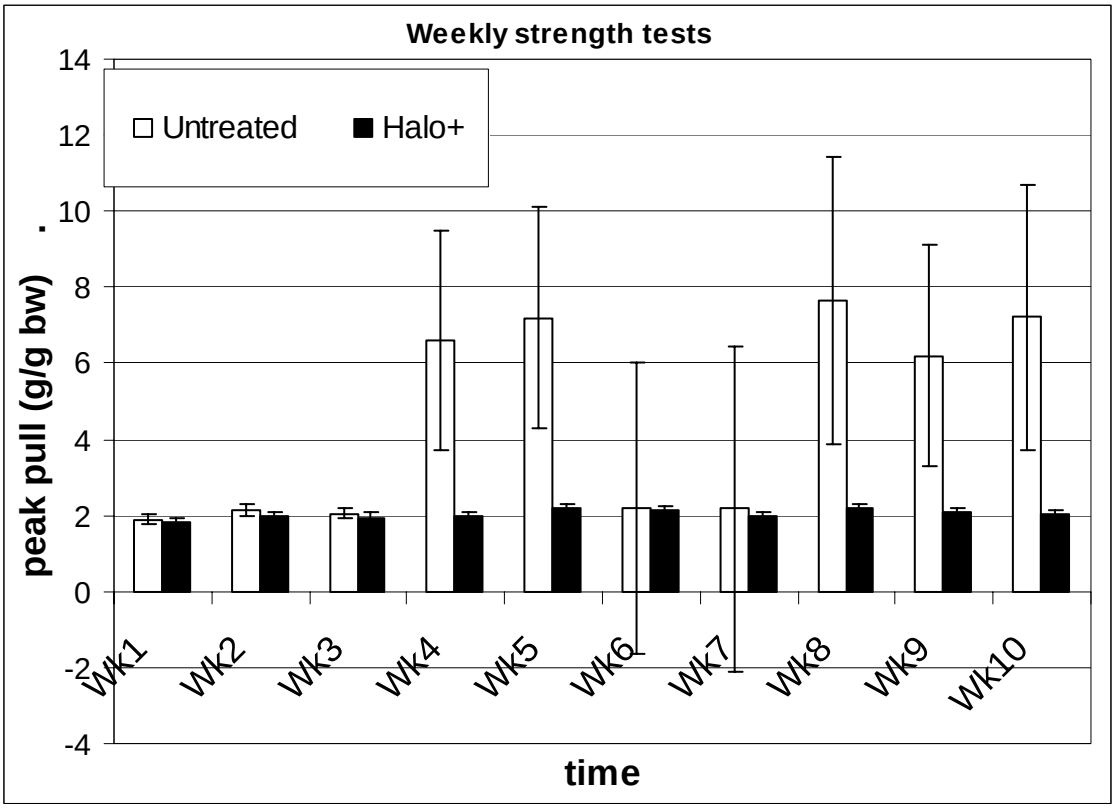
Weekly strength tests
Untreated
Halo+
peak pull (g/g bw)
14
12
10
8
6
4
2
0
-2
-4
Wk1
Wk2
Wk3
Wk4
Wk5
Wk6
Wk7
Wk8
Wk9
Wk10
time

Figure 12: Running apparatus, distance run

A: Apparatus for 24 hour voluntary running using a rodent wheel, switch, and automatic counter (on top of the cage).

B: Plot representing the average distance traveled weekly during voluntary exercise. Distance was normalized to body weight (mean ± SEM). Groups varied in size (n = 13-14 in the first 5 weeks; n = 9-10 in the second 5 weeks; n = 4-5 in final 2 weeks and EBD run). Note that the Untreated group ran more varied distances from week to week, while the Halo+ group stayed more consistent from week to week. In the final, EBD run there was a dramatic drop in both groups, however, the Untreated group drops much further than the Halo+ group.

C: A graph representing the distance traveled during the final, EBD run of voluntary exercise. This was 4 days after the penultimate running trial. Halo+ group ran a significantly longer distance than the Untreated group in this run ($p<0.05$). (Comparison is to untreated).

A

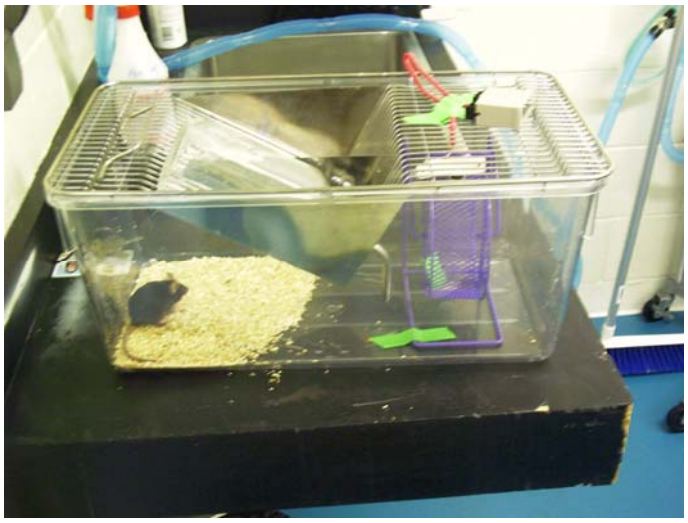

B

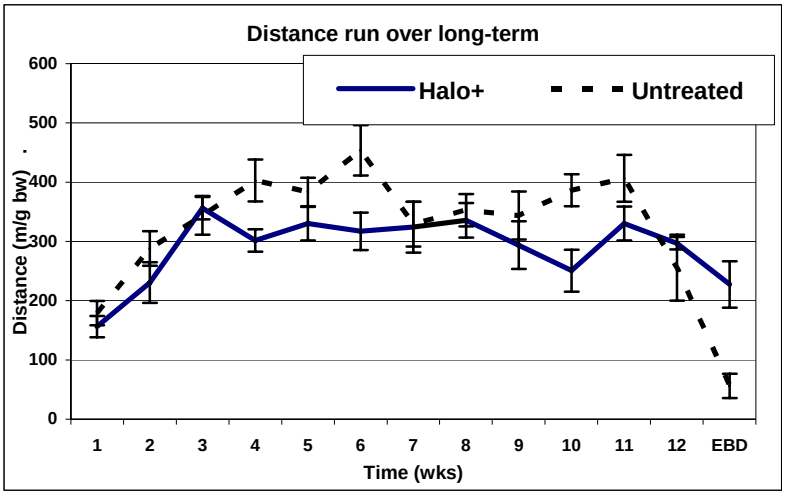
Distance run over long-term
Halo+
Untreated
Distance (m/g bw)
600
500
400
300
200
100
0
1
2
3
4
5
6
7
8
9
10
11
12
EBD
Time (wks)

C

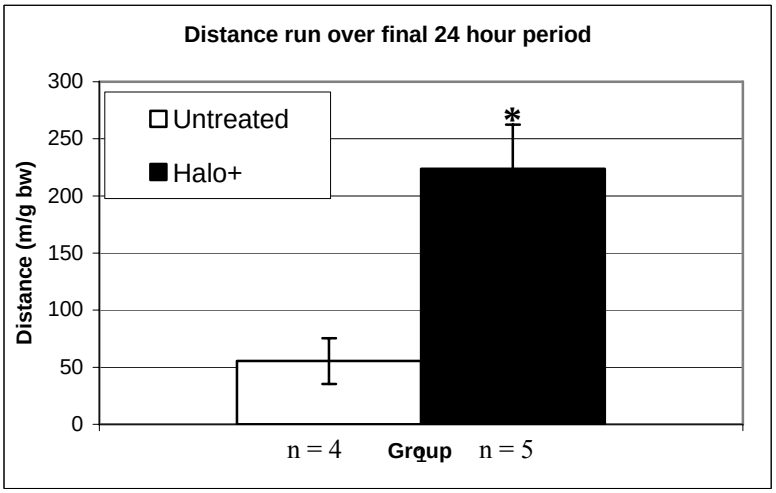
Distance run over final 24 hour period
Untreated
Halo+
Distance (m/g bw)
300
250
200
150
100
50
0
*
n = 4
Group
n = 5

Figure 13: Evans Blue Dye (EBD) photos and counts

A: Cross-section of quadriceps from a representative section of a treated mouse showing both EBD-positive and EBD-negative fibers. The photo is a montage of images taken at 100x magnification to form the entire tissue section. The Arrow points to an EBD-positive fiber. Note that the edges of each muscle section were not counted to eliminate any possible edge effect (as previously noticed in many samples and staining procedures).

B: Frequency distribution of the proportion of EBD-positive fibers. The Untreated group had a significantly higher proportion of EBD-positive fibers than the Halo+ group after 12 weeks of treatment (n = 3-5/group).

C: A scatter plot graph showing the relationship between the proportions of EBD-positive fibers to the distance run in the final running test. Linear-regression lines (from an Excel calculation) for datapoints in the two groups Halo-treated and Untreated,are also plotted. These curves show that in untreated mice, there was an increase in fiber damage as running distance increased. There was no relationship in Halo+ mice between the proportions of EBD-positive fibers and distance run as distance increased.

A

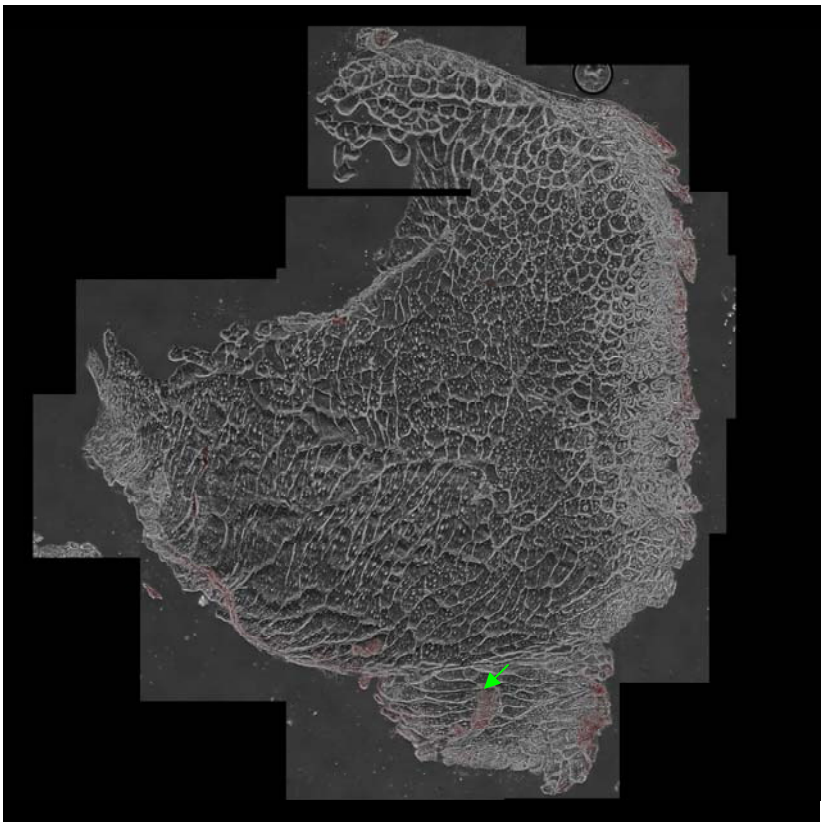

B

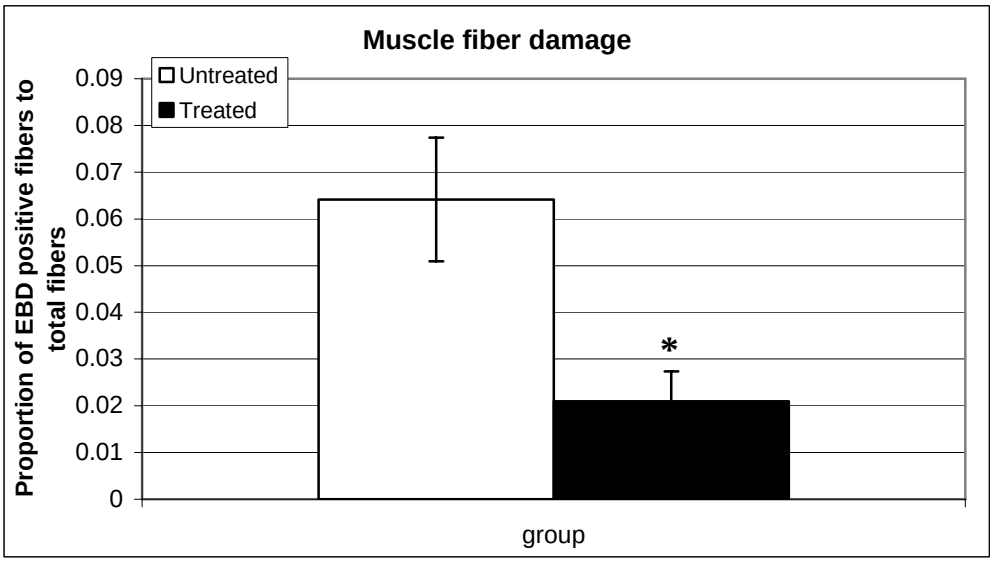
Muscle fiber damage
Untreated
Treated
Proportion of EBD positive fibers to total fibers
0.09
0.08
0.07
0.06
0.05
0.04
0.03
0.02
0.01
0
*
group

C

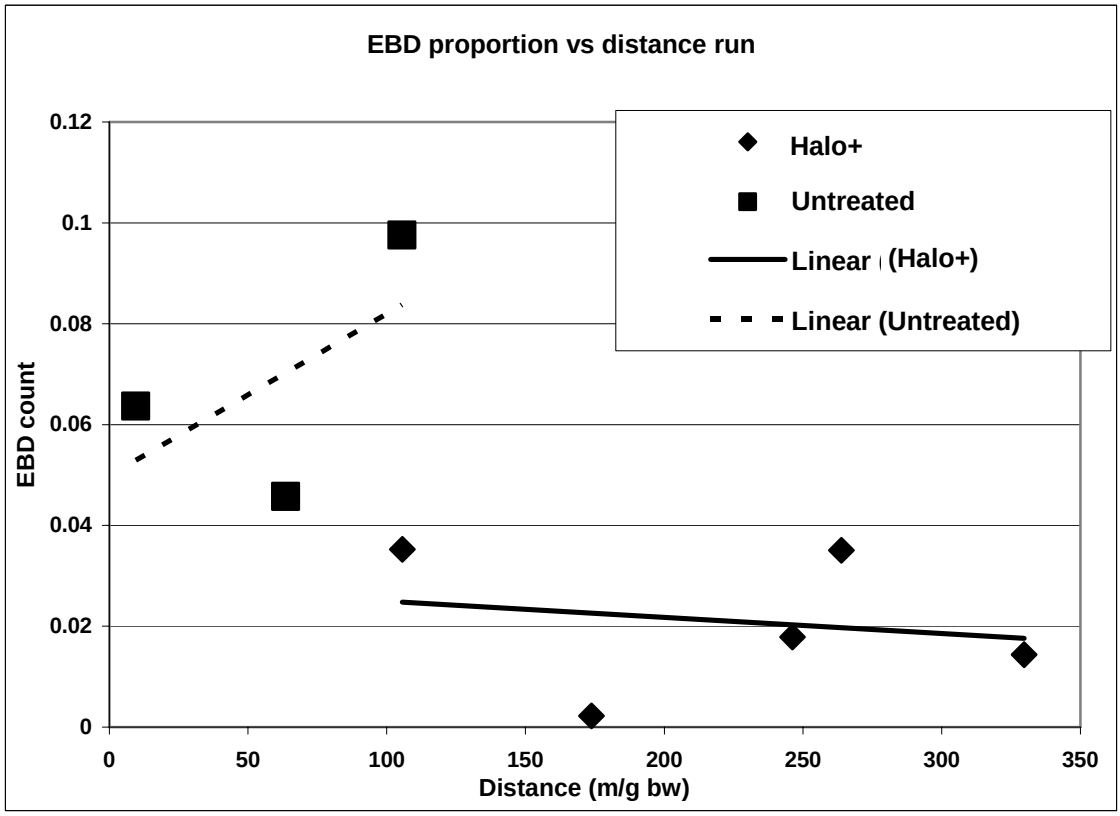
EBD proportion vs distance run
0.12
0.1
0.08
0.06
0.04
0.02
0
EBD count
0
50
100
150
200
250
300
350
Distance (m/g bw)
Halo+
Untreated
Linear (Halo+)
Linear (Untreated)

Figure 14: Respiratory dysfunction

A: Buxco Plethysmograph with four individual chambers for mice, sodium-lime filtration, and computer with software.

B: B is the tracings of a single experiment on a representative mouse from each of the Untreated and Halo+ groups. Graphs represent the breathing profiles of mice. The image on the top is an Untreated mouse and on the bottom is the profile of a Halo+ mouse. The large spikes are artifacts of the procedure, and represent the timing of each increasing dose of methacholine (see the tracing in panel C for the dose levels). Note that the slope of the tracing for the Untreated mouse increases with increasing doses of methacholine, while the Halo+ mouse has a breathing pattern which the tracing shows as remaining relatively stable and at baseline levels over the period of increasing doses of methacholine during the challenge test.

C: A Graph representing the response measured in Penh of the Halo+ and Untreated mice pooled at 10 (n = 5/group) and 12 weeks (n = 4-5/group) of treatment. Halo+ mice have a lower response to methacholine than Untreated mice. Also, note that Untreated mice begin to show increases in Penh after a dose of 12.5 mg/mL, while Penh of Halo+ mice does not begin to increase until a dose of 25 (mg/mL).

A

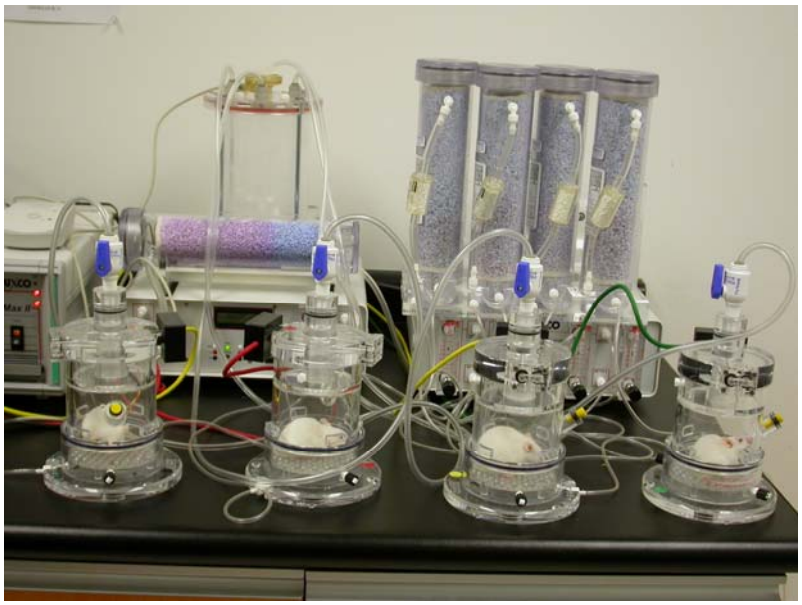

B

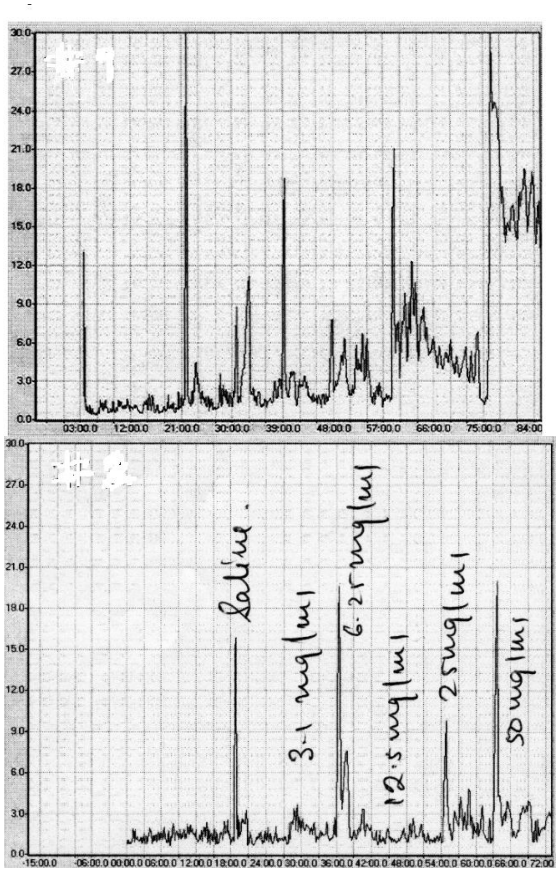

C

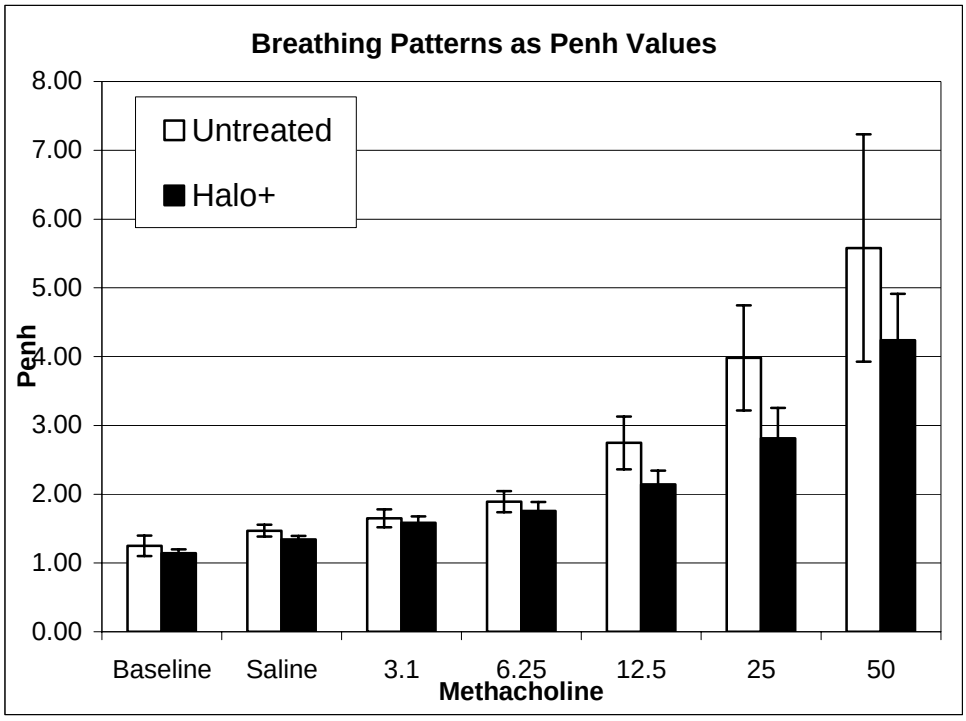
Breathing Patterns as Penh Values
8.00
7.00
6.00
5.00
4.00
3.00
2.00
1.00
0.00
Penh
Untreated
Halo+
Baseline
Saline
3.1
6.25
12.5
25
50
Methacholine

Figure 15: Vimentin protein content

A: Western blots first probed for vimentin (top panel) and then for GAPDH (lower panel in A). There was no difference at 5 weeks or 10 weeks between Untreated (UT) and Halo+ (Halo) groups (n = 4-5).

B: Graph of optical density per mg muscle scanned from Western blots (figure 14A) probed for vimentin. In the heart muscle there was no difference between Halo+ and Untreated mice at either 5 or 10 weeks of treatment.

A

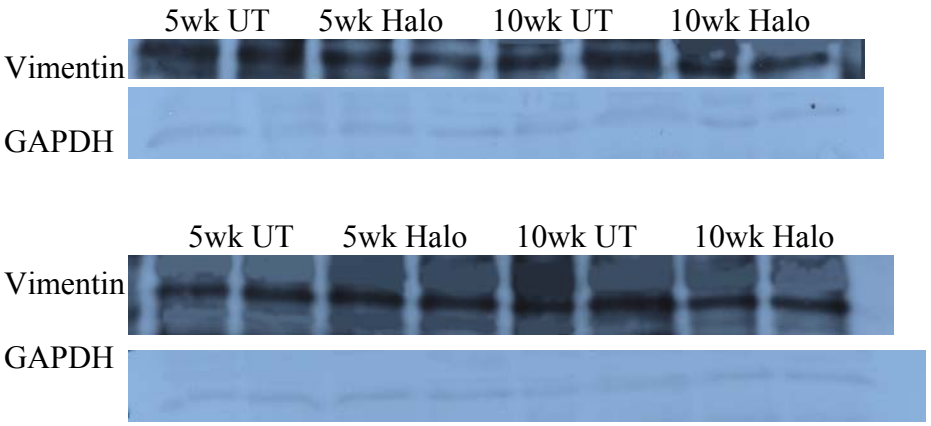
5wk UT
5wk Halo
10wk UT
10wk Halo
Vimentin
GAPDH
5wk UT
5wk Halo
10wk UT
10wk Halo
Vimentin
GAPDH

B

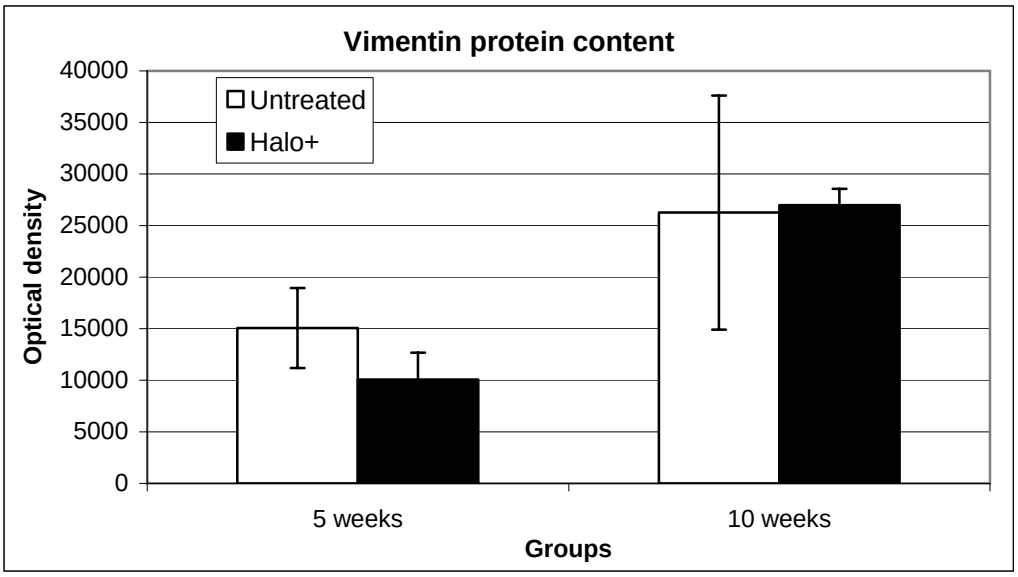
Vimentin protein content
Optical density
40000
35000
30000
25000
20000
15000
10000
5000
0
Untreated
Halo+
5 weeks
10 weeks
Groups

Figure 16: Summary of the discussion section, represented as a model of the pathways that were affected by Halo treatment, as determined by the findings of this thesis project.

Halo (mode of action unknown) increases HGF, this inhibits TGFβ and reduces the number of fibroblasts and myofibroblasts in the muscle. In addition to fewer myofibroblasts, a greater number of myofibroblasts undergo apoptosis as they have remodeled the tissue and muscle repair has occurred. Fewer myofibroblasts, in turn means less collagen expression and production, and less scar tissue. There is more muscle and less collagen; therefore the extracellular matrix becomes looser as fibrosis decreases. Muscles undergo repair more easily due to the decreases in fibrosis, increasing proliferation of muscle cells and reduction in the number of active myofibroblasts. This increases muscle function and reduces the ongoing progression of muscle damage from activity in muscular dystrophy.

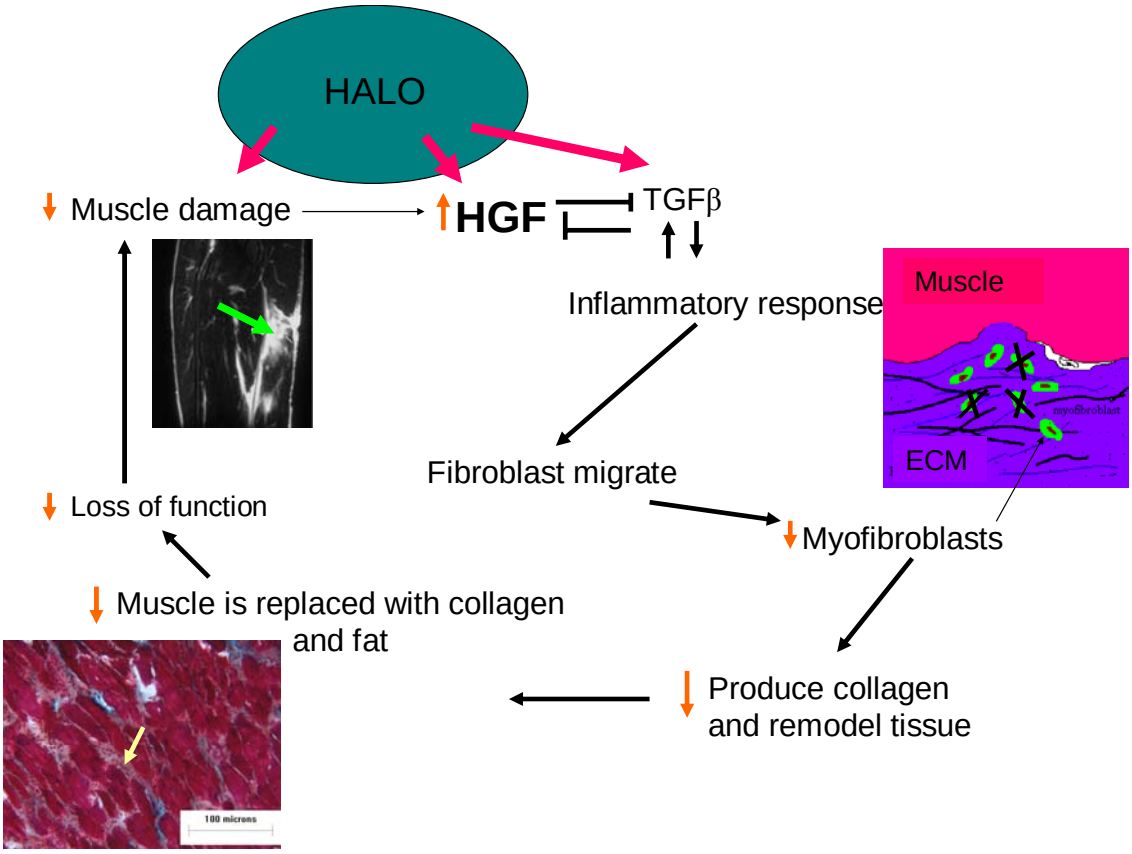
HALO
Muscle damage
HGF
TGFβ
Inflammatory response
Muscle
myofibroblast
ECM
Fibroblast migrate
Loss of function
Myofibroblasts
Muscle is replaced with collagen and fat
Produce collagen and remodel tissue
100 microns

Chapter 6. DISCUSSION

Results of these experiments are the first to our knowledge to demonstrate that fibrosis in dystrophic muscle can be treated with halofuginone hydrobromide (Halo). Halo reduced collagen I and collagen III expression in mdx muscle as measured by *in situ* hybridization; this is considered strong evidence of reduced myofibroblast activity after treatment, which is consistent with the findings of reduced α-smooth muscle actin and greater HGF in muscles after treatment.. Fibrosis decreased, increasing muscle cell proliferation, sparing dystrophic muscles from exercise-induced damage, increasing cardiorespiratory function, and decreasing the severity of disease progression.

1. COLLAGEN CONTENT

Collagen protein content was measured with numerous techniques. These included Sirius red, Masson's trichrome, dot blots for collagen I and III, and Western blots for collagen I (see below). The Western blots showed a significant difference after 5 weeks of treatment, but not after 10 weeks of treatment. However, none of the other techniques yielded any change in protein levels after treatment with Halo in any group.

Collagen content was previously shown to decrease after Halo treatment in mice and rats (Bruck *et al* 2001,Gnainsky *et al* 2004,Levi-Schaffer *et al* 1996,Nagler *et al* 1996,Nagler *et al* 1998,Nagler *et al* 1999,Nagler *et al* 2000,Nagler and Pines 1999,Pines *et al* 2001,Pines *et al* 2003). Some examples are: tight-skin (Tsk) mice, murine chronic graft versus host disease, murine scleroderma, and pulmonary fibrosis in the rat. The

mice and rats used in these studies suffered from fibrotic diseases where fibrosis was the primary disorder. In mdx mice and Duchenne muscular dystrophy (DMD) fibrosis is a secondary response to membrane degeneration (Finsterer and Stollberger 2003,Liu *et al* 1996b). It is possible that due to Halo's, still unknown, mode of action it cannot regulate the secondary fibrosis related to muscular dystrophy. Unlike other fibrotic conditions, collagen is continually produced in DMD; as muscle degenerates collagen is laid down in the ECM. Therefore, unless the issue of preventing muscle membrane damage is addressed, Halo treatment would not likely have a lasting effect. Collagen I and collagen III fibers create a meshwork in the ECM by cross-linking with themselves and with each other (von der 1981). It is possible that Halo alters the molecular conformation of collagen or alters the lysine residues that allow Schiff-base cross-links (Kagan and Trackman 1991) preventing fibers from cross-linking. Alternatively it may break the already-formed cross-links by activation of metalloproteinase activity. If Halo alters the balance between formation and degredation cross-links, there may be no change in collagen content. However, we would expect to see changes related to the impact of fibrosis, for example functional improvements.

Although the studies with Western blots did not show any significant difference after 10 weeks of treatment with Halo, they showed a trend for Halo to reduce collagen content in the quadriceps, heart and tibialis anterior. Interestingly, there seemed to be no observed trend to reduced collagen content in the diaphragm, where it was anticipated an antifibrotic effect would show most clearly. The diaphragm has the most extensive fibrosis of the muscle tissues (Stedman *et al* 1991) which may be partly necessary for its continued function. Therefore, Halo may not be able to resolve the extensive

extracellular network present in mdx diaphragm. However, we saw a trend for Halo to decrease collagen protein in other muscles after 10 weeks of treatment and a significant decrease after 5 weeks of treatment in the quadriceps, tibialis anterior and heart.

The techniques used to quantify collagen content are generally only semi-quantitative and may not be specific enough to detect subtle changes in. Sirius red has been used in many studies to quantify collagen (*e.g.*, (Gavish *et al* 2002,Hsu *et al* 2006,Pines *et al* 2001). However, after some investigation of the literature we found out that many researchers used the stain incorrectly, based on its specificity for collagen under polarized light (Sweat *et al* 1964). Since many investigators use epi-fluorescence or bright field measures of red and green areas, this difference in method may explain a contradiction in results. The changes in collagen content were very dramatic in the above examples; it is possible that are changes in the present study were simply too small to detect by chemical stains, such as Sirius red and Masson's trichrome.

As an aside, we noticed the central nuclei in mdx mouse muscle fibers were stained red with Sirius red. This was unexpected. However, the central nuclei were not birifringent, as that is a feature of the stain specific to collagen fiber orientation. Sirius red is an acidic dye that binds to basic materials in the tissue. This suggests there is a chemical difference in the central nuclei of dystrophic muscle tissue, as the peripheral muscle nuclei did not stain. Therefore, Sirius red may have potential to be used as a crude diagnostic tool. This observation also suggests that we may be able to get more insight in to the central nucleation of dystrophic muscle which persists for an unknown reason, by examining the chemical properties of central nuclei.

a) Developing a technique

Collagen is a large molecule with many strong covalent cross-links, and thus is difficult to penetrate an agarose gel. To overcome this problem, proteins were digested with collagenase (a matrix metalloproteinase) in an attempt to measure collagen protein content. Preliminary trials digesting protein samples for different lengths of time, as well as trials to determine the ideal concentration of collagenase were conducted (see figure C in *Appendix A*). At a 0.2% concentration of collagenase trials of digestion for 30 minutes to 2 hours were observed to have digested the collagen, leaving a clear band at 190kDa (the molecular weight of collagen I) as well as smaller bands, thought to be fragments of collagen of side molecules linked to collagen. The antibody was specific, as undigested proteins (a negative control) had no bands. Also, vitrogen (a positive control for collagen I) had only one band at 190kDa. Because, collagenase cleaves only semi-specifically (Sigma-Aldrich product information), the blots from digested protein extracts of the different muscles each had a different number of bands stained for collagen, suggesting that the collagen in each tissue has slightly different molecular and fibrillar morphology. We are as yet, unsure of what each band represents (possible break down products) or the exact mechanism of collagenase digestive activity in each tissue. However, from this work it appears that it is plausible and reproducible to use a collagenase digestion method to prepare protein extracts of muscle that will enable collagen protein to run on an SDS gel. This has lot of potential for future use, given that collagen studies with Western blotting techniques would be valuable additions to many studies.

For this study there was an observable trend for collagen I to decrease in the quadriceps, heart, and tibialis anterior after 10 weeks of Halo treatment and a significant

decrease in these tissues after 5 weeks of Halo treatment. However because of the technique (above) and the small sample size and variability, the significance of results may be disguised. This experiment should be repeated with a larger sample size and a repeat study (in progress) will collect tissues to address this question.

2. HGF PROTEIN CONTENT

HGF protein concentration in muscle tissue increased with 10 weeks of Halo treatment. HGF plays a critical role in satellite cell activation and proliferation (Nakamura *et al.*, 1989). HGF binds to c-met, a receptor on quiescent satellite cells, and stimulates satellite cell proliferation (Tatsumi *et al* 1998). Mdx mice have a large number of actively proliferating satellite cells because they are constantly undergoing degeneration, and therefore satellite cell stimulation (Reimann *et al* 2000). In this study HGF was higher, suggesting there would be a consequent increase in satellite cell activation and proliferation. HGF also stimulates cell migration (Liu 2004). As Halo decreases the amount of collagen and loosens the ECM, it is possible that satellite cells and the myofibroblasts produced by their activation could migrate more freely after Halo. Therefore it is possible that HGF is activated in some positive feedback loop involving Halo, due to satellite cell migration and that this activation causes further migration and repair. Because Halo+ mice do not have as much damage after 12 weeks of treatment (as seen in *chapter6, section6c*) as observed in muscle from untreated mdx mice, it is possible that the muscles in treated mice are undergoing a rapid regeneration at 10 weeks of treatment which would be consistent with there being a large increase in satellite cell

number, proliferation and migration to regenerate the muscles. Halo is therefore aiding in muscle regeneration and repairing damage due to dystrophy.

Recent work in the area of fibrosis has shown that HGF is an antifibrotic agent that antagonizes TGFβ (Liu 2002,Matsumoto and Nakamura 2001). Successful treatment with HGF in dermal sclerosis (Iwasaki *et al* 2006), lung fibrosis (Gazdhar *et al* 2006), and renal fibrosis (Herrero-Fresneda *et al* 2006) has reduced fibrosis by the inhibition of TGFβ. In the current work, HGF in muscle was increased by Halo treatment. This suggests Halo has an effect upstream to TGFβ and Smad3 potentially by activating HGF production, and decreases fibrosis in dystrophy.

3. ALPHA-SMOOTH MUSCLE ACTIN

Alpha-smooth muscle actin protein decreased with 10 weeks of Halo treatment. This can be interpreted as evidence that Halo decreased migration and/or differentiation by myofibroblasts in dystrophic muscle. Work by Yang and Liu (Yang and Liu 2003) has shown that HGF inhibits the expression of α-smooth muscle actin. Since, Halo increased HGF production in this study, it would be expected to inhibit myofibroblast activation and the production of α-smooth muscle actin by those cells. With a reduction in the number of myofibroblasts, collagen expression would decrease (see *chapter6, section4a*) and collagen production would be altered, resulting in an overall reduction in fibrosis.

4. MOLECULAR EFFECTS OF TREATMENT

a) Collagen I and collagen III expression

The level of collagen I and collagen III expression was used to quantify fibrosis and determine the effects of treatment on collagen production. Collagen I and collagen III expression decreased in the heart, quadriceps, tibialis anterior and diaphragm in all groups. This was expected, as seen in a pilot study by Mark Pines (unpublished) on young dystrophic mice in which, collagen expression decreased as Halo inhibited TGFβ, thereby inhibiting collagen transcription.

Surprisingly, central nuclei in regenerated muscle fibers were observed to express collagen I and collagen III in the tibialis anterior and quadriceps using *in situ* hybridization. To our knowledge there are no reports to date indicating that muscle fiber nuclei express or produce collagen. Notably this was a specific assay for collagen gene expression and the negative control experiments did not display such expression. Further research is needed to determine the mechanism behind this expression. Not only was collagen expressed by the central nuclei, Halo decreased that expression in the muscles. As there was no difference in central nucleation index with Halo treatment, this result suggests that Halo is having an effect in muscle tissue cells (in fibers with central nuclei and in mononucleated cells in the satellite position and nearby fibers) as well as in fibroblasts.

5. PROLIFERATION AND REPAIR

a) Ki67 staining

The number of muscle cells expressing Ki67, a marker of proliferation, increased after 5 weeks of Halo treatment. This may correlate with the rise of HGF protein (unfortunately HGF protein concentration in muscle was not studied in the 5 week treatment group). After 5 weeks of treatment, Halo stimulated myogenic repair; however after 10 weeks of treatment, fewer muscle cells expressed Ki67. This may indicate that the actively proliferating muscle cells have returned to the quiescent state as there is a significantly lower demand to repair damaged tissue (see *chapter6, section6c*).

The number of proliferating cells of the extracellular matrix regions of muscle tissue sections was decreased, according to the Ki67 assay. With muscle damage, inflammatory cells and fibroblasts migrate to the site of injury, where fibroblasts then (i.e., referring to the time after migration to injury) undergo proliferation and differentiation. After 5 weeks of treatment, muscles would have begun to repair (seen as increased muscle cell proliferation compared to muscle in untreated mice), so that myofibroblasts and fibroblasts would not be replacing damaged muscle fibers with collagen. Therefore fibroblasts and myofibroblasts would not be required to proliferate; these data are consistent with the findings for Ki67-positive cells in regions of fibrosis and muscle (decreased and increased respectively after 5 weeks treatment but without change from untreated mice after 10 weeks treatment). This result would also be consistent with there being a hypothetical increase in HGF (which was not studied in the 5-week treatment group), as HGF would no longer be stimulating myofibroblasts.

Therefore myofibroblast proliferation was decreased, in agreement with the decreased expression of α-smooth muscle actin (see *chapter6, section3*).

After 10 weeks of treatment, proliferation of cells in the ECM increased. This result is not consistent with data (see *chapter6, section2*) showing increased HGF in the same muscles. With an increase in HGF one would expect a decrease in myofibroblast activation (Liu 2004). Also there was a decrease in smooth muscle actin (see *chapter6, section3*) in the same muscles. This further suggests that there are fewer myofibroblasts present, which would lead to the expectation of finding less proliferation of myofibroblasts. The basis for these contradictory findings is not known. However, one could speculate that the counts of Ki67 positive cells in the ECM may include actively proliferative, migratory myoblasts, endothelial cells, Schwann cells, and inflammatory cells that each may show an increase in proliferation in a regenerating tissue that was undergoing significant remodeling (seen as a decrease in collagen expression), regeneration (see *chapter6, section6c*), and changes in collagen cross-linking or molecular structure. Alternatively, of the more than 20 statistical tests in this study, one might anticipate at least one finding of error in the results of statistical tests (finding significance where none was present, or finding no significance where there was a difference), since a statistical error as $p<0.05$ was used to determine significance.

6. FUNCTIONAL EFFECTS OF TREATMENT

a) Grip Strength

The profile of grip strength over 10 weeks of treatment showed no significant difference in grip strength with treatment by Halo. However, there was a large amount of variability in the untreated mice from week to week. The "yo-yoing" between different measurements may be partly indicative of the damage-repair cycle in mdx mice. Mdx mice undergo muscle damage and repair throughout their life, which worsens as they age (Carnwath and Shotton 1987,Coulton *et al* 1988b,Coulton *et al* 1988a,Torres and Duchen 1987). Interestingly, observations of the Halo+ group showed relatively little variation from week to week, and no decline in strength over the 10 week period. Previous work by Anderson *et al.* (2000) demonstrated that mdx mice treated with deflazacort have increased strength over time. However, that previous study examined young mice ages 2.5 weeks to 8 weeks old, and is therefore demonstrating only modest drug-related increases in strength in addition to typical increases in strength during development and maturation. In a study by Keeling *et al.* (2007) the long term strength of mdx mice was examined during treatment with corticosteroids. From 3 to 10 weeks-of-age, treated and untreated mice had the same strength; as time progressed from 10 to 24 weeks-of-age, strength in both groups of mice declined, but strength in the treated group declined at a much lower rate than in the untreated group. From 24 to 84 weeks-of-age, both groups of mice continued to show declining strength; however, the treated group remained stronger until the end of the study. Findings from the study by Keeling *et al.* (2007) corroborate the data from the current study, that Halo prevented a long term decline in muscle

strength. From this we can conclude that that Halo improves the functional outcomes by reducing the impact of disease progression.

b) Distance run

There was no significant difference week to week between treated and untreated groups in the distance that mice ran over a 24 hour interval. However, similar to observations of grip strength tests, treated mice ran relatively similar distances, consistently from week to week, whereas the distance run by untreated mice varied significantly from week to week. This supports the hypothesis developed above that Halo is stabilizing the damage-repair cycle seen in muscles of mdx mice, and improving the functional outcome.

Interestingly, in the final run prior to euthanasia and following EBD injection mice, the Halo+ mice ran significantly further than the untreated mice. This final trial of running was less than a week after the previous run (3 to 5 days), which makes it shorter than the interval between all the previous running trials. Exercise is known to accelerate the degeneration-regeneration cycle in mdx mice (Okano *et al* 2005), as fiber membranes lacking dystrophin are subject to exercise-induced damage. One week after running, limb muscles would be in the regeneration part of the cycle induced by the past run. With an interval less then a week between running trials, the muscles would not yet have regenerated and still have a lot of damage (McIntosh *et al* 1994,McIntosh and Anderson 1995). Therefore we would expect to observe a dramatic drop in the distance those mice could run when two trials were close together, as shown in untreated mice in this study. Since we observed no decrease between the final two running trials in Halo+ mice, Halo

would seem to be reducing the amount of exercise-induced damage (see *chapter6, section6c*), and therefore mice treated with Halo would be able to run further than untreated mice.

There is an interesting debate over the benefits of exercise for mdx mice and patients with DMD. In people suffering with conditions, such as DMD, the idea of physical activity can be daunting, due to pain, contractures due to fibrosis, and overall disability. However, without physical activity muscle undergoes atrophy; this is commonly seen in elderly people. This is a vicious cycle of inactivity causing more inactivity. Unlike the situation in the elderly or in people suffering with pain disorders, the DMD effect of exercise is a bit more controversial. Since exercise causes muscle fiber damage in DMD muscle, some physicians recommend that DMD patients do not engage in any significant physical activity. However, some research in mdx mice suggests that exercise can improve muscle strength, prevent atrophy, and improve fatigue-resistance by the conversion of glycolytic fibers to oxidative fibers (Hayes and Williams 1996). With age and moderate exercise, there was an improvement in age-related loss of tension produced by mdx muscles (Wineinger *et al* 1998). This suggested that low-levels of exercise are beneficial in reducing the effects of aging in mdx mice. Therefore exercise can improve the function of dystrophic muscle. Since our results suggest that Halo treatment may improve muscle regeneration and muscle performance, children suffering from DMD may be more able to participate in physical activity, and more willing to participate if they were able to receive Halo treatment. Therefore there is potential for Halo to be combined with moderate exercise for amelioration of muscle function in muscular dystrophy.

c) Membrane permeability (EBD)

Membrane damage was analyzed using a vital dye called Evan's Blue Dye (EBD). EBD binds to albumin in the body; when membranes are damaged, the EBD bound to albumin is able to permeate into damaged muscle fibers, for example in mdx muscle. In this study, the proportion of EBD-positive fibers was decreased as a result of 12 weeks of Halo treatment. As collagen content (or possibly collagen cross-linking) tended to decrease, we can speculate that satellite cells and myoblasts could have migrated more freely to repair damaged fibers. As seen from the results of the studies with Ki67 staining, there was increased muscle cell proliferation after 5 weeks of Halo treatment. This would be followed by muscle fiber regeneration and new muscle formation. By 12 weeks of treatment, muscles would have completed that repair. It is also possible that with decreased collagen content (or cross-linking) fibers may be better able to withstand exercise-induced damage as the inter-connection between fiber membrane, laminin, and ECM would be more fluid or flexible. Therefore, the proportion of EBD-positive fibers post exercise relates directly to muscle sparing from the functional deficit of dystrophy.

Interestingly, muscle membrane damage increased with increasing exercise in untreated mice, as we expected it might. However, there was no change in damage with increasing exercise in Halo+ mice. Halo therefore prevented functional defecits (exercise-induced fiber damage) seen in dystrophic muscle and improved overall performance. This is an important finding, as it speaks to the significant potential for treatment with Halo in dystrophy

d) Respiration

Barometric plethysmography is commonly used to characterize asthmatic symptomatology in children, as young as one to two years old (Bisgaard and Nielsen 2005,Nielsen and Bisgaard 2005). Despite some initial debate in the efficacy of Penh measurements, scientists have confirmed the validity of the Penh data (Lomask 2006) and clinicians continue to use it as a diagnostic measure. This technique has also been used in many mouse studies (*e.g.*, (Sausbier *et al* 2006) as a means of assessing respiratory function.

In the current study, Halo+ mice had a lower response to a methacholine challenge than untreated mice. Due to the important role of the diaphragm in respiration and the severe disease pathology of the diaphragm in mdx mouse dystrophy, we hypothesized that treatment-related improvement in the diaphragm tissue would be ameliorating respiratory function. As shown above, although collagen content did not change in the diaphragm, collagen expression was decreased by Halo. Therefore, while we are uncertain of the accuracy of our Western blot assay for collagen content or speculation about changes in the structure of collagen, the improved function of treated mice demonstrated using plethysmography likely reflected some effect of Halo on the mdx mouse diaphragm muscle leading us to believe either the assays for collagen content are not accurate enough or there is some other change to collagen that must be investigated.

The intercostal muscles were not assessed for collagen content or expression, although they play an important role in respiration. It is conceivable that dystrophy in

these muscles collagen content was reduced by Halo treatment, resulting in improved respiratory function, as assessed with plethysmography.

It is also possible that Halo caused an alteration in lung function itself unrelated to dystrophy. The literature and work by Mark Pines (Nagler *et al* 1996,Nagler *et al* 1998,Nagler *et al* 1999,Nagler *et al* 2000,Pines *et al* 2001,Pines and Nagler 1998) suggests that Halo only effects so-called "pathological collagen"; however because the exact mechanism by which collagen effects changes in respiratory and muscle functions is still unknown, we cannot confirm this is the case. After careful review, there is no literature on distinctive forms of collagen in pathological as compared to normal muscle (or other) tissue. To evaluate whether Halo affects "normal collagen" deposition, cross-linking with age, or remodeling in repair of function of normal tissue, including lung. Experiments in which C57 mice are treated with Halo are required.

e) Cardiomyopathy

There was a significant improvement in cardiac function after 5 weeks of treatment with Halo. Ventricular contraction was synchronus, as opposed to dys-kinetic contraction (abnormal motions of the ventricular wall) contraction that was present in untreated mice, and also in the baseline findings of the treatment group prior to the start of Halo treatment. A group of young mice were also treated with Halo. Echocardiography studies in the group of younger mice also showed that there was a resolution of ventricular dyskinesis in treated compared with untreated mice. There was no quantitative change in LV measurements after treatment, but this was not unexpected as it is rare to see these changes. There was no change in left ventricular hypertrophy that

is typically observed in mdx mouse cardiomyopathy (Anderson *et al* 1994). However, qualitative differences suggest that Halo improved cardiac dysfunction in mdx mouse, a condition that is characteristic of DMD.

Chapter 7. SUMMARY AND CONCLUSIONS

This work shows that with treatment by Halo, HGF was increased in muscle; this is thought to decrease myofibroblast activation and proliferation, resulting in reduced expression of collagen and decreased collagen content, therefore reducing fibrosis. As a consequence of reduced fibrosis, muscle repair was more effective and new damage (e.g., from exercise) was reduced. In addition, there were significant functional improvements after treatment for 5 or 10 weeks and the progression of disease was slowed. Therefore, we accept the hypothesis that Halo can reduce fibrosis, thereby improving function (figure 16).

This research is especially important because it shows a resolution of pre-existing fibrosis and a reduction of new collagen synthesis. Studies by Pines (unpublished) suggest a dose-dependent effect of Halo on fibrosis in young mice. Therefore, with a higher dose of Halo, there may be an even greater benefit to muscle and function. This research has stimulated several questions as to the exact details and pathway by which Halo has its effect. It will be critical to gain that information before clinical studies can begin in appropriate, ethical trials.

Chapter 8. BIBLIOGRAPHY

1. Adams GR, Haddad F, Baldwin KM (1999), Time course of changes in markers of myogenesis in overloaded rat skeletal muscles, *J.Appl.Physiol* 87: 1705-1712

2. Alberts B, Johnson A, Walter P, Lewis J, Raff M, Roberts K (2002), *Molecular Biology of the Cell*, Taylor and Francis,

3. Allen RE, Sheehan SM, Taylor RG, Kendall TL, Rice GM (1995), Hepatocyte growth factor activates quiescent skeletal muscle satellite cells in vitro, *J.Cell Physiol* 165: 307-312

4. Amalfitano A, Chamberlain JS (1996), The mdx-amplification-resistant mutation system assay, a simple and rapid polymerase chain reaction-based detection of the mdx allele, *Muscle Nerve* 19: 1549-1553

5. Amthor H, Nicholas G, McKinnell I, Kemp CF, Sharma M, Kambadur R, Patel K (2004), Follistatin complexes Myostatin and antagonises Myostatin-mediated inhibition of myogenesis, *Dev.Biol.* 270: 19-30

6. Anderson J, Pilipowicz O (2002), Activation of muscle satellite cells in single-fiber cultures, *Nitric.Oxide.* 7: 36-41

7. Anderson JE (2000), A role for nitric oxide in muscle repair: nitric oxide-mediated activation of muscle satellite cells, *Mol.Biol.Cell* 11: 1859-1874

8. Anderson JE, Bressler BH, Ovalle WK (1988), Functional regeneration in the hindlimb skeletal muscle of the mdx mouse, *J.Muscle Res.Cell Motil.* 9: 499-515

9. Anderson JE, Liu L, Kardami E (1994), The effects of hyperthyroidism on muscular dystrophy in the mdx mouse: greater dystrophy in cardiac and soleus muscle, *Muscle Nerve* 17: 64-73

10. Anderson JE, McIntosh LM, Poettcker R (1996), Deflazacort but not prednisone improves both muscle repair and fiber growth in diaphragm and limb muscle in vivo in the mdx dystrophic mouse, *Muscle Nerve* 19: 1576-1585

11. Anderson JE, Ovalle WK, Bressler BH (1987), Electron microscopic and autoradiographic characterization of hindlimb muscle regeneration in the mdx mouse, *Anat.Rec.* 219: 243-257

12. Anderson JE, Vargas C (2003), Correlated NOS-Imu and myf5 expression by satellite cells in mdx mouse muscle regeneration during NOS manipulation and deflazacort treatment, *Neuromuscul.Disord.* 13: 388-396

13. Anderson JE, Weber M, Vargas C (2000), Deflazacort increases laminin expression and myogenic repair, and induces early persistent functional gain in mdx mouse muscular dystrophy, *Cell Transplant.* 9: 551-564

14. Archer JD, Vargas CC, Anderson JE (2006), Persistent and improved functional gain in mdx dystrophic mice after treatment with L-arginine and deflazacort, *FASEB J.* 20: 738-740

15. Armstrong RB (1990), Initial events in exercise-induced muscular injury, *Med.Sci.Sports Exerc.* 22: 429-435

16. Backman E, Henriksson KG (1995), Low-dose prednisolone treatment in Duchenne and Becker muscular dystrophy, *Neuromuscul.Disord.* 5: 233-241

17. Badalamente MA, Stracher A (2000), Delay of muscle degeneration and necrosis in mdx mice by calpain inhibition, *Muscle Nerve* 23: 106-111

18. Barthelmai W (1965), [On the effect of corticoid administration on creatine phosphokinase in progressive muscular dystrophy], *Verh.Dtsch.Ges.Inn.Med.* 71: 624-626

19. Bartlett RJ, Stockinger S, Denis MM, Bartlett WT, Inverardi L, Le TT, thi MN, Morris GE, Bogan DJ, Metcalf-Bogan J, Kornegay JN (2000), In vivo targeted repair of a point mutation in the canine dystrophin gene by a chimeric RNA/DNA oligonucleotide, *Nat.Biotechnol.* 18: 615-622

20. Belles-Isles M, Roy R, Dansereau G, Goulet M, Roy B, Bouchard JP, Tremblay JP (1993), Rapid selection of donor myoblast clones for muscular dystrophy therapy using cell surface expression of NCAM, *Eur.J.Histochem.* 37: 375-380

21. Bernasconi P, Di Blasi C, Mora M, Morandi L, Galbiati S, Confalonieri P, Cornelio F, Mantegazza R (1999), Transforming growth factor-beta1 and fibrosis in congenital muscular dystrophies, *Neuromuscul.Disord.* 9: 28-33

22. Bernasconi P, Torchiana E, Confalonieri P, Brugnoni R, Barresi R, Mora M, Cornelio F, Morandi L, Mantegazza R (1995), Expression of transforming growth factor-beta 1 in dystrophic patient muscles correlates with fibrosis. Pathogenetic role of a fibrogenic cytokine, *J.Clin.Invest* 96: 1137-1144

23. Bertorini T, Palmieri G, Bhattacharya S (1982a), Beneficial effects of dantrolene sodium in exercise-induced muscle pains: calcium mediated?, *Lancet* 1: 616-617

24. Bertorini TE, Bhattacharya SK, Palmieri GM, Chesney CM, Pifer D, Baker B (1982b), Muscle calcium and magnesium content in Duchenne muscular dystrophy, *Neurology* 32: 1088-1092

25. Bertorini TE, Cornelio F, Bhattacharya SK, Palmieri GM, Dones I, Dworzak F, Brambati B (1984), Calcium and magnesium content in fetuses at risk and prenecrotic Duchenne muscular dystrophy, *Neurology* 34: 1436-1440

26. Bertorini TE, Palmieri GM, Griffin JW, Igarashi M, McGee J, Brown R, Nutting DF, Hinton AB, Karas JG (1988), Effect of chronic treatment with the calcium antagonist diltiazem in Duchenne muscular dystrophy, *Neurology* 38: 609-613

27. Best TM, Hunter KD (2000), Muscle injury and repair, *Phys.Med.Rehabil.Clin.N.Am.* 11: 251-266

28. Biggar WD, Gingras M, Fehlings DL, Harris VA, Steele CA (2001), Deflazacort treatment of Duchenne muscular dystrophy, *J.Pediatr.* 138: 45-50

29. Bischoff R (1990), Control of satellite cell proliferation, *Adv.Exp.Med.Biol.* 280: 147-157

30. Bischoff R (1997), Chemotaxis of skeletal muscle satellite cells, *Dev.Dyn.* 208: 505-515

31. Bischoff R, Heintz C (1994), Enhancement of skeletal muscle regeneration, *Dev.Dyn.* 201: 41-54

32. Bisgaard H, Nielsen KG (2005), Plethysmographic measurements of specific airway resistance in young children, *Chest* 128: 355-362

33. Blake DJ, Kroger S (2000), The neurobiology of duchenne muscular dystrophy: learning lessons from muscle?, *Trends Neurosci.* 23: 92-99

34. Blake DJ, Weir A, Newey SE, Davies KE (2002), Function and genetics of dystrophin and dystrophin-related proteins in muscle, *Physiol Rev.* 82: 291-329

35. Bodensteiner JB, Engel AG (1978), Intracellular calcium accumulation in Duchenne dystrophy and other myopathies: a study of 567,000 muscle fibers in 114 biopsies, *Neurology* 28: 439-446

36. Bogdanovich S, Krag TO, Barton ER, Morris LD, Whittemore LA, Ahima RS, Khurana TS (2002), Functional improvement of dystrophic muscle by myostatin blockade, *Nature* 420: 418-421

37. Bonni S, Wang HR, Causing CG, Kavsak P, Stroschein SL, Luo K, Wrana JL (2001), TGF-beta induces assembly of a Smad2-Smurf2 ubiquitin ligase complex that targets SnoN for degradation, *Nat.Cell Biol.* 3: 587-595

38. Bradley WG, Fulthorpe JJ (1978), Studies of sarcolemmal integrity in myopathic muscle, *Neurology* 28: 670-677

39. Bressler BH, Jasch LG, Ovalle WK, Slonecker CE (1983), Changes in isometric contractile properties of fast-twitch and slow-twitch skeletal muscle of C57BL/6J dy2J/dy2J dystrophic mice during postnatal development, *Exp.Neurol.* 80: 457-470

40. Brooke MH, Fenichel GM, Griggs RC, Mendell JR, Moxley R, Miller JP, Province MA (1983), Clinical investigation in Duchenne dystrophy: 2. Determination of the "power" of therapeutic trials based on the natural history, *Muscle Nerve* 6: 91-103

41. Brown JC, Timpl R (1995), The collagen superfamily, *Int.Arch.Allergy Immunol.* 107: 484-490

42. Brown SC, Lucy JA (1993), Dystrophin as a mechanochemical transducer in skeletal muscle, *Bioessays* 15: 413-419

43. Bruck R, Genina O, Aeed H, Alexiev R, Nagler A, Avni Y, Pines M (2001), Halofuginone to prevent and treat thioacetamide-induced liver fibrosis in rats, *Hepatology* 33: 379-386

44. Bruckner P, Prockop DJ (1981), Proteolytic enzymes as probes for the triple-helical conformation of procollagen, *Anal.Biochem.* 110: 360-368

45. Bulfield G, Siller WG, Wight PA, Moore KJ (1984), X chromosome-linked muscular dystrophy (mdx) in the mouse, *Proc.Natl.Acad.Sci.U.S.A* 81: 1189-1192

46. Burridge K, Chrzanowska-Wodnicka M (1996), Focal adhesions, contractility, and signaling, *Annu.Rev.Cell Dev.Biol.* 12: 463-518

47. Butler J, Shapiro MD, Jassal D, Neilan T, Nichols J, Ferencik M, Brady TJ, Hoffmann U, Cury RC (2007), Comparison of multidetector computed tomography and two-dimensional transthoracic echocardiography for left ventricular assessment in patients with heart failure, *Am.J.Cardiol.* 99: 247-249

48. Carnwath JW, Shotton DM (1987), Muscular dystrophy in the mdx mouse: histopathology of the soleus and extensor digitorum longus muscles, *J.Neurol.Sci.* 80: 39-54

49. Carpenter JL, Hoffman EP, Romanul FC, Kunkel LM, Rosales RK, Ma NS, Dasbach JJ, Rae JF, Moore FM, McAfee MB, . (1989), Feline muscular dystrophy with dystrophin deficiency, *Am.J.Pathol.* 135: 909-919

50. Carpenter S, Karpati G (1979), Duchenne muscular dystrophy: plasma membrane loss initiates muscle cell necrosis unless it is repaired, *Brain* 102: 147-161

51. Carter GT, Wineinger MA, Walsh SA, Horasek SJ, Abresch RT, Fowler WM, Jr. (1995), Effect of voluntary wheel-running exercise on muscles of the mdx mouse, *Neuromuscul.Disord.* 5: 323-332

52. Cerletti M, Negri T, Cozzi F, Colpo R, Andreetta F, Croci D, Davies KE, Cornelio F, Pozza O, Karpati G, Gilbert R, Mora M (2003), Dystrophic phenotype of canine X-linked muscular dystrophy is mitigated by adenovirus-mediated utrophin gene transfer, *Gene Ther.* 10: 750-757

53. Chan YS, Li Y, Foster W, Horaguchi T, Somogyi G, Fu FH, Huard J (2003), Antifibrotic effects of suramin in injured skeletal muscle after laceration, *J.Appl.Physiol* 95: 771-780

54. Choi ET, Callow AD, Sehgal NL, Brown DM, Ryan US (1995), Halofuginone, a specific collagen type I inhibitor, reduces anastomotic intimal hyperplasia, *Arch.Surg.* 130: 257-261

55. Clegg CH, Linkhart TA, Olwin BB, Hauschka SD (1987), Growth factor control of skeletal muscle differentiation: commitment to terminal differentiation occurs in G1 phase and is repressed by fibroblast growth factor, *J.Cell Biol.* 105: 949-956

56. Coirault C, Pignol B, Cooper RN, Butler-Browne G, Chabrier PE, Lecarpentier Y (2003), Severe muscle dysfunction precedes collagen tissue proliferation in mdx mouse diaphragm, *J.Appl.Physiol* 94: 1744-1750

57. Cooper BJ, Valentine BA, Wilson S, Patterson DF, Concannon PW (1988a), Canine muscular dystrophy: confirmation of X-linked inheritance, *J.Hered.* 79: 405-408

58. Cooper BJ, Winand NJ, Stedman H, Valentine BA, Hoffman EP, Kunkel LM, Scott MO, Fischbeck KH, Kornegay JN, Avery RJ, . (1988b), The homologue of the Duchenne locus is defective in X-linked muscular dystrophy of dogs, *Nature* 334: 154-156

59. Coulton GR, Curtin NA, Morgan JE, Partridge TA (1988a), The mdx mouse skeletal muscle myopathy: II. Contractile properties, *Neuropathol.Appl.Neurobiol.* 14: 299-314

60. Coulton GR, Morgan JE, Partridge TA, Sloper JC (1988b), The mdx mouse skeletal muscle myopathy: I. A histological, morphometric and biochemical investigation, *Neuropathol.Appl.Neurobiol.* 14: 53-70

61. Dangain J, Vrbova G (1984), Muscle development in mdx mutant mice, *Muscle Nerve* 7: 700-704

62. Darby I, Skalli O, Gabbiani G (1990), Alpha-smooth muscle actin is transiently expressed by myofibroblasts during experimental wound healing, *Lab Invest* 63: 21-29

63. Decary S, Mouly V, Butler-Browne GS (1996), Telomere length as a tool to monitor satellite cell amplification for cell-mediated gene therapy, *Hum.Gene Ther.* 7: 1347-1350

64. Di Guglielmo GM, Le Roy C, Goodfellow AF, Wrana JL (2003), Distinct endocytic pathways regulate TGF-beta receptor signalling and turnover, *Nat.Cell Biol.* 5: 410-421

65. Di Sario A, Bendia E, Macarri G, Candelaresi C, Taffetani S, Marzioni M, Omenetti A, De Minicis S, Trozzi L, Benedetti A (2004), The anti-fibrotic effect of pirfenidone in rat liver fibrosis is mediated by downregulation of procollagen alpha1(I), TIMP-1 and MMP-2, *Dig.Liver Dis.* 36: 744-751

66. Doevendans PA, Daemen MJ, de Muinck ED, Smits JF (1998), Cardiovascular phenotyping in mice, *Cardiovasc.Res.* 39: 34-49

67. Drachman DB, Toyka KV, Myer E (1974), Prednisone in Duchenne muscular dystrophy, *Lancet* 2: 1409-1412

68. Duance VC, Stephens HR, Dunn M, Bailey AJ, Dubowitz V (1980), A role for collagen in the pathogenesis of muscular dystrophy?, *Nature* 284: 470-472

69. Dugina V, Fontao L, Chaponnier C, Vasiliev J, Gabbiani G (2001), Focal adhesion features during myofibroblastic differentiation are controlled by intracellular and extracellular factors, *J.Cell Sci.* 114: 3285-3296

70. Dupont-Versteegden EE, McCarter RJ, Katz MS (1994), Voluntary exercise decreases progression of muscular dystrophy in diaphragm of mdx mice, *J.Appl.Physiol* 77: 1736-1741

71. Durbeej M, Henry MD, Campbell KP (1998), Dystroglycan in development and disease, *Curr.Opin.Cell Biol.* 10: 594-601

72. Edwards DR, Leco KJ, Beaudry PP, Atadja PW, Veillette C, Riabowol KT (1996), Differential effects of transforming growth factor-beta 1 on the expression of matrix metalloproteinases and tissue inhibitors of metalloproteinases in young and old human fibroblasts, *Exp.Gerontol.* 31: 207-223

73. Eppert K, Scherer SW, Ozcelik H, Pirone R, Hoodless P, Kim H, Tsui LC, Bapat B, Gallinger S, Andrulis IL, Thomsen GH, Wrana JL, Attisano L (1996), MADR2 maps to 18q21 and encodes a TGFbeta-regulated MAD-related protein that is functionally mutated in colorectal carcinoma, *Cell* 86: 543-552

74. Ervasti JM, Campbell KP (1991), Membrane organization of the dystrophin-glycoprotein complex, *Cell* 66: 1121-1131

75. Ervasti JM, Campbell KP (1993), A role for the dystrophin-glycoprotein complex as a transmembrane linker between laminin and actin, *J.Cell Biol.* 122: 809-823

76. Fichtner-Feigl S, Strober W, Kawakami K, Puri RK, Kitani A (2006), IL-13 signaling through the IL-13alpha2 receptor is involved in induction of TGF-beta1 production and fibrosis, *Nat.Med.* 12: 99-106

77. Finsterer J, Stollberger C (2003), The heart in human dystrophinopathies, *Cardiology* 99: 1-19

78. Finsterer J, Stollberger C, Feichtinger H (2006), Noncompaction in Duchenne muscular dystrophy: frustrated attempt to create a compensatory left ventricle?, *Cardiology* 105: 223-225

79. Fisher I, Abraham D, Bouri K, Hoffman EP, Muntoni F, Morgan J (2005), Prednisolone-induced changes in dystrophic skeletal muscle, *FASEB J.* 19: 834-836

80. Florini JR, Magri KA (1989), Effects of growth factors on myogenic differentiation, *Am.J.Physiol* 256: C701-C711

81. Franco A, Jr., Lansman JB (1990), Calcium entry through stretch-inactivated ion channels in mdx myotubes, *Nature* 344: 670-673

82. Fraser RD, MacRae TP, Miller A, Suzuki E (1983), Molecular conformation and packing in collagen fibrils, *J.Mol.Biol.* 167: 497-521

83. Gabbiani G, Chaponnier C, Huttner I (1978), Cytoplasmic filaments and gap junctions in epithelial cells and myofibroblasts during wound healing, *J.Cell Biol.* 76: 561-568

84. Gabbiani G, Ryan GB, Majne G (1971), Presence of modified fibroblasts in granulation tissue and their possible role in wound contraction, *Experientia* 27: 549-550

85. Gaschen FP, Hoffman EP, Gorospe JR, Uhl EW, Senior DF, Cardinet GH, III, Pearce LK (1992), Dystrophin deficiency causes lethal muscle hypertrophy in cats, *J.Neurol.Sci.* 110: 149-159

86. Gavish Z, Pinthus JH, Barak V, Ramon J, Nagler A, Eshhar Z, Pines M (2002), Growth inhibition of prostate cancer xenografts by halofuginone, *Prostate* 51: 73-83

87. Gazdhar A, Fachinger P, van Leer C, Pierog J, Gugger M, Friis R, Schmid RA, Geiser T (2006), Gene transfer of hepatocyte growth factor by electroporation reduces bleomycin-induced lung fibrosis, *Am.J.Physiol Lung Cell Mol.Physiol*

88. Ge Y, Molloy MP, Chamberlain JS, Andrews PC (2004), Differential expression of the skeletal muscle proteome in mdx mice at different ages, *Electrophoresis* 25: 2576-2585

89. Gelse K, Poschl E, Aigner T (2003), Collagens--structure, function, and biosynthesis, *Adv.Drug Deliv.Rev.* 55: 1531-1546

90. Giboda M, Smith JM, Prichard RK (1994), Reduction in tissue egg load and maintenance of resistance to challenge in mice infected with Schistosoma mansoni, following combined treatment with praziquantel and an antifibrotic agent, *Ann.Trop.Med.Parasitol.* 88: 385-395

91. Gillies M, Su T, Sarossy M, Hollows F (1993), Interferon-alpha 2b inhibits proliferation of human Tenon's capsule fibroblasts, *Graefes Arch.Clin.Exp.Ophthalmol.* 231: 118-121

92. Gnainsky Y, Spira G, Paizi M, Bruck R, Nagler A, Abu-Amara SN, Geiger B, Genina O, Monsonego-Ornan E, Pines M (2004), Halofuginone, an inhibitor of collagen synthesis by rat stellate cells, stimulates insulin-like growth factor binding protein-1 synthesis by hepatocytes, *J.Hepatol.* 40: 269-277

93. Goldberg HA, Maeno M, Domenicucci C, Qi ZN, Sodek J (1988), Identification of small collagenous proteins with properties of procollagen alpha 1 (I) pN-propeptide in fetal porcine calvarial bone, *Coll.Relat Res.* 8: 187-197

94. Goldspink G, Fernandes K, Williams PE, Wells DJ (1994), Age-related changes in collagen gene expression in the muscles of mdx dystrophic and normal mice, *Neuromuscul.Disord.* 4: 183-191

95. Gollins H, McMahon J, Wells KE, Wells DJ (2003), High-efficiency plasmid gene transfer into dystrophic muscle, *Gene Ther.* 10: 504-512

96. Granchelli JA, Avosso DL, Hudecki MS, Pollina C (1996), Cromolyn increases strength in exercised mdx mice, *Res.Commun.Mol.Pathol.Pharmacol.* 91: 287-296

97. Granot I, Bartov I, Plavnik I, Wax E, Hurwitz S, Pines M (1991), Increased skin tearing in broilers and reduced collagen synthesis in skin in vivo and in vitro in response to the coccidiostat halofuginone, *Poult.Sci.* 70: 1559-1563

98. Grinnell F (1994), Fibroblasts, myofibroblasts, and wound contraction, *J.Cell Biol.* 124: 401-404

99. Grobet L, Martin LJ, Poncelet D, Pirottin D, Brouwers B, Riquet J, Schoeberlein A, Dunner S, Menissier F, Massabanda J, Fries R, Hanset R, Georges M (1997), A deletion in the bovine myostatin gene causes the double-muscled phenotype in cattle, *Nat.Genet.* 17: 71-74

100. Grounds MD, Garrett KL, Lai MC, Wright WE, Beilharz MW (1992), Identification of skeletal muscle precursor cells in vivo by use of MyoD1 and myogenin probes, *Cell Tissue Res.* 267: 99-104

101. Hahn A, Bach JR, Delaubier A, Renardel-Irani A, Guillou C, Rideau Y (1997), Clinical implications of maximal respiratory pressure determinations for individuals with Duchenne muscular dystrophy, *Arch.Phys.Med.Rehabil.* 78: 1-6

102. Hahn SA, Schutte M, Hoque AT, Moskaluk CA, da Costa LT, Rozenblum E, Weinstein CL, Fischer A, Yeo CJ, Hruban RH, Kern SE (1996), DPC4, a candidate tumor suppressor gene at human chromosome 18q21.1, *Science* 271: 350-353

103. Halevy O, Nagler A, Levi-Schaffer F, Genina O, Pines M (1996), Inhibition of collagen type I synthesis by skin fibroblasts of graft versus host disease and scleroderma patients: effect of halofuginone, *Biochem.Pharmacol.* 52: 1057-1063

104. Hamelmann E, Schwarze J, Takeda K, Oshiba A, Larsen GL, Irvin CG, Gelfand EW (1997), Noninvasive measurement of airway responsiveness in allergic mice using barometric plethysmography, *Am.J.Respir.Crit Care Med.* 156: 766-775

105. Hantai D, Labat-Robert J, Grimaud JA, Fardeau M (1985), Fibronectin, laminin, type I, III and IV collagens in Duchenne's muscular dystrophy, congenital muscular dystrophies and congenital myopathies: an immunocytochemical study, *Connect.Tissue Res.* 13: 273-281

106. Hara H, Nolan PM, Scott MO, Bucan M, Wakayama Y, Fischbeck KH (2002), Running endurance abnormality in mdx mice, *Muscle Nerve* 25: 207-211

107. Harris AK (1988), Fibroblasts and myofibroblasts, *Methods Enzymol.* 163: 623-642

108. Hawke TJ, Garry DJ (2001), Myogenic satellite cells: physiology to molecular biology, *J.Appl.Physiol* 91: 534-551

109. Hayes A, Williams DA (1996), Beneficial effects of voluntary wheel running on the properties of dystrophic mouse muscle, *J.Appl.Physiol* 80: 670-679

110. Hemler ME (1999), Dystroglycan versatility, *Cell* 97: 543-546

111. Henry MD, Campbell KP (1999), Dystroglycan inside and out, *Curr.Opin.Cell Biol.* 11: 602-607

112. Herrero-Fresneda I, Torras J, Franquesa M, Vidal A, Cruzado JM, Lloberas N, Fillat C, Grinyo JM (2006), HGF gene therapy attenuates renal allograft scarring by preventing the profibrotic inflammatory-induced mechanisms, *Kidney Int.* 70: 265-274

113. Hill JJ, Davies MV, Pearson AA, Wang JH, Hewick RM, Wolfman NM, Qiu Y (2002), The myostatin propeptide and the follistatin-related gene are inhibitory binding proteins of myostatin in normal serum, *J.Biol.Chem.* 277: 40735-40741

114. Hill JJ, Qiu Y, Hewick RM, Wolfman NM (2003a), Regulation of myostatin in vivo by growth and differentiation factor-associated serum protein-1: a novel protein with protease inhibitor and follistatin domains, *Mol.Endocrinol.* 17: 1144-1154

115. Hill M, Wernig A, Goldspink G (2003b), Muscle satellite (stem) cell activation during local tissue injury and repair, *J.Anat.* 203: 89-99

116. Hoffman EP, Brown RH, Jr., Kunkel LM (1987a), Dystrophin: the protein product of the Duchenne muscular dystrophy locus, *Cell* 51: 919-928

117. Hoffman EP, Monaco AP, Feener CC, Kunkel LM (1987b), Conservation of the Duchenne muscular dystrophy gene in mice and humans, *Science* 238: 347-350

118. Hoodless PA, Haerry T, Abdollah S, Stapleton M, O'Connor MB, Attisano L, Wrana JL (1996), MADR1, a MAD-related protein that functions in BMP2 signaling pathways, *Cell* 85: 489-500

119. Hsu YC, Hsiao M, Chien YW, Lee WR (2006), Exogenous nitric oxide stimulated collagen type I expression and TGF-beta1 production in keloid fibroblasts by a cGMP-dependent manner, *Nitric.Oxide.*

120. Hulmes DJ, Wess TJ, Prockop DJ, Fratzl P (1995), Radial packing, order, and disorder in collagen fibrils, *Biophys.J.* 68: 1661-1670

121. Hurme T, Kalimo H (1992), Adhesion in skeletal muscle during regeneration, *Muscle Nerve* 15: 482-489

122. Iannaccone ST, Nanjiani Z (2001), Duchenne Muscular Dystrophy, *Curr.Treat.Options.Neurol.* 3: 105-117

123. Ibraghimov-Beskrovnaya O, Ervasti JM, Leveille CJ, Slaughter CA, Sernett SW, Campbell KP (1992), Primary structure of dystrophin-associated glycoproteins linking dystrophin to the extracellular matrix, *Nature* 355: 696-702

124. Ikeda K, Mitsumoto H (1993), In vivo and in vitro muscle tensions in wobbler mouse motor neuron disease, *Muscle Nerve* 16: 979-981

125. Ionasescu V, Lara-Braud C, Zellweger H, Ionasescu R, Burmeister L (1977), Fibroblast cultures in Duchenne muscular dystrophy. Alterations in synthesis and secretion of collagen and noncollagen proteins, *Acta Neurol.Scand.* 55: 407-417

126. Ishikawa H (1966), Electron microscopic observations of satellite cells with special reference to the development of mammalian skeletal muscles, *Z.Anat.Entwicklungsgesch.* 125: 43-63

127. Ishitobi M, Haginoya K, Zhao Y, Ohnuma A, Minato J, Yanagisawa T, Tanabu M, Kikuchi M, Iinuma K (2000), Elevated plasma levels of transforming growth factor beta1 in patients with muscular dystrophy, *Neuroreport* 11: 4033-4035

128. Ito T, Williams JD, Fraser DJ, Phillips AO (2004), Hyaluronan regulates transforming growth factor-beta1 receptor compartmentalization, *J.Biol.Chem.* 279: 25326-25332

129. Itoh S, Landstrom M, Hermansson A, Itoh F, Heldin CH, Heldin NE, ten Dijke P (1998), Transforming growth factor beta1 induces nuclear export of inhibitory Smad7, *J.Biol.Chem.* 273: 29195-29201

130. Iwasaki T, Imado T, Kitano S, Sano H (2006), Hepatocyte growth factor ameliorates dermal sclerosis in the tight-skin mouse model of scleroderma, *Arthritis Res.Ther.* 8: R161

131. Jagadha V, Becker LE (1988), Brain morphology in Duchenne muscular dystrophy: a Golgi study, *Pediatr.Neurol.* 4: 87-92

132. Jassal DS, Desai SC, Neilan TG, Avery E, Vlahakes GJ, Agnihotri AK (2006), The impact of spontaneous echocardiographic contrast in patients with left atrial enlargement undergoing cardiac valvular surgery, *J.Cardiothorac.Vasc.Anesth.* 20: 772-776

133. Johnson SE, Allen RE (1993), Proliferating cell nuclear antigen (PCNA) is expressed in activated rat skeletal muscle satellite cells, *J.Cell Physiol* 154: 39-43

134. Joulia D, Bernardi H, Garandel V, Rabenoelina F, Vernus B, Cabello G (2003), Mechanisms involved in the inhibition of myoblast proliferation and differentiation by myostatin, *Exp.Cell Res.* 286: 263-275

135. Junquiera LC, Junqueira LC, Brentani RR (1979), A simple and sensitive method for the quantitative estimation of collagen, *Anal.Biochem.* 94: 96-99

136. Kadler K (1995), Extracellular matrix 1: Fibril-forming collagens, *Protein Profile.* 2: 491-619

137. Kadler KE, Holmes DF, Trotter JA, Chapman JA (1996), Collagen fibril formation, *Biochem.J.* 316 (Pt 1): 1-11

138. Kagan HM, Trackman PC (1991), Properties and function of lysyl oxidase, *Am.J.Respir.Cell Mol.Biol.* 5: 206-210

139. Kambadur R, Sharma M, Smith TP, Bass JJ (1997), Mutations in myostatin (GDF8) in double-muscled Belgian Blue and Piedmontese cattle, *Genome Res.* 7: 910-916

140. Karpati G, Carpenter S, Prescott S (1988), Small-caliber skeletal muscle fibers do not suffer necrosis in mdx mouse dystrophy, *Muscle Nerve* 11: 795-803

141. Kavsak P, Rasmussen RK, Causing CG, Bonni S, Zhu H, Thomsen GH, Wrana JL (2000), Smad7 binds to Smurf2 to form an E3 ubiquitin ligase that targets the TGF beta receptor for degradation, *Mol.Cell* 6: 1365-1375

142. Keeling RM, Golumbek PT, Streif EM, Connolly AM (2007), Weekly oral prednisolone improves survival and strength in male mdx mice, *Muscle Nerve* 35: 43-48

143. Khan MA (1993), Corticosteroid therapy in Duchenne muscular dystrophy, *J.Neurol.Sci.* 120: 8-14

144. Khillan JS, Li SW, Prockop DJ (1994), Partial rescue of a lethal phenotype of fragile bones in transgenic mice with a chimeric antisense gene directed against a mutated collagen gene, *Proc.Natl.Acad.Sci.U.S.A* 91: 6298-6302

145. Khurana TS, Prendergast RA, Alameddine HS, Tome FM, Fardeau M, Arahata K, Sugita H, Kunkel LM (1995), Absence of extraocular muscle pathology in Duchenne's muscular dystrophy: role for calcium homeostasis in extraocular muscle sparing, *J.Exp.Med.* 182: 467-475

146. Kingsley DM (1994), The TGF-beta superfamily: new members, new receptors, and new genetic tests of function in different organisms, *Genes Dev.* 8: 133-146

147. Krippendorf BB, Riley DA (1993), Distinguishing unloading- versus reloading-induced changes in rat soleus muscle, *Muscle Nerve* 16: 99-108

148. Kuhn K (1995), Basement membrane (type IV) collagen, *Matrix Biol.* 14: 439-445

149. Kuivaniemi H, Tromp G, Prockop DJ (1991), Mutations in collagen genes: causes of rare and some common diseases in humans, *FASEB J.* 5: 2052-2060

150. Langley B, Thomas M, Bishop A, Sharma M, Gilmour S, Kambadur R (2002), Myostatin inhibits myoblast differentiation by down-regulating MyoD expression, *J.Biol.Chem.* 277: 49831-49840

151. Laptev AV, Lu Z, Colige A, Prockop DJ (1994), Specific inhibition of expression of a human collagen gene (COL1A1) with modified antisense oligonucleotides. The most effective target sites are clustered in double-stranded regions of the predicted secondary structure for the mRNA, *Biochemistry* 33: 11033-11039

152. Law PK, Goodwin TG, Fang Q, Hall TL, Quinley T, Vastagh G, Duggirala V, Larkin C, Florendo JA, Li L, Jackson T, Yoo TJ, Chase N, Neel M, Krahn T, Holcomb R (1997a), First human myoblast transfer therapy continues to show dystrophin after 6 years, *Cell Transplant.* 6: 95-100

153. Law PK, Goodwin TG, Fang Q, Quinley T, Vastagh G, Hall T, Jackson T, Deering MB, Duggirala V, Larkin C, Florendo JA, Li LM, Yoo TJ, Chase N, Neel M, Krahn T, Holcomb RL (1997b), Human gene therapy with myoblast transfer, *Transplant.Proc.* 29: 2234-2237

154. Laws N, Hoey A (2004), Progression of kyphosis in mdx mice, *J.Appl.Physiol* 97: 1970-1977

155. Leeuwenburgh C, Ji LL (1995), Glutathione depletion in rested and exercised mice: biochemical consequence and adaptation, *Arch.Biochem.Biophys.* 316: 941-949

156. Lefaucheur JP, Pastoret C, Sebille A (1995), Phenotype of dystrophinopathy in old mdx mice, *Anat.Rec.* 242: 70-76

157. Levi-Schaffer F, Nagler A, Slavin S, Knopov V, Pines M (1996), Inhibition of collagen synthesis and changes in skin morphology in murine graft-versus-host disease and tight skin mice: effect of halofuginone, *J.Invest Dermatol.* 106: 84-88

158. Levitt RC, Mitzner W (1988), Expression of airway hyperreactivity to acetylcholine as a simple autosomal recessive trait in mice, *FASEB J.* 2: 2605-2608

159. Lim LE, Campbell KP (1998), The sarcoglycan complex in limb-girdle muscular dystrophy, *Curr.Opin.Neurol.* 11: 443-452

160. Lin J, Arnold HB, Della-Fera MA, Azain MJ, Hartzell DL, Baile CA (2002), Myostatin knockout in mice increases myogenesis and decreases adipogenesis, *Biochem.Biophys.Res.Commun.* 291: 701-706

161. Liu F, Hata A, Baker JC, Doody J, Carcamo J, Harland RM, Massague J (1996a), A human Mad protein acting as a BMP-regulated transcriptional activator, *Nature* 381: 620-623

162. Liu J, Lissens W, Devroey P, Liebaers I, Van Steirteghem A (1996b), Cystic fibrosis, Duchenne muscular dystrophy and preimplantation genetic diagnosis, *Hum.Reprod.Update.* 2: 531-539

163. Liu Y (2002), Hepatocyte growth factor and the kidney, *Curr.Opin.Nephrol.Hypertens.* 11: 23-30

164. Liu Y (2004), Hepatocyte growth factor in kidney fibrosis: therapeutic potential and mechanisms of action, *Am.J.Physiol Renal Physiol* 287: F7-16

165. Lomask M (2006), Further exploration of the Penh parameter, *Exp.Toxicol.Pathol.* 57 Suppl 2: 13-20

166. Lord JP, Portwood MM, Lieberman JS, Fowler WM, Jr., Berck P (1987), Upper extremity functional rating for patients with Duchenne muscular dystrophy, *Arch.Phys.Med.Rehabil.* 68: 151-154

167. Lossos IS, Izbicki G, Or R, Goldstein RH, Breuer R (2000), The effect of suramin on bleomycin-induced lung injury, *Life Sci.* 67: 2873-2881

168. Love DR, Forrest SM, Smith TJ, England S, Flint T, Davies KE, Speer A (1989), Molecular analysis of Duchenne and Becker muscular dystrophies, *Br.Med.Bull.* 45: 659-680

169. Lu QL, Mann CJ, Lou F, Bou-Gharios G, Morris GE, Xue SA, Fletcher S, Partridge TA, Wilton SD (2003), Functional amounts of dystrophin produced by skipping the mutated exon in the mdx dystrophic mouse, *Nat.Med.* 9: 1009-1014

170. Lynch GS, Hinkle RT, Chamberlain JS, Brooks SV, Faulkner JA (2001), Force and power output of fast and slow skeletal muscles from mdx mice 6-28 months old, *J.Physiol* 535: 591-600

171. Massague J (1998), TGF-beta signal transduction, *Annu.Rev.Biochem.* 67: 753-791

172. Matsuda R, Nishikawa A, Tanaka H (1995), Visualization of dystrophic muscle fibers in mdx mouse by vital staining with Evans blue: evidence of apoptosis in dystrophin-deficient muscle, *J.Biochem.(Tokyo)* 118: 959-964

173. Matsumoto K, Nakamura T (2001), Hepatocyte growth factor: renotropic role and potential therapeutics for renal diseases, *Kidney Int.* 59: 2023-2038

174. Mauro A (1961), Satellite cell of skeletal muscle fibers, *J.Biophys.Biochem.Cytol.* 9: 493-495

175. McArdle A, Edwards RH, Jackson MJ (1994), Time course of changes in plasma membrane permeability in the dystrophin-deficient mdx mouse, *Muscle Nerve* 17: 1378-1384

176. McGaha TL, Kodera T, Spiera H, Stan AC, Pines M, Bona CA (2002a), Halofuginone inhibition of COL1A2 promoter activity via a c-Jun-dependent mechanism, *Arthritis Rheum.* 46: 2748-2761

177. McGaha TL, Phelps RG, Spiera H, Bona C (2002b), Halofuginone, an inhibitor of type-I collagen synthesis and skin sclerosis, blocks transforming-growth-factor-beta-mediated Smad3 activation in fibroblasts, *J.Invest Dermatol.* 118: 461-470

178. McIntosh L, Granberg KE, Briere KM, Anderson JE (1998), Nuclear magnetic resonance spectroscopy study of muscle growth, mdx dystrophy and glucocorticoid treatments: correlation with repair, *NMR Biomed.* 11: 1-10

179. McIntosh LM, Anderson JE (1995), Hypothyroidism prolongs and increases mdx muscle precursor proliferation and delays myotube formation in normal and dystrophic limb muscle, *Biochem.Cell Biol.* 73: 181-190

180. McIntosh LM, Pernitsky AN, Anderson JE (1994), The effects of altered metabolism (hypothyroidism) on muscle repair in the mdx dystrophic mouse, *Muscle Nerve* 17: 444-453

181. McKoy G, Ashley W, Mander J, Yang SY, Williams N, Russell B, Goldspink G (1999), Expression of insulin growth factor-1 splice variants and structural genes in rabbit skeletal muscle induced by stretch and stimulation, *J.Physiol* 516 (Pt 2): 583-592

182. McLennan IS (1993), Resident macrophages (ED2- and ED3-positive) do not phagocytose degenerating rat skeletal muscle fibres, *Cell Tissue Res.* 272: 193-196

183. McPherron AC, Lawler AM, Lee SJ (1997), Regulation of skeletal muscle mass in mice by a new TGF-beta superfamily member, *Nature* 387: 83-90

184. McPherron AC, Lee SJ (2002), Suppression of body fat accumulation in myostatin-deficient mice, *J.Clin.Invest* 109: 595-601

185. Mendell JR, Moxley RT, Griggs RC, Brooke MH, Fenichel GM, Miller JP, King W, Signore L, Pandya S, Florence J, . (1989), Randomized, double-blind six-month trial of prednisone in Duchenne's muscular dystrophy, *N.Engl.J.Med.* 320: 1592-1597

186. Merly F, Lescaudron L, Rouaud T, Crossin F, Gardahaut MF (1999), Macrophages enhance muscle satellite cell proliferation and delay their differentiation, *Muscle Nerve* 22: 724-732

187. Meyer OA, Tilson HA, Byrd WC, Riley MT (1979), A method for the routine assessment of fore- and hindlimb grip strength of rats and mice, *Neurobehav.Toxicol.* 1: 233-236

188. Mishima M, Kawakami K, Fukunaga T, Sugiura N, Hirai T, Oku Y, Fukui M, Chin K, Ohi M, Kuno K (1996), Validity of a random noise oscillation and body box system for the measurement of the respiratory impedance of small animals, *Front Med.Biol.Eng* 7: 163-175

189. Miura S, Takeshita T, Asao H, Kimura Y, Murata K, Sasaki Y, Hanai JI, Beppu H, Tsukazaki T, Wrana JL, Miyazono K, Sugamura K (2000), Hgs (Hrs), a FYVE domain protein, is involved in Smad signaling through cooperation with SARA, *Mol.Cell Biol.* 20: 9346-9355

190. Mokri B, Engel AG (1975), Duchenne dystrophy: electron microscopic findings pointing to a basic or early abnormality in the plasma membrane of the muscle fiber, *Neurology* 25: 1111-1120

191. Morgan JE (1990), Practical aspects of myoblast implantation: investigations on two inherited myopathies in animals, *Adv.Exp.Med.Biol.* 280: 89-94

192. Murakami N, McLennan IS, Nonaka I, Koishi K, Baker C, Hammond-Tooke G (1999), Transforming growth factor-beta2 is elevated in skeletal muscle disorders, *Muscle Nerve* 22: 889-898

193. Myllyharju J, Kivirikko KI (2001), Collagens and collagen-related diseases, *Ann.Med.* 33: 7-21

194. Nagler A, Firman N, Feferman R, Cotev S, Pines M, Shoshan S (1996), Reduction in pulmonary fibrosis in vivo by halofuginone, *Am.J.Respir.Crit Care Med.* 154: 1082-1086

195. Nagler A, Genina O, Lavelin I, Ohana M, Pines M (1999), Halofuginone, an inhibitor of collagen type I synthesis, prevents postoperative adhesion formation in the rat uterine horn model, *Am.J.Obstet.Gynecol.* 180: 558-563

196. Nagler A, Gofrit O, Ohana M, Pode D, Genina O, Pines M (2000), The effect of halofuginone, an inhibitor of collagen type i synthesis, on urethral stricture formation: in vivo and in vitro study in a rat model, *J.Urol.* 164: 1776-1780

197. Nagler A, Pines M (1999), Topical treatment of cutaneous chronic graft versus host disease with halofuginone: a novel inhibitor of collagen type I synthesis, *Transplantation* 68: 1806-1809

198. Nagler A, Rivkind AI, Raphael J, Levi-Schaffer F, Genina O, Lavelin I, Pines M (1998), Halofuginone--an inhibitor of collagen type I synthesis--prevents postoperative formation of abdominal adhesions, *Ann.Surg.* 227: 575-582

199. Nakamura T, Nishizawa T, Hagiya M, Seki T, Shimonishi M, Sugimura A, Tashiro K, Shimizu S (1989), Molecular cloning and expression of human hepatocyte growth factor, *Nature* 342: 440-443

200. Nakao A, Afrakhte M, Moren A, Nakayama T, Christian JL, Heuchel R, Itoh S, Kawabata M, Heldin NE, Heldin CH, ten Dijke P (1997a), Identification of Smad7, a TGFbeta-inducible antagonist of TGF-beta signalling, *Nature* 389: 631-635

201. Nakao A, Imamura T, Souchelnytskyi S, Kawabata M, Ishisaki A, Oeda E, Tamaki K, Hanai J, Heldin CH, Miyazono K, ten Dijke P (1997b), TGF-beta receptor-mediated signalling through Smad2, Smad3 and Smad4, *EMBO J.* 16: 5353-5362

202. Nakao A, Roijer E, Imamura T, Souchelnytskyi S, Stenman G, Heldin CH, ten Dijke P (1997c), Identification of Smad2, a human Mad-related protein in the transforming growth factor beta signaling pathway, *J.Biol.Chem.* 272: 2896-2900

203. Nathan CF (1987), Secretory products of macrophages, *J.Clin.Invest* 79: 319-326

204. Neilan TG, Januzzi JL, Lee-Lewandrowski E, Ton-Nu TT, Yoerger DM, Jassal DS, Lewandrowski KB, Siegel AJ, Marshall JE, Douglas PS, Lawlor D, Picard MH, Wood MJ (2006), Myocardial injury and ventricular dysfunction related to training levels among nonelite participants in the Boston marathon, *Circulation* 114: 2325-2333

205. Nguyen HX, Tidball JG (2003a), Expression of a muscle-specific, nitric oxide synthase transgene prevents muscle membrane injury and reduces muscle inflammation during modified muscle use in mice, *J.Physiol* 550: 347-356

206. Nguyen HX, Tidball JG (2003b), Interactions between neutrophils and macrophages promote macrophage killing of rat muscle cells in vitro, *J.Physiol* 547: 125-132

207. Nguyen HX, Tidball JG (2003c), Null mutation of gp91phox reduces muscle membrane lysis during muscle inflammation in mice, *J.Physiol* 553: 833-841

208. Nielsen KG, Bisgaard H (2005), Hyperventilation with cold versus dry air in 2- to 5-year-old children with asthma, *Am.J.Respir.Crit Care Med.* 171: 238-241

209. Nishi M, Yasue A, Nishimatu S, Nohno T, Yamaoka T, Itakura M, Moriyama K, Ohuchi H, Noji S (2002), A missense mutant myostatin causes hyperplasia without hypertrophy in the mouse muscle, *Biochem.Biophys.Res.Commun.* 293: 247-251

210. Ohlendieck K (1996), Towards an understanding of the dystrophin-glycoprotein complex: linkage between the extracellular matrix and the membrane cytoskeleton in muscle fibers, *Eur.J.Cell Biol.* 69: 1-10

211. Okano T, Yoshida K, Nakamura A, Sasazawa F, Oide T, Takeda S, Ikeda S (2005), Chronic exercise accelerates the degeneration-regeneration cycle and downregulates insulin-like growth factor-1 in muscle of mdx mice, *Muscle Nerve* 32: 191-199

212. Orimo S, Hiyamuta E, Arahata K, Sugita H (1991), Analysis of inflammatory cells and complement C3 in bupivacaine-induced myonecrosis, *Muscle Nerve* 14: 515-520

213. Pastoret C, Sebille A (1995a), Age-related differences in regeneration of dystrophic (mdx) and normal muscle in the mouse, *Muscle Nerve* 18: 1147-1154

214. Pastoret C, Sebille A (1995b), mdx mice show progressive weakness and muscle deterioration with age, *J.Neurol.Sci.* 129: 97-105

215. Petrof BJ, Shrager JB, Stedman HH, Kelly AM, Sweeney HL (1993), Dystrophin protects the sarcolemma from stresses developed during muscle contraction, *Proc.Natl.Acad.Sci.U.S.A* 90: 3710-3714

216. Piez KA, Carrillo AL (1964), HELIX FORMATION BY SI, *Biochemistry* 3: 908-914

217. Pines M, Domb A, Ohana M, Inbar J, Genina O, Alexiev R, Nagler A (2001), Reduction in dermal fibrosis in the tight-skin (Tsk) mouse after local application of halofuginone, *Biochem.Pharmacol.* 62: 1221-1227

218. Pines M, Nagler A (1998), Halofuginone: a novel antifibrotic therapy, *Gen.Pharmacol.* 30: 445-450

219. Pines M, Snyder D, Yarkoni S, Nagler A (2003), Halofuginone to treat fibrosis in chronic graft-versus-host disease and scleroderma, *Biol.Blood Marrow Transplant.* 9: 417-425

220. Prockop DJ, Kivirikko KI (1995), Collagens: molecular biology, diseases, and potentials for therapy, *Annu.Rev.Biochem.* 64: 403-434

221. Quinlan JG, Hahn HS, Wong BL, Lorenz JN, Wenisch AS, Levin LS (2004), Evolution of the mdx mouse cardiomyopathy: physiological and morphological findings, *Neuromuscul.Disord.* 14: 491-496

222. Reimann J, Irintchev A, Wernig A (2000), Regenerative capacity and the number of satellite cells in soleus muscles of normal and mdx mice, *Neuromuscul.Disord.* 10: 276-282

223. Rhodes K, Rippe RA, Umezawa A, Nehls M, Brenner DA, Breindl M (1994), DNA methylation represses the murine alpha 1(I) collagen promoter by an indirect mechanism, *Mol.Cell Biol.* 14: 5950-5960

224. Ricard-Blum S, Ruggiero F (2005), The collagen superfamily: from the extracellular matrix to the cell membrane, *Pathol.Biol.(Paris)* 53: 430-442

225. Roberts RG, Bobrow M, Bentley DR (1992), Point mutations in the dystrophin gene, *Proc.Natl.Acad.Sci.U.S.A* 89: 2331-2335

226. Robertson TA, Papadimitriou JM, Grounds MD (1992), Fusion between a myogenic cell in the satellite cell position and undamaged adult myofibre segments, *Experientia* 48: 394-395

227. Rossert JA, Chen SS, Eberspaecher H, Smith CN, de Crombrugghe B (1996), Identification of a minimal sequence of the mouse pro-alpha 1(I) collagen

promoter that confers high-level osteoblast expression in transgenic mice and that binds a protein selectively present in osteoblasts, *Proc.Natl.Acad.Sci.U.S.A* 93: 1027-1031

228. Rowland LP (1976), Pathogenesis of muscular dystrophies, *Arch.Neurol.* 33: 315-321

229. Sabourin LA, Rudnicki MA (2000), The molecular regulation of myogenesis, *Clin.Genet.* 57: 16-25

230. Sampaolesi M, Blot S, D'Antona G, Granger N, Tonlorenzi R, Innocenzi A, Mognol P, Thibaud JL, Galvez BG, Barthelemy I, Perani L, Mantero S, Guttinger M, Pansarasa O, Rinaldi C, Cusella De Angelis MG, Torrente Y, Bordignon C, Bottinelli R, Cossu G (2006), Mesoangioblast stem cells ameliorate muscle function in dystrophic dogs, *Nature* 444: 574-579

231. Sausbier M, Zhou XB, Beier C, Sausbier U, Wolpers D, Maget S, Martin C, Dietrich A, Ressmeyer AR, Renz H, Schlossmann J, Hofmann F, Neuhuber W, Gudermann T, Uhlig S, Korth M, Ruth P (2006), Reduced rather than enhanced cholinergic airway constriction in mice with ablation of the large conductance Ca2+-activated K+ channel, *FASEB J.*

232. Schultz E, Gibson MC, Champion T (1978), Satellite cells are mitotically quiescent in mature mouse muscle: an EM and radioautographic study, *J.Exp.Zool.* 206: 451-456

233. Schultz E, Jaryszak DL, Valliere CR (1985), Response of satellite cells to focal skeletal muscle injury, *Muscle Nerve* 8: 217-222

234. Schultz E, McCormick KM (1994), Skeletal muscle satellite cells, *Rev.Physiol Biochem.Pharmacol.* 123: 213-257

235. Scott JM, Li S, Harper SQ, Welikson R, Bourque D, DelloRusso C, Hauschka SD, Chamberlain JS (2002), Viral vectors for gene transfer of micro-, mini-, or full-length dystrophin, *Neuromuscul.Disord.* 12 Suppl 1: S23-S29

236. Serini G, Bochaton-Piallat ML, Ropraz P, Geinoz A, Borsi L, Zardi L, Gabbiani G (1998), The fibronectin domain ED-A is crucial for myofibroblastic phenotype induction by transforming growth factor-beta1, *J.Cell Biol.* 142: 873-881

237. Serini G, Gabbiani G (1999), Mechanisms of myofibroblast activity and phenotypic modulation, *Exp.Cell Res.* 250: 273-283

238. Seyedin SM, Rosen DM (1990), Matrix proteins of the skeleton, *Curr.Opin.Cell Biol.* 2: 914-919

239. Sharma M, Kambadur R, Matthews KG, Somers WG, Devlin GP, Conaglen JV, Fowke PJ, Bass JJ (1999), Myostatin, a transforming growth factor-beta

superfamily member, is expressed in heart muscle and is upregulated in cardiomyocytes after infarct, *J.Cell Physiol* 180: 1-9

240. Sicinski P, Geng Y, Ryder-Cook AS, Barnard EA, Darlison MG, Barnard PJ (1989), The molecular basis of muscular dystrophy in the mdx mouse: a point mutation, *Science* 244: 1578-1580

241. Singer II, Kawka DW, Kazazis DM, Clark RA (1984), In vivo co-distribution of fibronectin and actin fibers in granulation tissue: immunofluorescence and electron microscope studies of the fibronexus at the myofibroblast surface, *J.Cell Biol.* 98: 2091-2106

242. Skrabek RQ, Anderson JE (2001), Metabolic shifts and myocyte hypertrophy in deflazacort treatment of mdx mouse cardiomyopathy, *Muscle Nerve* 24: 192-202

243. Spencer MJ, Croall DE, Tidball JG (1995), Calpains are activated in necrotic fibers from mdx dystrophic mice, *J.Biol.Chem.* 270: 10909-10914

244. Spencer MJ, Mellgren RL (2002), Overexpression of a calpastatin transgene in mdx muscle reduces dystrophic pathology, *Hum.Mol.Genet.* 11: 2645-2655

245. Spencer MJ, Montecino-Rodriguez E, Dorshkind K, Tidball JG (2001), Helper (CD4(+)) and cytotoxic (CD8(+)) T cells promote the pathology of dystrophin-deficient muscle, *Clin.Immunol.* 98: 235-243

246. Spencer MJ, Tidball JG (1996), Calpain translocation during muscle fiber necrosis and regeneration in dystrophin-deficient mice, *Exp.Cell Res.* 226: 264-272

247. St Pierre BA, Tidball JG (1994), Macrophage activation and muscle remodeling at myotendinous junctions after modifications in muscle loading, *Am.J.Pathol.* 145: 1463-1471

248. Stedman HH, Sweeney HL, Shrager JB, Maguire HC, Panettieri RA, Petrof B, Narusawa M, Leferovich JM, Sladky JT, Kelly AM (1991), The mdx mouse diaphragm reproduces the degenerative changes of Duchenne muscular dystrophy, *Nature* 352: 536-539

249. Stein CA (1993), Suramin: a novel antineoplastic agent with multiple potential mechanisms of action, *Cancer Res.* 53: 2239-2248

250. Straub V, Rafael JA, Chamberlain JS, Campbell KP (1997), Animal models for muscular dystrophy show different patterns of sarcolemmal disruption, *J.Cell Biol.* 139: 375-385

251. Stroschein SL, Bonni S, Wrana JL, Luo K (2001), Smad3 recruits the anaphase-promoting complex for ubiquitination and degradation of SnoN, *Genes Dev.* 15: 2822-2836

252. Sweat F, Puchtler H, Rosenthal SI (1964), SIRIUS RED F3BA AS A STAIN FOR CONNECTIVE TISSUE, *Arch.Pathol.* 78: 69-72

253. Tatsumi R, Anderson JE, Nevoret CJ, Halevy O, Allen RE (1998), HGF/SF is present in normal adult skeletal muscle and is capable of activating satellite cells, *Dev.Biol.* 194: 114-128

254. Thies RS, Chen T, Davies MV, Tomkinson KN, Pearson AA, Shakey QA, Wolfman NM (2001), GDF-8 propeptide binds to GDF-8 and antagonizes biological activity by inhibiting GDF-8 receptor binding, *Growth Factors* 18: 251-259

255. Thioudellet C, Blot S, Squiban P, Fardeau M, Braun S (2002), Current protocol of a research phase I clinical trial of full-length dystrophin plasmid DNA in Duchenne/Becker muscular dystrophies. Part I: rationale, *Neuromuscul.Disord.* 12 Suppl 1: S49-S51

256. Thompson JP, Simkevich CP, Holness MA, Kang AH, Raghow R (1991), In vitro methylation of the promoter and enhancer of Pro alpha 1(I) collagen gene leads to its transcriptional inactivation, *J.Biol.Chem.* 266: 2549-2556

257. Tian XL, Yao W, Guo ZJ, Gu L, Zhu YJ (2006), Low dose pirfenidone suppresses transforming growth factor beta-1 and tissue inhibitor of metalloproteinase-1, and protects rats from lung fibrosis induced by bleomycina, *Chin Med.Sci.J.* 21: 145-151

258. Tidball JG, Berchenko E, Frenette J (1999), Macrophage invasion does not contribute to muscle membrane injury during inflammation, *J.Leukoc.Biol.* 65: 492-498

259. Torres LF, Duchen LW (1987), The mutant mdx: inherited myopathy in the mouse. Morphological studies of nerves, muscles and end-plates, *Brain* 110 (Pt 2): 269-299

260. Tsukazaki T, Chiang TA, Davison AF, Attisano L, Wrana JL (1998), SARA, a FYVE domain protein that recruits Smad2 to the TGFbeta receptor, *Cell* 95: 779-791

261. Unemori EN, Pickford LB, Salles AL, Piercy CE, Grove BH, Erikson ME, Amento EP (1996), Relaxin induces an extracellular matrix-degrading phenotype in human lung fibroblasts in vitro and inhibits lung fibrosis in a murine model in vivo, *J.Clin.Invest* 98: 2739-2745

262. Varghese S (2006), Matrix metalloproteinases and their inhibitors in bone: an overview of regulation and functions, *Front Biosci.* 11: 2949-2966

263. Verrecchia F, Vindevoghel L, Lechleider RJ, Uitto J, Roberts AB, Mauviel A (2001), Smad3/AP-1 interactions control transcriptional responses to TGF-beta in a promoter-specific manner, *Oncogene* 20: 3332-3340

264. Vierck J, O'Reilly B, Hossner K, Antonio J, Byrne K, Bucci L, Dodson M (2000), Satellite cell regulation following myotrauma caused by resistance exercise, *Cell Biol.Int.* 24: 263-272

265. Vilquin JT, Brussee V, Asselin I, Kinoshita I, Gingras M, Tremblay JP (1998), Evidence of mdx mouse skeletal muscle fragility in vivo by eccentric running exercise, *Muscle Nerve* 21: 567-576

266. Von der MK (1981), Localization of collagen types in tissues, *Int.Rev.Connect.Tissue Res.* 9: 265-324

267. Wagner KR, McPherron AC, Winik N, Lee SJ (2002), Loss of myostatin attenuates severity of muscular dystrophy in mdx mice, *Ann.Neurol.* 52: 832-836

268. Walia B, Wang L, Merlin D, Sitaraman SV (2003), TGF-beta down-regulates IL-6 signaling in intestinal epithelial cells: critical role of SMAD-2, *FASEB J.* 17: 2130-2132

269. Walther MM, Rehak NN, Venzon D, Myers CE, Linehan WM, Figg WD (2000), Suramin administration is associated with a decrease in serum calcium levels, *World J.Urol.* 18: 388-391

270. Walther Z, May LT, Sehgal PB (1988), Transcriptional regulation of the interferon-beta 2/B cell differentiation factor BSF-2/hepatocyte-stimulating factor gene in human fibroblasts by other cytokines, *J.Immunol.* 140: 974-977

271. Wan M, Shi X, Feng X, Cao X (2001), Transcriptional mechanisms of bone morphogenetic protein-induced osteoprotegrin gene expression, *J.Biol.Chem.* 276: 10119-10125

272. Watkins SC, Cullen MJ (1986), A quantitative comparison of satellite cell ultrastructure in Duchenne muscular dystrophy, polymyositis, and normal controls, *Muscle Nerve* 9: 724-730

273. Watkins SC, Cullen MJ (1988), A quantitative study of myonuclear and satellite cell nuclear size in Duchenne's muscular dystrophy, polymyositis and normal human skeletal muscle, *Anat.Rec.* 222: 6-11

274. Wehling M, Spencer MJ, Tidball JG (2001), A nitric oxide synthase transgene ameliorates muscular dystrophy in mdx mice, *J.Cell Biol.* 155: 123-131

275. Weintraub H (1993), The MyoD family and myogenesis: redundancy, networks, and thresholds, *Cell* 75: 1241-1244

276. Winand NJ, Edwards M, Pradhan D, Berian CA, Cooper BJ (1994), Deletion of the dystrophin muscle promoter in feline muscular dystrophy, *Neuromuscul.Disord.* 4: 433-445

277. Wineinger MA, Abresch RT, Walsh SA, Carter GT (1998), Effects of aging and voluntary exercise on the function of dystrophic muscle from mdx mice, *Am.J.Phys.Med.Rehabil.* 77: 20-27

278. Wozniak AC, Anderson JE (2007), Nitric oxide-dependence of satellite stem cell activation and quiescence on normal skeletal muscle fibers, *Dev.Dyn.* 236: 240-250

279. Wrogemann K, Pena SD (1976), Mitochondrial calcium overload: A general mechanism for cell-necrosis in muscle diseases, *Lancet* 1: 672-674

280. Yablonka-Reuveni Z, Rivera AJ (1994), Temporal expression of regulatory and structural muscle proteins during myogenesis of satellite cells on isolated adult rat fibers, *Dev.Biol.* 164: 588-603

281. Yang J, Liu Y (2003), Delayed administration of hepatocyte growth factor reduces renal fibrosis in obstructive nephropathy, *Am.J.Physiol Renal Physiol* 284: F349-F357

282. Yang S, Alnaqeeb M, Simpson H, Goldspink G (1996), Cloning and characterization of an IGF-1 isoform expressed in skeletal muscle subjected to stretch, *J.Muscle Res.Cell Motil.* 17: 487-495

283. Yingling JM, Das P, Savage C, Zhang M, Padgett RW, Wang XF (1996), Mammalian dwarfins are phosphorylated in response to transforming growth factor beta and are implicated in control of cell growth, *Proc.Natl.Acad.Sci.U.S.A* 93: 8940-8944

284. Yoshioka M, Okuno T, Honda Y, Nakano Y (1980), Central nervous system involvement in progressive muscular dystrophy, *Arch.Dis.Child* 55: 589-594

285. Yu M, Sato H, Seiki M, Spiegel S, Thompson EW (1997), Calcium influx inhibits MT1-MMP processing and blocks MMP-2 activation, *FEBS Lett.* 412: 568-572

286. Yuan W, Varga J (2001), Transforming growth factor-beta repression of matrix metalloproteinase-1 in dermal fibroblasts involves Smad3, *J.Biol.Chem.* 276: 38502-38510

287. Zeman RJ, Zhang Y, Etlinger JD (1994), Clenbuterol, a beta 2-agonist, retards wasting and loss of contractility in irradiated dystrophic mdx muscle, *Am.J.Physiol* 267: C865-C868

288. Zhang W, Ou J, Inagaki Y, Greenwel P, Ramirez F (2000), Synergistic cooperation between Sp1 and Smad3/Smad4 mediates transforming growth factor

beta1 stimulation of alpha 2(I)-collagen (COL1A2) transcription, *J.Biol.Chem.* 275: 39237-39245

289. Zhang XL, Topley N, Ito T, Phillips A (2005), Interleukin-6 regulation of transforming growth factor (TGF)-beta receptor compartmentalization and turnover enhances TGF-beta1 signaling, *J.Biol.Chem.* 280: 12239-12245

290. Zhang Y, Chang C, Gehling DJ, Hemmati-Brivanlou A, Derynck R (2001), Regulation of Smad degradation and activity by Smurf2, an E3 ubiquitin ligase, *Proc.Natl.Acad.Sci.U.S.A* 98: 974-979

291. Zhao Y, Haginoya K, Sun G, Dai H, Onuma A, Iinuma K (2003), Platelet-derived growth factor and its receptors are related to the progression of human muscular dystrophy: an immunohistochemical study, *J.Pathol.* 201: 149-159

292. Zhu H, Kavsak P, Abdollah S, Wrana JL, Thomsen GH (1999a), A SMAD ubiquitin ligase targets the BMP pathway and affects embryonic pattern formation, *Nature* 400: 687-693

293. Zhu HJ, Iaria J, Sizeland AM (1999b), Smad7 differentially regulates transforming growth factor beta-mediated signaling pathways, *J.Biol.Chem.* 274: 32258-32264

294. Zhu X, Topouzis S, Liang LF, Stotish RL (2004), Myostatin signaling through Smad2, Smad3 and Smad4 is regulated by the inhibitory Smad7 by a negative feedback mechanism, *Cytokine* 26: 262-272

295. Ziesche R, Block LH (2000), Mechanisms of antifibrotic action of interferon gamma-1b in pulmonary fibrosis, *Wien.Klin.Wochenschr.* 112: 785-790

Chapter 9. APPENDIX A

Figure A

A: Stimuli involved in activation, proliferation and differentiation of satellite cells (based on ideas from (Hawke and Garry 2001).

B: Summary of satellite cell activity. Muscle injury stimulates activation of satellite cells through the mechanisms above, and cells proliferate. Satellite cells migrate to the site of injury and either fuse with existing muscle fibers or form new muscle fibers, leaving regenerated and repaired fibers with centralized nuclei (based on ideas from (Hawke and Garry 2001).

A

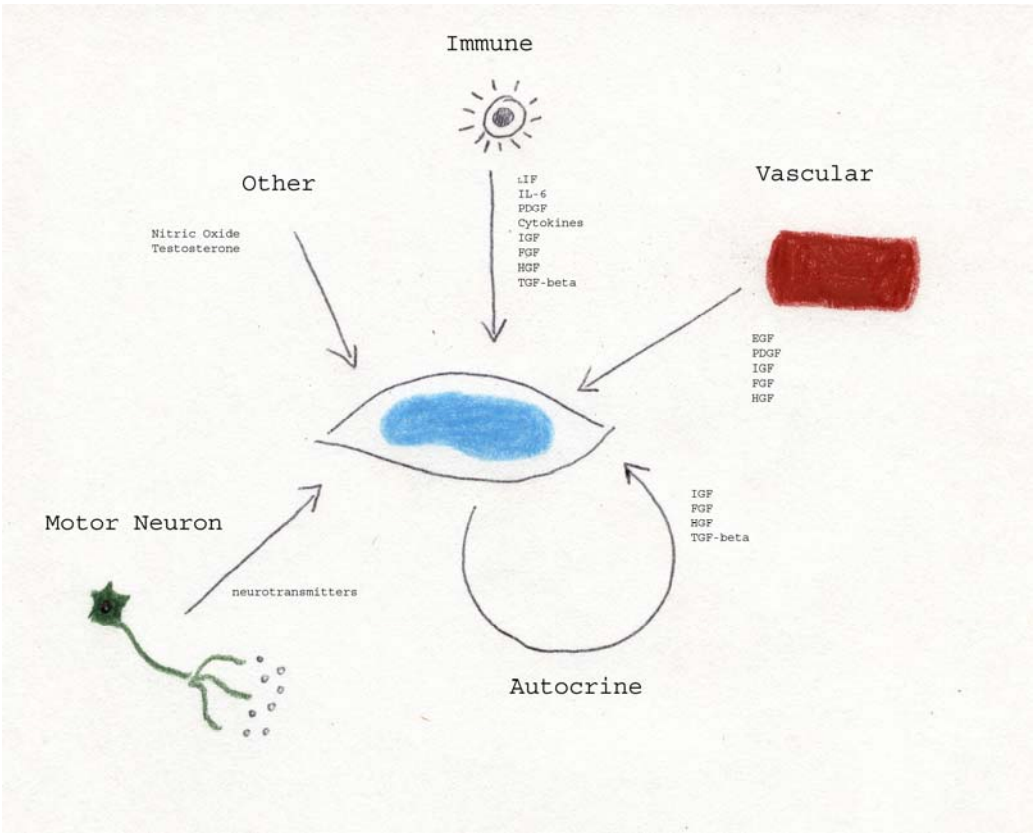
Immune
Other
Vascular
Nitric Oxide
Testosterone
LIF
IL-6
PDGF
Cytokines
IGF
FGF
HGF
TGF-beta
EGF
PDGF
IGF
FGF
HGF
IGF
FGF
HGF
TGF-beta
Motor Neuron
neurotransmitters
Autocrine

B

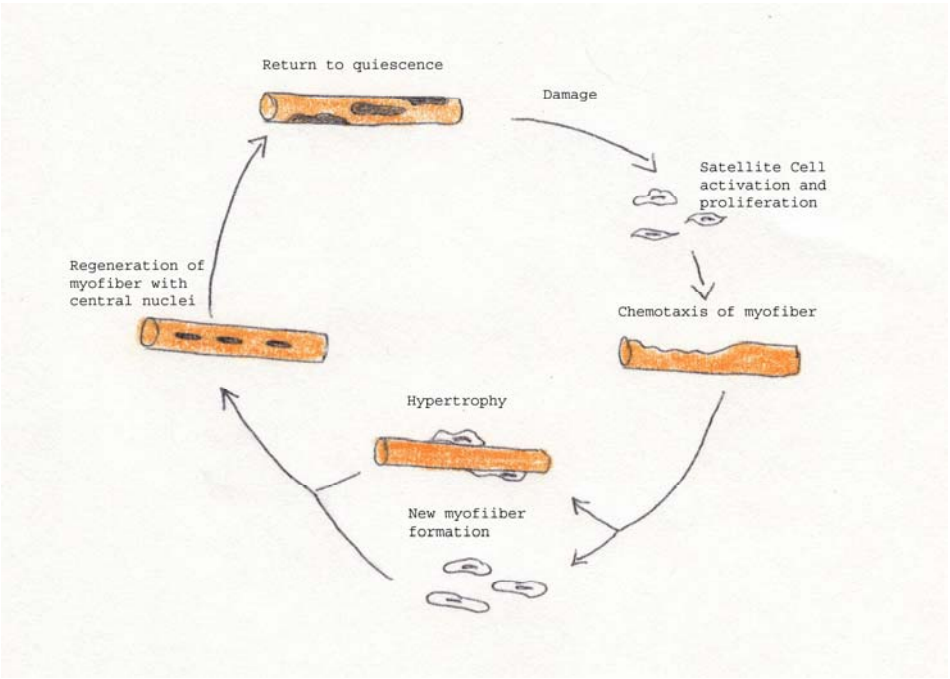
Return to quiescence
Damage
Satellite Cell
activation and
proliferation
Regeneration of
myofiber with
central nuclei
Chemotaxis of myofiber
Hypertrophy
New myofiiber
formation

Figure B

A: Collagen fibril assembly: Pro-collagen α-chains are synthesized in the golgi apparatus, where hydroxylation, glycosylation, and triple helix formation occurs. Triple helices are secreted out of the cell, the ends are cleaved off forming a collagen molecule, the molecules form a fibril, and then aggregate to form a collagen fiber (based of ideas from (Alberts *et al* 2002).

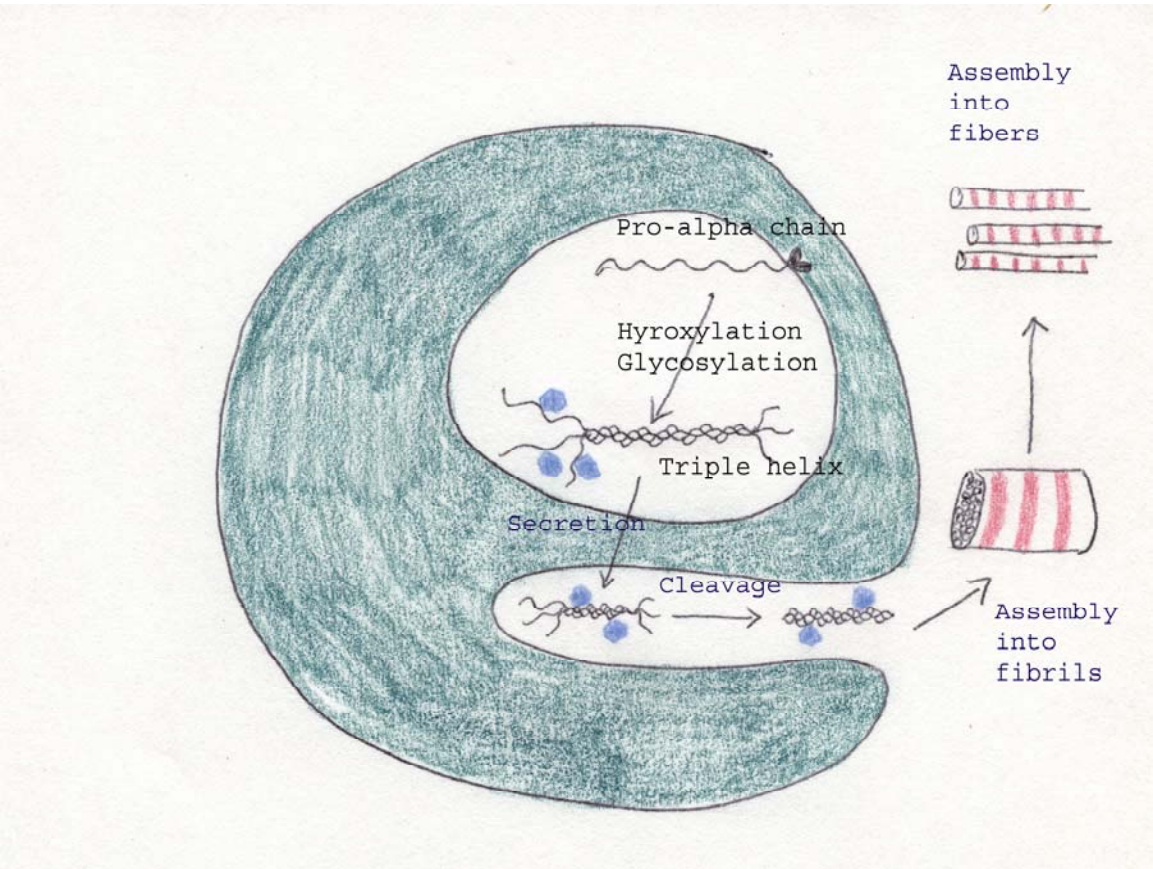

Figure C

A: Trial of collagenase digestion technique, using a sample of tibialis anterior from a young mdx mouse. Incubation times were 5 minutes, 15 minutes, 30 minutes, and 180 minutes. Bands were present at the 190kDa weight, as well as further down on the gel.

B: Second trial with Vitrogen as a positive control. Tibialis anterior and Vitrogen samples were incubated for 5 minutes, 10 minutes, 30 minutes, and 180 minutes. Bands appeared at all time points for Vitrogen (2 bands); however, bands at the 190kDa molecular weight were only present after 30 and 180 minutes incubation of the muscle samples.

A

5 15 30 180 - controls

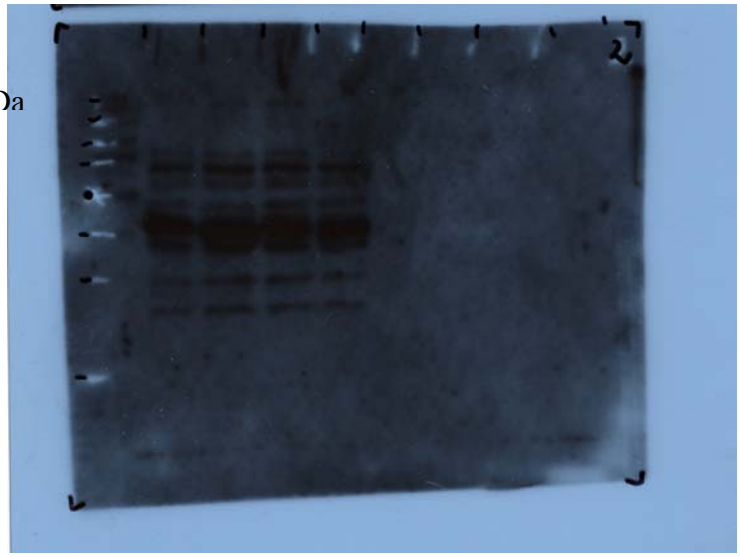

B

Muscle Vitrogen

5 10 30 180 5 10 30 180

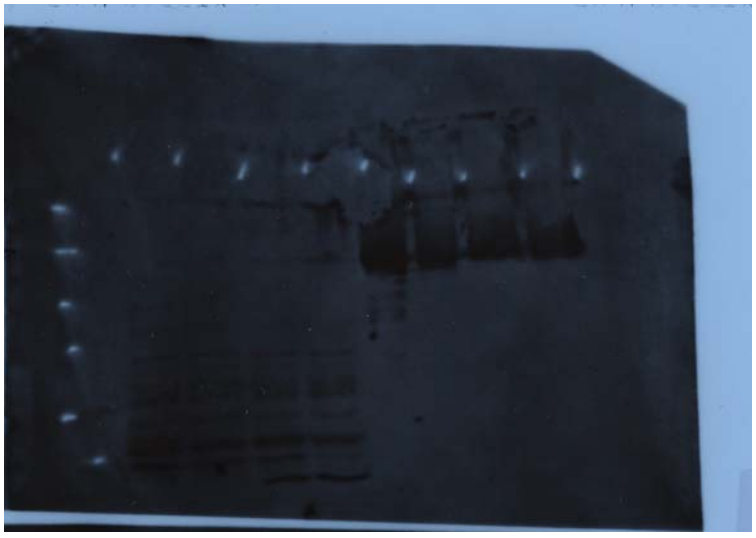

Chapter 10. APPENDIX B

RECIPES

a) Protein Analysis

-0.05M Tris-HCL

Tris Base	3.03 g
pH to 6.8.	
Bring to 50 mL mark with ddH_2O	

-1.5M Tris-HCL

Tris Base	9.09 g
pH to 8.8.	
Bring to 50 mL mark with ddH_2O	

-2.5M Tris-HCL

Tris-HCl	29.55 g
pH to 7.2.	
Bring to 75 mL mark with ddH_2O	

-Seperating gel

ddH_2O	4.9 mL
30% Acrylamide/Bis	2.4 mL
1.5M Tris-HCL	2.5 mL
10% SDS	0.1 mL
10% APS	0.1 mL
TEMED	0.006 mL

-Stacking gel

ddH_2O	5.5 mL
30% Acrylamide/Bis	1.3 mL
1.5M Tris-HCL	1.0 mL
10% SDS	0.08 mL
10% APS	0.08 mL
TEMED	0.008 mL

-Acrylamide

Acrylamide	14.6 g
N'N'-bis-methylene	0.4 g
Bring to 50 mL with ddH_2O.	

-10% SDS(Sodium Dodecyl Sulphate: aka Sodium Lauryl Sulphate)

SDS	10 g

ddH_2O	70 mL
pH to 7.2	
Bring to 100 mL with ddH_2O	

-10%APS (Ammonium Persulfate)

Ammonium persulfate	100 mg
ddH_2O	1 mL

-Sample Buffer (GELS)

ddH_2O	4.0 mL
0.5M Tris-HCL	1.0 mL
Glycerol	0.8 mL
10% SDS	1.6 mL
2-β-mercaptoethanol	0.4 mL
0.05% bromophenol blue	0.2 mL

-Sample Buffer (DOT BLOTS)

ddH_2O	2.1 mL
0.5M Tris-HCL	0.5 mL
Glycerol	0.4 mL
10% SDS	0.8 mL
2-β-mercaptoethanol	0.2 mL

-Running Buffer

Tris Base	3.25 g
Glycine	14.425 g
SDS	1 g
Bring to 1 L with ddH_2O	

-Transfer Buffer

Tris Base	5.82 g
Glycine	2.93 g
Methanol	200 mL
Bring to 1 L with ddH_2O	

-Blocking Buffer (0.05 M Tris-HCl; 0.3% Tween 20; 5% Milk Powder)

0.05M Tris	500 mL
Tween 20	1.5 mL
Tris+Tween	50 mL
Skim milk powder	2.5 g

-10 x PBS (Phosphate Buffered Saline)

NaCl	80 g
KCl	2 g
$Na_2HPO_4.7H_2O$	27.2 g

KH_2PO_4	2.4 g	

-Buffer 3

Tris Base	12.11 g	
NaCl	5.84 g	
$MgCl_2.6H_2O$	10.16 g	
ddH_2O	200 mL	
pH to 9.5		
Bring to 1L with ddH_2O		

-Stripping solution

10% SDS	20 mL	
Tris (pH6.8)	12.5 mL	
2-β-mercaptoethanol	700 µL	
Bring to 100 mL with ddH_2O		

b) Immunostaining

- Primary antibody diluent

1x PBS	9 mL	
Horse Serum	1 mL	10 %
Bovine Serum Albumin	0.1 g	1 %
10% Na azide*	10 uL	0.1 %

-Secondary antibosy diluent

Bovine Serum Albumin	0.1 g	1 %
1x PBS	10 mL	

- Bis Benzimide

1 uM Bis Benzimide	10.68 uL
ddH_2O	500 mL

-Ethidium Bromide

Ethidium Bromide	4 uL
1x PBS	50 mL

-DAB working solution

DAB	1 mL
1x PBS	50 mL
Colour intensifier	0.1 mL

-Colour intensifier

$NiCl_2.6H_2O$	0.5g
$CoCl_2.6H_2O$	0.5g
ddH_2O	10 mL

c) In situ hybridization

- DEPC water

DEPC (Diethyl pyrocarbonate)	1 mL
100% ethanol	9 mL
DEPC + ethanol	10mL
ddH_2O	1L

-Hybridization buffer (digoxigenin-labelled probes)

Deionized Formamide	25 mL
50% Dextran Sulphate	10 mL
20x SSC	12.5 mL
50x Denhardt's Solution	2 mL
10% N-Lauroyl Sarcosine	0.5 uL
Boehringer Blocking Reagent	1.0 g

Bring up to 50 mL with DEPC water

-50% Dextran sulphate

Dextran Sulphate	5.0 g
DEPC treated water	8.0 mL

Bring up to a 10 mL with DEPC ddH_2O

-Formamide deionization

Resin Beads TMD-8	5 g
Formamide	50 mL

-Dehardt's solution (50x)

Ficol	5 g
Polyvinylpyrrolidone	5 g
Bovine Serum Albumin	5 g

Bring up to 500 mL with DEPC ddH_2O

-12% Paraformaldehyde

Paraformaldehyde	12 g
1xPBS	100 mL
1 M NaOH	couple drops

-20x Standard saline citrate (SSC)

NaCl (3 M)	175.33 g
Trisodium Citrate (0.3 M)*	88.2 g
DEPC ddH_2O	300 mL

pH to 7.0.

Bring up to 1L with DEPC ddH_2O

10x Standard saline citrate (SSC)

NaCl (1.5 M)	87.67 g
Trisodium Citrate (0.15 M)*	44.1 g
DEPC ddH_2O	300 mL

Bring up to 1L with DEPC ddH_2O

-10% N-Lauroyl sarcosine

N-Lauroyl Sarcosine	5 g
DEPC ddH_2O	30 mL

Bring up to 50 mL mark with DEPC ddH_2O

-0.5M EDTA

EDTA	186.1 g
DEPC ddH_2O	800 mL

pH to 8.0 with 5M NaOH

Bring to 1000 mL with DEPC ddH_2O

-Buffer 1

Maleic Acid (100 mM)	11.607 g
NaCl (150 mM)	8.766 g
NaOH pellets	approx. 7 g
DEPC ddH_2O	800 mL

pH to 7.5

Bring up to 1L with DEPC ddH_2O

-Buffer 2

Roche Blocking Reagent	1.0 g
Buffer 1	100 mL

-Buffer 4

Tris base (10 mM)	1.211 g
EDTA (1 mM)	0.372 g
ddH_2O	800 mL

pH to 8.0.

Bring up to 1L with ddH_2O

-2x SSC 0.1% SDS

20x SSC	100 mL
SDS	1 g

Bring up to 1 L with DEPC ddH_2O

-RNAse A stock

RNase A	100 mg
0.01M Sodium Acetate	6 mL

pH to 7.4 with 1M Tris (pH 7.4).

Bring to 10 mL with sterile ddH_2O.

-0.01M Sodium acetate

$NaCH_3COO.3H_2O$	0.136 g
ddH_2O	90 mL

pH to 5.2 with glacial acetic acid.

Bring up to 100 mL with ddH_2O

-Colour solution

BCIP	0.175 mg/mL
NBT	0.35 mg/mL

Levamisole	240 ug/mL

-BCIP

BCIP	0.05 g
100 % Dimethylformamide	1 mL

-NBT

NBT	0.05 g
70 % Dimethylformamide	1 mL

-Levamisole stock

Levamisole	0.024 g
Buffer 3	1 mL

-Harris' Hematoxylin

Ammonium	10 g
Hematoxylin	0.5 g
Mercuric Oxide	0.25 g
Glacial Acetic Acid	2 - 4 mL
Absolute Ethanol	10 mL
Distilled water	100 mL